TRANSPORT PROPERTIES OF PROTON-EXCHANGE MEMBRANES: EFFECT OF SUPERCRITICAL-FLUID PROCESSING AND CHEMICAL FUNCTIONALITY

by

Juan Carlos Pulido Ayazo

A thesis submitted in partial fulfillment of the requirements for the degree of

DOCTOR OF PHILOSOPHY
in
CHEMICAL ENGINEERING

UNIVERSITY OF PUERTO RICO
MAYAGÜEZ CAMPUS
2010

Approved by:

_____	_____
David Suleiman Rosado, PhD President, Graduate Committee	Date
_____	_____
Madeline Torres-Lugo, PhD Member, Graduate Committee	Date
_____	_____
L. Antonio Estévez De Vidts, PhD Member, Graduate Committee	Date
_____	_____
Jaime Benítez Rodríguez, PhD Member, Graduate Committee	Date
_____	_____
Jayanta Banerjee, PhD Representative of Graduate Studies	Date
_____	_____
David Suleiman Rosado, PhD Chairperson of the Department	Date

ABSTRACT

Nafion® membranes commonly used in direct methanol fuel cells (DMFC), are tipically limited by high methanol permeability (also known as the cross-over limitation). These membranes have phase segregated sulfonated ionic domains in a perfluorinated backbone, which makes processing challenging and limited by phase equilibria considerations. This study used supercritical fluids (SCFs) as a processing alternative, since the gas-like mass transport properties of SCFs allow a better penetration into the membranes and the use of polar co-solvents influenced their morphology, fine-tuning the physical and transport properties in the membrane. Measurements of methanol permeability and proton conductivity were performed to the Nafion® membranes processed with SCFs at 40ºC and 200 bar and the co-solvents as: acetone, tetrahydrofuran (THF), isopropyl alcohol, HPLC-grade water, acetic acid, cyclohexanone. The results obtained for the permeability data were of the order of 10^{-8}-10^{-9} cm^2/s, two orders of magnitude lower than unprocessed Nafion.

Proton conductivity results obtained using AC impedance electrochemical spectroscopy was between 0.02 and 0.09 S/cm, very similar to the unprocessed Nafion. SCF processing with ethanol as co-solvent reduced the methanol permeability by two orders of magnitude, while the proton conductivity was only reduced by 4%. XRD analysis made to the treated samples exhibited a decreasing pattern in the crystallinity, which affects the transport properties of the membrane. Also, SAXS profiles of the Nafion membranes processed were obtained with the goal of determining changes produced by the SCF processing in the hydrophilic domains of the polymer.

With the goal of searching for new alternatives in proton exchange membranes (PEMs) triblock copolymer of poly(styrene-isobutylene-styrene) (SIBS) and poly(styrene-isobutylene-styrene) SEBS were studied. These sulfonated tri-block copolymers had lower methanol permeabilities, but also lower proton conductivity, even with blends of these and blends with Nafion membranes. Other alternative studied was the functionalization of the membranes SIBS with metallic cations, which decreased the methanol permeability in the membranes containing the cations Mg^{2+}, Zn^{2+} and Al^{3+}, while the proton conductivity was maintained more or less constant. The permeation of methanol vapor was investigated and the behavior through the membranes studied followed a pattern of Fick's Law, while the pattern shown by the permeation in liquid phase was non-Fickian.

RESUMEN

Las membranas Nafion® son comúnmente usadas en celdas de combustible operadas con metanol (DMFC), las cuales están muy limitadas en su funcionamiento por la alta permeabilidad de metanol a través de dicha membrana (fenómeno conocido como permeación de metanol). Estas membranas muestran una segregación de fases de sus dominios iónicos sulfonados ligados a su cadena principal perfluorinada, el cual hace de su procesamiento todo un reto limitado por consideraciones de equilibrio de fases. Este estudio utilizó fluidos supercríticos como una alternativa de procesamiento, ya que las propiedades de transporte de masa son similares a las de los gases, lo que permite una mejor penetración en la membrana y la utilización de co-solventes polares influenció su morfología y varió sus propiedades físicas y de transporte. Las medidas de permeabilidad de metanol y conductividad protónica fueron hechas a las membranas Nafion® procesadas con fluido supercrítico y co-solventes como: acetona, tetrahidrofurano (THF), alcohol isopropílico, agua, ácido acético y ciclohexanona. Los resultados obtenidos para los datos de permeabilidad fueron del orden de 10^{-8}-10^{-9} cm^2/s, dos órdenes de magnitud más bajos que en el Nafion® sin procesar.

Los resultados de conductividad protónica fueron obtenidos usando espectroscopía electroquímica de impedancia AC y estuvieron entre 0.02 y 0.09 S/cm, muy similares a los del Nafion® sin procesar. El procesamiento supercrítico usando etanol como cosolvente redujo la permeabilidad por dos órdenes de magnitud, mientras la reducción en la conductividad protónica fue sólo del 4%. Análisis de XRD y SAXS fueron realizados a las membranas con el objetivo de determinar cambios estructurales en el polímero. Los análisis de XRD hechos a las membranas tratadas exhibieron una disminución en el patrón de cristalinidad, lo que podría afectar las propiedades de transporte de la membrana. Los perfiles obtenidos con la técnica SAXS demostraron cambios producidos por el SCF en los dominios hidrofílicos de la membrana.

Con el objetivo de buscar nuevas alternativas de membranas de intercambio protónico, se estudian los copolímeros de SIBS y SEBS. Estos copolímeros sulfonados tienen más baja permeabilidad al metanol, pero también baja conductividad protónica. Otra alternativa estudiada fue la funcionalización de las membranas SIBS con cationes metálicos, los cuales disminuyeron la permeabilidad al metanol en la membranas conteniendo cationes como Mg^{2+}, Zn^{2+} y Al^{3+}, mientras la conductividad protónica se mantuvo más o menos constante. La permeación de vapor de metanol se estudió y ésta se ajustó a un patrón de ley de Fick, mientras que el patrón de permeación en fase líquida fue no Fickiano.

To my loved family . . .

Gladys and Felymar

ACKNOWLEDGEMENTS

During the development of my graduate studies in the University of Puerto Rico, several people and institutions collaborated directly and indirectly with my research. With their help it was possible for me to finish my work. That is why I wish to dedicate this section to recognize their support.

I want to start expressing a sincere acknowledgement to my advisor, Dr. David Suleiman Rosado, for providing me the opportunity to do research under his guidance and supervision. I received motivation, encouragement and technical support from him during all my studies.

I want to thank the motivation, inspiration and support of my loved wife Gladys and my beautiful daughter Felymar.

I would also like to thank my family in Colombia, for their unconditional support, inspiration and love.

A special thanks to my friends Boris Rentería and Leonel Quiñones for their help and support in the material characterization techniques as the XRD and TGA analysis. I am completely grateful to them for their valuable help for the completion of this work.

Finally, I would like to acknowledge the financial support from U.S. Department of Defense through Grant # DAAD19-03-1-0141 and from the Research and Development Center of the University of Puerto Rico, Mayagüez Campus. They provided the funding and the resources for the development of this research.

Table of Contents

List of Tables

Tables **Page**

List of Figures

Figures **Page**

1 INTRODUCTION

The requirements of new energy sources that are clean and of a great performance have been of interest in the last years. For this reason, researchers have focused on the development of new energy technologies such as fuel cells. In this technology it is necessary to employ membranes with a high selectivity for protons, while maintaining low permeability of the fuel used (*e.g.,* methanol).

New polymeric materials have been used in the synthesis of these membranes. Nafion® is the material with the best physical and chemical properties to be used as membranes in these cells. However, other polymers such as tri-block copolymers SEBS (styrene-ethylene-isobutylene-styrene) and SIBS (styrene-isobutylene-styrene) have been considered as alternative membranes to Nafion®.

This research focuses on finding new methods for the modification of polymers used in the fabrication of membranes for fuel cells. The modification of the physical or chemical properties of these polymers is necessary for better performance of the membranes in the fuel cells. Structural modifications of the polymers were done with supercritical fluids, which produced changes in their properties such as: permeability, proton conductivity, glass transition temperature and melting point.

The understanding obtained from this research can lead to more selective membranes (low permeability to the fuel used), while maintaining high proton conductivity, which can be

used in fuel cells. With the supercritical fluid processing of these polymers the morphology of these amorphous polymers will be fine tuned. This investigation elucidated the transport mechanism through experimental and modeling efforts.

1.1 Motivation

The most recent developments in separation processes have been towards the development of new membranes that can combine high selectivity, with low cost and stability. A separation process uses selective membranes to particular compounds such as: acids, alkalis organic solvents, gases and nitrate, iodide, sodium, and potassium ions. Ion exchange membranes have been used in this field, as separators for electrolysis of electrolyte solutions, desalinate electrolyte solutions, and pervaporation to dehydrate organic solvents [1].

Other common application of the membranes is in fuel cells, where they should be capable of separating protons from compounds as methanol for the generation of energy; these are denominated proton exchange membranes (PEM). In fuel cells, the membrane must have a high proton conductivity and low permeability to the fuel; this way it is possible to achieve a better performance of the cell. There are polymer materials, which exhibit a high proton conductivity; these are perfluorosulfonated polymer (Nafion®), SEBS, SIBS and oxo-acid such as polybenzimidazole (PBI).

Studying the impact of the SCF on the polymers to modify the transport properties (*e.g.,* permeability, diffusivity) of these materials, plays an important role in the application as barrier materials for food packaging and to be used in chemical protective clothing (CPC)

and stronger but lighter material among others applications. In CPC it is necessary to block selectively the transport of chemical and biochemical compounds while allowing water (from sweat) to be removed from the body.

In the last few years, researchers have shown that some thermoplastic polymers can reversibly swell using supercritical carbon dioxide. This phenomenon has been used to impregnate compounds as proteins (fluorescently-labeled) and bioactive compounds into a polymeric matrix [2]. The main polymers used as bioactive and biodegradable polymers are the PMMA (polymethylmethacrylate), (PLA) poly(lactic acid) and PLGA poly(lactic acid-co-glycolic acid).

1.2 Literature Review

A variety of studies have dealt with processing or modification of polymers, which could be classified in two areas: conventional processes and supercritical fluid processing. These conventional processes can be further sub-divided into chemical or physical such as: annealing temperature, film formation (casting solvent versus heat pressed), casting solvent and sulfonation. A variety of sulfonic acid (or sulfonated) polymers have been synthesized such as: ether sulfone, polyether ether ketone and S-SIBS, which have generated particular interest for its relationship between morphology and transport properties. This is the main goal of the optimization of the membranes used in the fuel cells.

Suleiman et al. [3], studied various sulfonated poly(styrene-isobutylene-styrene) (S-SIBS) and styrene-ethylene-isobuthylene-styrene (S-SEBS) ionomers by conventional processing

methods such as: casting solvent versus heat pressed and processing solvent. The study focused on the polymer properties affected by the solvent-polymer interactions. They found a linear and direct relationship between the sulfonation degree of S-SIBS and its solubility in the solvents studied (THF, Benzene, Chloroform, Methylene chloride, Cyclohexanone). In this study, they found out that the degradation temperature was approximately 450°C regardless of the sulfonation level, which was approximately 16°C higher than the unsulfonated polymer. This describes additional thermal stability from the interconnection of the sulfonic groups. Also they found out that this block copolymer desulfonates at approximately 290°C.

Okada et al. [4] studied transport and equilibrium properties of Nafion® membranes with sodium and hydrogen ions, using 11 different aqueous solutions of HCl and NaCl to equilibrate the membranes. The membrane conductivity was measured using AC impedance spectroscopy and it changed linearly with the concentration of hydrogen ions in the membrane. They also found that Nafion® membranes have a slightly higher affinity to sodium ions than for hydrogen ions. Unfortunately, results demonstrated that a possible sodium ion contamination (and others cations) in the fuel cell membranes may produce dried membrane and therefore a reduction in the efficiency of the fuel cell. This is because these ions, once entered into the membrane, are difficult to remove.

In recent years, polymers such as: Nafion®, polysulfone, SIBS, SEBS, PBI and PMMA have been processed with supercritical carbon dioxide with the goal of understanding how the supercritical fluids interact with these polymeric materials. The study of these interactions

between supercritical CO_2 and polymers at a molecular level will help to the understanding of the origin of phenomena such as the plasticizing on glass polymers. Most of the SCF processing has taken place in our lab; however, this investigation evaluated transport properties and materials characterization in detail for the first him.

Ramírez, C., [5] studied the processing of SEBS and SIBS with supercritical carbon dioxide at different processing conditions. The variables studied were: temperature, pressure, sulfonation percent, and the addition of a co-solvent (acetone, toluene or none). In addition to SCF CO_2, she quantified the thermal changes using a thermogravimetric analyzer (TGA), where the most significant effects were caused by the degree of sulfonation and the co-solvent effects.

Ocasio, M., [6] investigated the effect of supercritical fluid processing on the physical properties of Nafion® and SEBS. She used various cosolvents (tetrahydrofuran, acetone, methylene chloride, isopropyl alcohol, methanol, acetonitrile, glacial acetic acid, ciclohexanone or water) to influence the polymer-SCF interactions. The material characterization used thermogravimetric analysis. With this technique she found out that the degradation temperature of the membranes was significantly influenced by the co-solvents used and the processing conditions. Also, the sulfonic side-groups of the sulfonated polymers were thermally unstable and that the chemical environment with the SCF did not exert any effect on the degradation temperature of the polymer.

Marrero [7] studied the possible changes in thermodynamic equilibrium properties, specifically the ion exchange capacity (IEC), of poly(styrene-isobutylene-styrene) block copolymer processed with SCF CO_2 to several processing conditions. The technique used for the measurements of the IEC was an acid-base titration with NaOH. The variables studied were the immersion time of the membrane in a NaCl solution (2 M) and the weight of the membrane sampled. Also, she studied the kinetic effect of the IEC. She found out that the time necessary for the membrane to reach the equilibrium was over 24 hours, since the ions must diffuse through the membrane.

Kazarian [8] studied the changes in chemical properties of polymers such as PMMA (polymethyl methacrylate) when subjected to SCFs by means of ATR-IR spectroscopy. The study was based on understanding the plasticizing phenomena of SCF CO_2 on glassy polymers. The analysis measured spectra of polymers subjected to high-pressure gas, supercritical fluid, or near-critical water. The author used in situ ATR-IR spectroscopy to measure absorption and swelling of polymers under high-pressure CO_2. The in situ ATR-IR spectroscopy was applied to study the formation of stereo-complex of PMMA induced by high-pressure CO_2. The ATR-IR method allowed to observe SCF CO_2-induced melting of polyethylene glycol and to monitor the impregnation of pharmaceuticals into the molten polymer, which is important in the development of SCF processing of polymer/drug formulations.

Kojima et al. [9] studied the phase behavior of crosslinked polyisoprene rubber (PIR) with supercritical carbon dioxide. They performed visual swelling measurements based on the

sample dimensions using a high-pressure view cell. The change in the degree of swelling with time provided a diffusion coefficient of CO_2 in crosslinked PIR. They found out that the relationship between the degree of swelling and CO_2 pressure can be described by a sigmoidal curve in the pressure range studied (0.1 to 20 MPa) at 323 K.

Sproule et al. [2] used the reversible swelling phenomena (with SCF CO_2) of thermoplastic polymers to enhance the impregnation of protein (fluorescently-labeled) into a polymethylmethacrylate (PMMA) matrix. They applied a laser dilatometry technique to measure SCF CO_2 swelling and desorption from a polymer in situ. They achieved successful impregnation of a protein into CO_2-swollen PMMA, indicating the efficacy of producing protein-polymer biomedical materials using SCF technology.

1.3 Overview of Chapters

The first chapter develops the necessary motivation for the project and a literature review. Chapter 2 deals with background theory such as: diffusion, permeation and transport models. Chapter 3 presents the SCF processing of the Nafion® membranes with different co-solvents; experiments and material characterization, the data analysis were related to the transport properties like permeability and proton conductivity. Chapter 4 presents the study about sulfonated tri-block copolymer membranes such as SIBS, SEBS and physical blends of these. The resulting membranes are analyzed using: Thermal characterization (TGA, DSC), analysis of transport properties and structural analysis (by means of the XRD technique) are presented to explain the results. Chapter 5 deals with the SIBS membranes functionalized with different metal cations, of methanol permeability and conductivity. Finally, conclusions and the recommendations are presented in chapters 6 and 7 respectively.

2 THEORETICAL BACKGROUND

2.1 Diffusion and Permeation

The process of diffusion or permeation of a substance through polymeric materials cannot be described easily by a concentration-dependent form of Fick's law with constant boundary conditions, specially when the penetrant causes a swelling phenomenon on the polymer. This is the case of the so-called glassy polymers which exhibit 'anomalous' or 'non-Fickian' behavior. On the other hand, in the rubbery polymers the diffusion is generally Fickian. This distinction arises because polymers in the rubbery state respond rapidly to changes in their condition; however, the properties of a glassy polymer tend to be time-dependent. Some deviations from Fickian behavior are associated with the finite rates at which the polymer structure may change in response to the sorption or desorption of penetrant molecules.

Anomalous effects may be directly related to the influence of the changing polymer structure on solubility and diffusional mobility, or they may result from the internal stresses exerted by one part of the medium on another as diffusion proceeds.

Polymers usually show a wide spectrum of relaxation times associated with structural changes, but all of them decrease as temperature or penetrant concentration is increased and motion of the polymer segments enhanced. At a given concentration, the change from the glassy to the rubbery state is said to occur at the glass transition temperature. A sorption process, for example, can be influenced by those segmental motions which occur at about the same rate or slower than the motivating diffusion process. In rubbery polymers, well above their glass transition temperature, the polymer chains adjust so quickly to the presence of the penetrant that they do not cause diffusion anomalies.

Crank [10] has identified, according to the relative rates of diffusion and polymer relaxation, three classes of diffusion (Figure 2.1):

(a) Fickian diffusion, occurs when the rate of diffusion is much less than the rate of relaxation.

(b) Sigmoid diffusion, the other extreme, occurs when the diffusion is very rapid compared to the relaxation processes.

(c) Non-Fickian or anomalous diffusion, occurs when the rates of diffusion and relaxation are comparable.

(d) The term pseudo-Fickian has been used to describe sorption-desorption profiles of the same general shape and disposition, but for which persists for a shorter time.

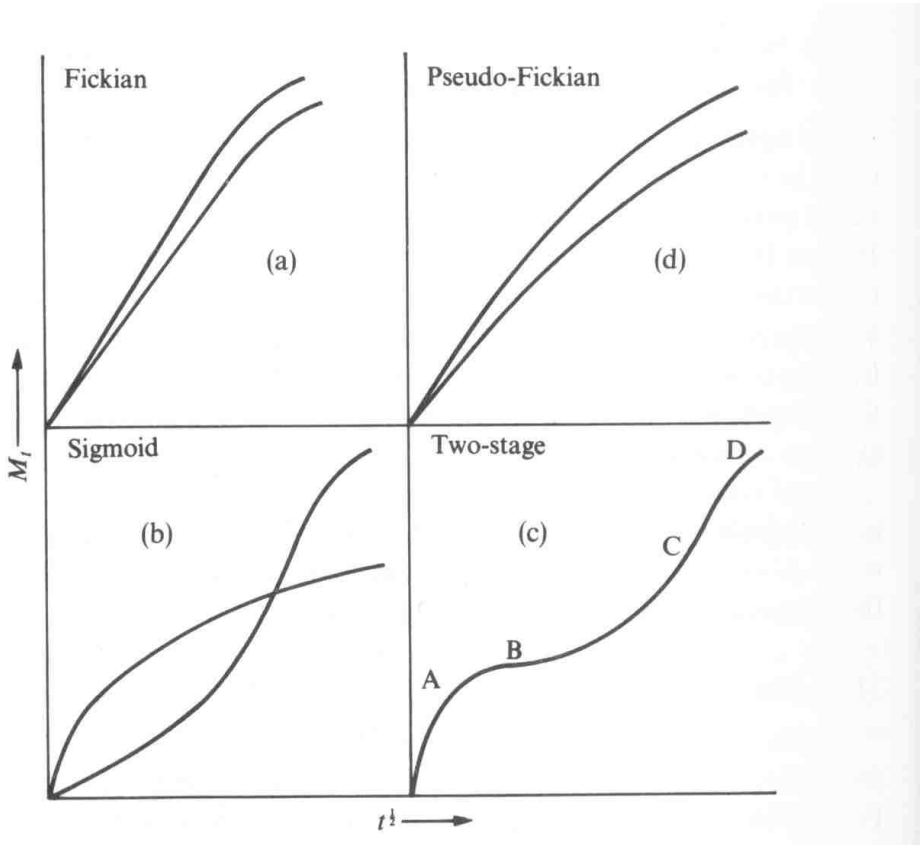

Figure 2.1 Kinds of Permeation

t: time

M: molar flux

Case (a) systems are controlled by the diffusion coefficient, while case (b) is controlled by the constant velocity of an advancing front which marks the innermost limit of penetration of the diffusant and is the boundary between swollen gel and glassy core. Case (b) is also a second extreme or limiting case with respect to the shape of the sorption-time curve. If the amount sorbed at time t is denoted by Kt^n, with K and n constants, then case (b) systems are characterized by n=1 and case (a) systems by n=½.

Non-Fickian systems lie between case (a) and case (b) in that n takes an intermediate value between ½ and 1, or changes sigmoidally from one to another. Also, non-Fickian behavior requires two or more parameters to describe the interacting diffusion and relaxation effects inherent in it.

2.2 Transport in Proton Exchange Membranes (PEM)

A synthetic membrane is a barrier that controls transport rates of one or various species diffusing through it. These can be permeable, or semipermeable to certain species. Some parameters control the performance of the membranes, such as: selectivity, permeability and flux, while factors such as temperature and hydration affect the transport through the membrane.

In the last few years, membrane material science has developed new materials of different structures and performance, as PBI (polybenzimidazole), polysulfone, PEEK (polyether ether ketone) and PES (polyether sulfone) to be used as synthetic membranes in separation processes and fuel cells [11]. Synthetic membranes can be classified as: symmetric or asymmetric according to its structure and functionality. Some membranes are composed of layers of different polymeric materials, which give special properties of mass transfer or electrical properties according to their use. Synthetic membranes have several characteristics, which determine their chemical or physical properties, such as: the molecular weight of the

monomer and structural characteristics (homopolymer or copolymer, linear or branched, and level of crosslinking).

Other membranes called proton exchange membranes (PEM) are used mainly in fuel cells for the transport of positively charged molecules and to prevent cross mixing of the positive and negative electrolytes, allowing the transport of ions to complete the circuit during the passage of current. The most commonly PEM used for fuel cells and electrolytic processes is Nafion®, which is a perfluorinated ionomer copolymer. Nafion® is a polytetrafluoroethylene with sulfonic pendant groups bound to the perfluorinated backbone by fluoroether side chains (Figure 2.2). Nafion® is used due to its excellent mechanical, chemical strength and its high ionic conductivity.

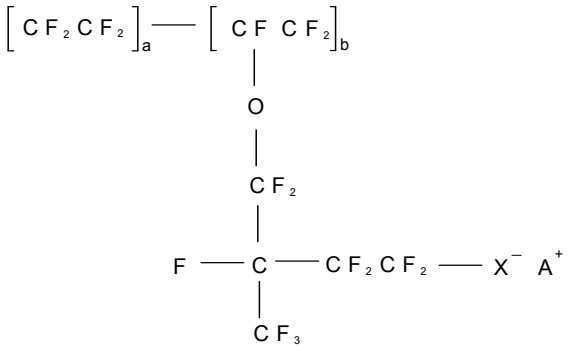

where

X^-: is the anion SO_3^-
A^+: is the cation H^+ or a metal cation such as Na^+

Figure 2.2 Nafion® Perfluorinated Ionomer

An ideal PEM should exhibit a high electrical conductivity combined with a high ionic permeability, not only to promote productivity, but also to reduce the operating cost. The membrane conductivity can be increased by the increasing ionic charge density. A factor that affects the generation of electric current in the fuel cells is the transport of water and ions, through the membrane, due to ionic conductivity which decreases strongly when the membrane is dry.

Other types of ion exchange membranes used in fuel cells are perfluoroalkyl sulfonated, which have excellent conductivity and cation selectivity. The polymer structure of these membranes consists of a linear backbone of fluorocarbons chains and ethylether pendant groups with sulfonic acid cation exchange sites [12].

The transport of protons and methanol in the PEM is a critical function due to its importance for the generation of power in the fuel cells. The transport of protons has been described by the Nerst-Plank equation, given by:

$$-j_p = D_p C_p \left(\frac{\nabla C_p}{C_p} + z_p \frac{F \nabla \psi}{RT} \right) \qquad (1)$$

where,

j_p: proton flux

D_p: Diffusion coefficient

C_p: Concentration

z_p: Charge

F: Faraday's constant

R: Gas constant

T: Temperature

ψ: Electrostatic potential

Equation (1) can be simplified if the concentration of protons (C_p) and membrane thickness are constant:

$$j_p = \left(\frac{D_p C_p F}{RT} \right) \frac{\Delta \psi}{L} \qquad (2)$$

Another parameter in the diffusion of protons in the fuel cells is the Proton conductivity (σ_p), which is defined by:

$$\sigma_p = \frac{D_p C_p F^2}{RT} \qquad (3)$$

while the methanol diffusion is described by the well-known Fick's law:

$$-j_m = D_m \frac{\partial C_m}{\partial X} \qquad (4)$$

where,

D_m: Methanol diffusion

C_m: Methanol concentration

If the methanol concentration is constant in the side of the anode (donor) (Figure 2.3), and it is given by C_{mo}, then the Fick's law for methanol diffusion can be expressed as:

$$j_m = \frac{D_m K_m C_{m_o}}{L} \qquad (5)$$

where,

K_m: Partition coefficient (the ratio of methanol concentration inside the membrane to that in the adjacent solution).

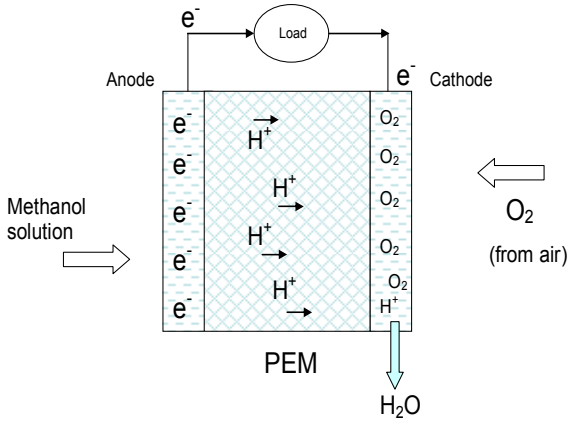

Figure 2.3 Schematic representation of a methanol//O_2 fuel cell

Another parameter that influences on the performance of the fuel cells is the permeability (P_m) of the methanol and the selectivity to the protons of the membrane. These parameters are defined by the following equations [13]:

$$P_m = D_m K_m \qquad (6)$$

The permeability is defined as the ratio of methanol concentration inside the membrane to that in the adjacent solution.

$$\beta = \frac{j_p}{j_m} = \frac{\sigma_p}{P_m}\left(\frac{\Delta\psi}{FC_{m_o}}\right) \qquad (7)$$

The selectivity of the membrane (β) can be defined as the ratio of fluxes, the ratio of proton flux (j_p) to methanol flux (j_m), given by equation (7), which is the result of the combination of the equations (2), (3) and (5). This is expressed in terms of the proton conductivity (σ_p) and methanol permeability (P_m) [13]:

$$\alpha = \frac{\sigma_p}{P_m} \qquad (8)$$

It is important to note that these two parameters (conductivity and permeability) are proportional to their respective diffusion coefficients. A high selectivity (β) is required for a best performance of the DMFC, which is reached with high proton conductivity and low permeability to methanol.

2.3 Transport Models

The transport of a compound through polymer membranes can be described by various models. Some models are based in thermodynamic and statistical principles, and others are based on correlation of the physical properties of the membrane with the observed transport phenomena. There are at least seven models available that describe the transport phenomena; all seven of them can be applied to the liquid-membrane systems, but only two can describe the gas-membrane systems, the solution diffusion model and solution diffusion imperfection model [14]. The following are the models proposed:

1. Frictional model
2. Irreversible thermodynamics
3. Solution diffusion model
4. Solution diffusion imperfection model
5. Finely porous model
6. Diffusion viscous flow model
7. Preferential sorption capillary flow model

Although these are the available models, we will only discuss in detail the solution diffusion model, because this model can be applied to gas-membrane and liquid-membrane systems [14] and the classical free volume model.

2.3.1 Solution diffusion model

This model was proposed by Graham in 1866. The model describes the transport of gases through a membrane as a three steps process: sorption of gas onto the membrane, diffusion through the membrane due to an applied concentration (or pressure) gradient and desorption of gas. The first and last steps are considered dependent of the characteristics of membrane material and the gas or liquid.

In this model it is assumed that an isothermal homogenous stationary membrane in which particles at a position *r* are dissolved with a local concentration *c(r)*. The particle flux is given by

$$J(r) = c(r)v(r) \qquad (9)$$

It is considered the motion of particles of an *i*-th species, where the average velocity of the dissolved particles *v(r)* is proportional to the thermodynamic driving force (which is the negative gradient of chemical potential).

$$v(r) = \frac{1}{\gamma} F_{th} = -\frac{1}{\gamma} \nabla \mu(r) \qquad (10)$$

Where F_{th} is the thermodynamic force, γ is the frictional coefficient of the particles and μ the chemical potential of the dissolved particles, which is given by

$$\mu(r) = \mu^0 + RT \ln c(r) + \mu_e(r) \qquad (11)$$

Where μ^0 is the standard chemical potential of the ideal gas phase based on unit molar concentration. $\mu_e(r)$ is the excess chemical potential of the dissolved species respect to the ideal gas state. Combining the equations 9, 10 and 11:

$$J(r) = -\frac{RT}{\gamma}\nabla c(r) - \frac{c(r)}{\gamma}\nabla \mu_e(r) \qquad (12)$$

The frictional coefficient γ is related to the diffusion constant D by

$$\gamma = \frac{RT}{D} \qquad (13)$$

This way equation 12 can be rewritten as:

$$J(r) = -D \exp\left(-\frac{\mu_e(r)}{RT}\right) \cdot \nabla \left\{ c(r) \exp\left(\frac{\mu_e(r)}{RT}\right) \right\} \qquad (14)$$

If we consider a membrane with thickness d, which is in contact with concentrations c_1 and c_2 ($\Delta c = c_2 - c_1$) and we assumed there is equilibrium at both interfaces, then for a stationary flux $J(r)$ is assumed that $c(r)$ is a linear function of the coordinate and the concentration gradient is equal to $\Delta c/d$, due to μ_e is considered to be constant through homogeneous membrane.

Hence equation 14 is reduced to

$$J = -DS\frac{\Delta c}{d} \qquad (15)$$

where

$$S = \exp\left(-\frac{\mu_e}{RT}\right) \qquad (16)$$

$$P = DS \qquad (17)$$

Equation 15 is the mathematical expression for the solution-diffusion model, where the product of diffusion coefficient D and solubility factor S is called the permeability coefficient P, defined by the ratio between the flux J of the permeant species and its concentration gradient Δc over the membrane thickness d.

2.3.2 The classical free volume model

It is well known that the mechanical and rheological properties of a polymer are influenced by molecular motion or chain flexibility of the polymer molecules, which in turn depends upon the microscopic free-volume holes, present mainly in the amorphous region in the polymer. In addition, the free-volume holes facilitate the permeation or transport of a substance through a polymer by providing suitable pathways. In general, the free-volume concept is widely accepted in view of its ability to predict many properties of polymers at molecular level [15]. However, the free-volume model does not offer a detailed microscopic description of the penetrant-polymer system, but attempts to relate the diffusion coefficient to the free-volume available in the system, usually from statistical considerations.

The free-volume model is based on the idea that a penetrant can only move through the 'free volume' in the polymer and that thus the diffusion can be described using a statistical description of this free volume [14]. Free volume has been shown to have a strong influence in diffusion and permeation properties [16].

Transport properties such as the permeability coefficient and proton conductivity are influenced by the free-volume available in the polymeric membrane. The permeability coefficient, P, is comprised of both kinetic and thermodynamic factors which in principle

depend on different aspects of the substance/polymer pair (Equation 17). However, for a given penetrant, the diffusion coefficient, D, varies from polymer to polymer a great deal more than does the solubility coefficient. While the diffusion coefficient may depend on many issues, the free volume of the polymer is among the most important. Thus, the permeability coefficient for a given penetrant in a series of polymers can be reasonably well correlated in terms of free volume of the following form [17]:

$$D = Ae^{-\frac{B}{V_f}} \qquad (18)$$

$$P = A^* e^{-\frac{B^*}{V_f}} \qquad (19)$$

where A and B are constants for a particular substance. The fractional free volume, V_f, has been defined as

$$V_f = \frac{(V - V_o)}{V} \qquad (20)$$

Here, V is defined as specific volume of the polymer (may be expressed as volume per unit mass or mole of repeat unit) which is obtained from experimental measurement of the polymer density at the temperature of interest. The term V_o is the volume occupied by the polymer chains. It can be determined by the Bondi's group contribution method where the occupied volume is computed from the van der Waals volumes, $(V_w)_k$, of the various groups in the polymer structure by

$$V_o = 1.3\sum_{k=1}^{K}(V_w)_k \qquad (21)$$

where K is the total number of groups into which the repeat unit structure of the polymer is divided. The factor of 1.3 was estimated by Bondi from the packing densities of molecular crystals at absolute zero and accounts for the fact that this volume is greater than the molecular volume; a major approximation is that a single universal value of 1.3 is assumed to apply for all groups and structures[17].

`

3 SUPERCRITICAL-FLUID PROCESSING OF NAFION® MEMBRANES

Despite all advantages in the development of proton exchanged membranes (PEM) for fuel cell applications, Nafion remains the most commonly used PEM for direct methanol fuel cells (DMFC). Nafion® is a non-crosslinked ion exchanged polymer (ionomer) with a perfluorinated backbone and sulfonate ionic groups attached to perfluorovinylether side chains. The semi-crystalline structure of Nafion® is separated in two microphases: a hydrophobic perfluorinated region (backbone) and hydrophilic domains formed by the ionic clusters. It has excellent resistance to chemicals due to the perfluorinated backbone , and high proton conductivity caused by the sulfonic groups. Unfortunately, since the transport mechanism for protons and methanol is the same (from sulfonic group to sulfonic group); the employment of this membrane at the fuel cell has the problem of methanol crossover from the anode to the cathode, which reduces the cathode potential and decreases the cell efficiency. Over 40% of the methanol used in the DMFC can be wasted across Nafion® membranes.

Different authors have investigated ways to modify Nafion® with the goal of decreasing the methanol crossover, while maintaining the proton conductivity high and therefore increase the performance and efficiency of the DMFC. The most common approaches involve Nafion® nano-composite membranes (NNM) (*e.g.,* of organosilica with sulfonated diphenyldimethosylane) to change the polymer morphology and pursue different transport mechanisms between the membranes reducing the methanol permeability; unfortunately, most of NNM approaches also decrease the proton conductivity proportional to the reduction in methanol permeability.

Solvent effects have also been studied to pursue morphological changes in the membrane. One of such study used small polar protic solvents (*e.g.,* methanol, ethanol, 2-propanol and

water) on Nafion® membranes. Proton conductivity results showed a reduction in the alcohol environment, while the aqueous environment maintained the high values commonly found in Nafion®; unfortunately, the study did not include methanol permeability.

Another important study of Nafion® membranes was performed by Elabd and Napadensky. They measured proton conductivity normal to the plane and in the plane of Nafion® membranes revealing that there are variations with the direction of the measurement.

There are numerous other physical and chemical modifications to Nafion® membranes as well as many alternative membranes that have been created as competitors to Nafion® membranes. This description is not intended to be comprehensive but simply an overview to point out some the chemical and physical modifications that helped guide this study. This investigation used supercritical fluids (SCFs) as a processing alternative, since the gas-like mass transport properties of SCFs allow for better penetrations into the membrane and the use of co-solvents of different chemical size, polarity and functionality could also influence the membrane morphology, and fine-tuning the physical and transport properties. SCF processed membranes were then characterized for methanol permeability and proton conductivity.

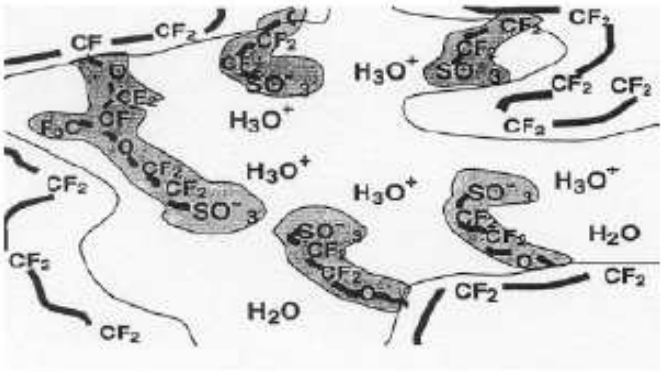

Figure 3.1 Clusters network in the Nafion® structure

3.1 Chemicals used

SFE-grade CO_2 (99.98% purity) was obtained from Scott Specialty Gases. Nafion® membrane N117 was obtained from Ion Power, Inc. Acetone (HPLC grade), toluene (HPLC grade), methanol (HPLC grade), ethanol, water (HPLC grade), tetrahydrofuran (99% purity), cyclohexanone (99% purity), dichloromethane (HPLC grade), acetonitrile (HPLC grade), and acetic acid (99.7% purity), were obtained from Sigma-Aldrich Chemical Company. They were used without any further treatment.

3.2 Supercritical-Fluid Processing

In recent years, the technology of supercritical fluids has attracted a particular interest by chemists and chemical engineers in seeking new polymeric materials with specific properties. Supercritical-fluid processing consists in exposing the polymer to a supercritical environment with the goal to modify its orientation arrangement (morphology), and properties, such as physical, chemical, mechanical and electrical properties. The modification of some properties by this method coupled with proper characterization of the material can be used in numerous applications.

The substance most used as a supercritical fluid is carbon dioxide because it is non-toxic, non-flammable, chemically inert, and inexpensive. Also its critical conditions (Tc = 31.1°C, Pc = 73.8 bar) are easily obtained. After being used in the process, it can be removed by a simple depressurization. Also, its density can be "tuned" with small changes in the pressure or temperature.

In this research, Nafion® membrane samples were saturated by immersion in a co-solvent (such as: acetone, toluene, acetonitrile, HPLC-grade water, isopropanol) for one hour and then they were processed with supercritical carbon dioxide (at 40°C and 200 bars) using a supercritical fluid extractor for one hour at a flow of 0.45 mL/min (Figure 3.2). The carbon dioxide was first withdrawn from the cylinder into a high-pressure syringe pump (ISCO 260D) before entering the extraction chamber, where the sample was placed at constant

temperature of 40˚C. The pressure and temperature were selected to have a high SCF density and were maintained constant. The syringe pump was used to maintain the pressure at a constant value of 200 bar. After one hour, the extractor was allowed to decompress using a coaxially-heated restrictor to overcome the Joule-Thompson effect.

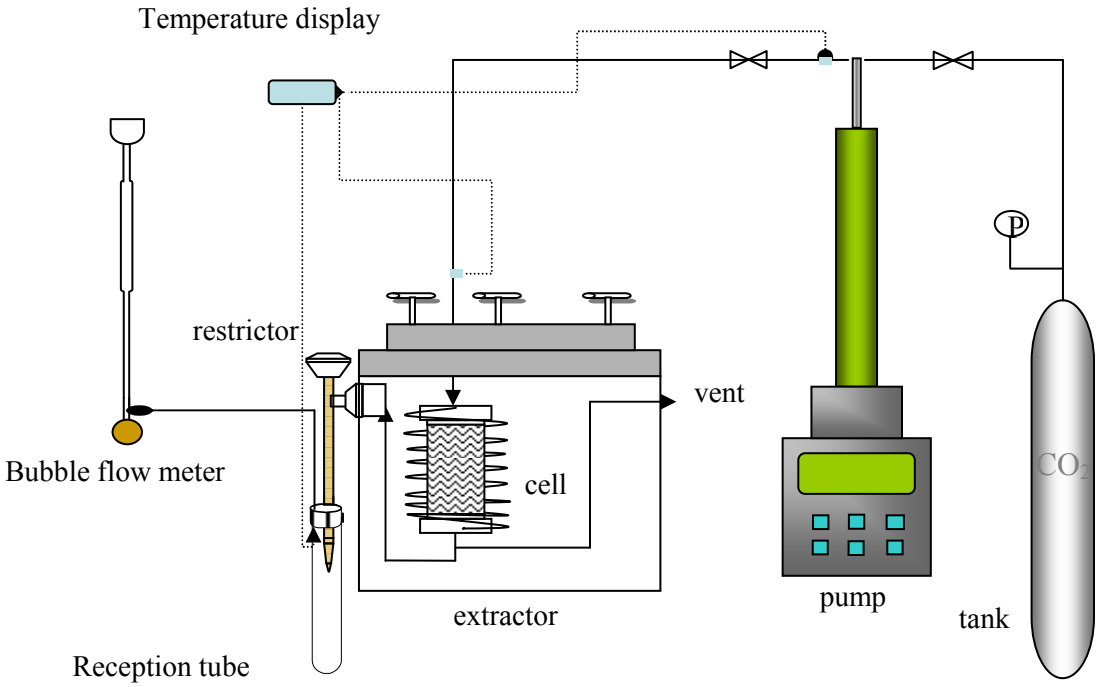

Figure 3.2 Supercritical-fluid extractor (ISCO)

3.3 Permeability Measurements in Liquid Phase

The methanol permeability of each Nafion® membrane sample processed with different co-solvents and $SCCO_2$ was measured using a FT-IR spectrophotometer. The Nafion® sample was clamped on a permeation cell and the sample was always maintained wetted with liquid methanol solution (Figure 3.3). The methanol concentration on one side of the membrane was maintained constant, while samples were taken from the other side of the membrane and analyzed in the FT-IR spectrometer, which measured the variation of methanol concentration as a function of time (a measure of the methanol that permeates through the membrane).

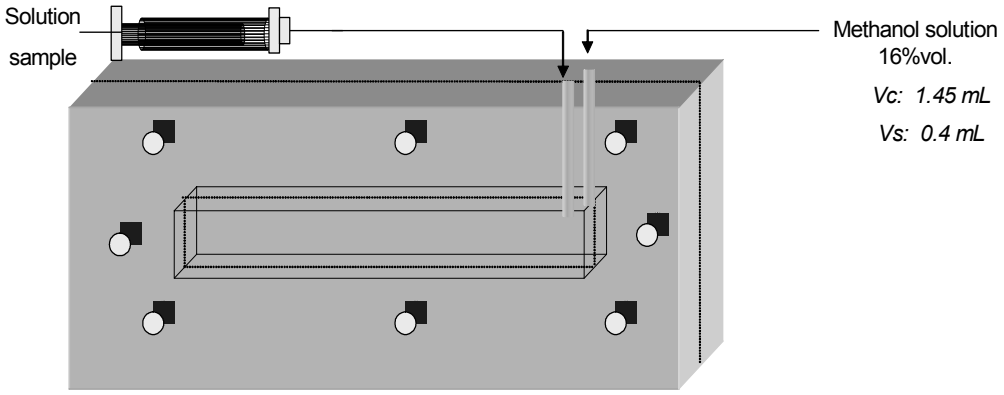

Figure 3.3 Permeation cell used in the experiments

A calibration curve was made with methanol solutions of known concentrations (Figure 3.4). The absorbance of the methanol peaks were correlated with the methanol concentration. Infrared spectra were recorded throughout each experiment at 30 min intervals using 64 scans and 4 cm^{-1} resolution for each collected spectrum.

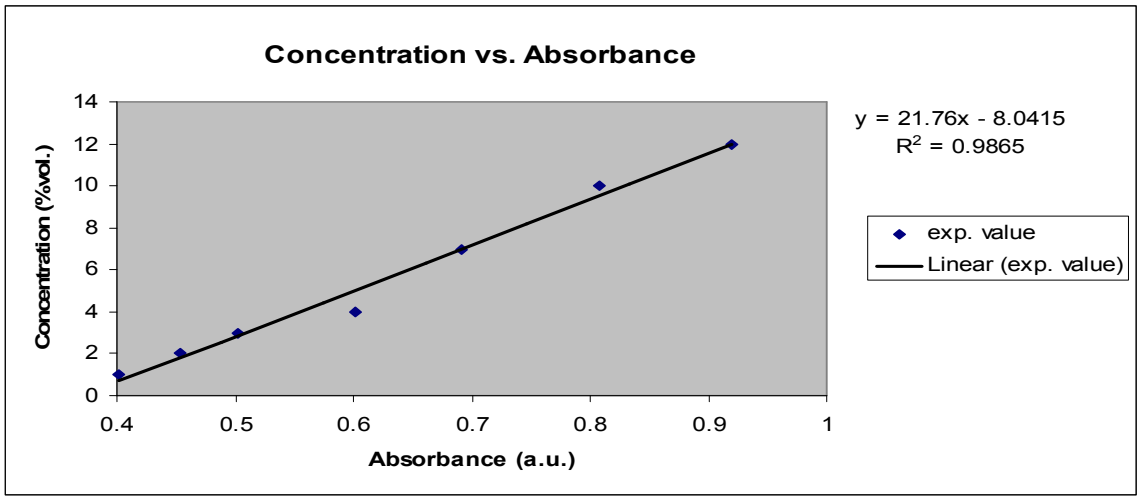

Figure 3.4 Calibration curve methanol concentrations versus absorbances

The permeability measurements were validated using a side-by-side fiber glass diffusion cell where a Nafion® sample was placed and each half-cell has a reservoir for deionized water and methanol solution respectively. The permeation of the methanol was recorded from a half-cell to another.

Using the continuity equation for diffusion in plane geometry it is possible to obtain a formula for the calculation of the methanol permeability through a membrane:

$$C_m(t) = \frac{PCA}{Vd}\left(t - \frac{d^2}{6D}\right) \qquad (22)$$

Where:

C_m: Methanol concentration below the membrane

C: Methanol concentration upper part of the membrane (constant)

A: Area of membrane surface in contact with methanol

t: time

d: membrane thickness

D: Diffusion coefficient

P: Permeability coefficient

The permeability coefficient (P) is determined from the slope of the plots methanol concentration versus time ($C_m(t)$ vs. t). Rearranging the equation 22:

$$\frac{C_m(t)Vd}{AC} = P\left(t - \frac{d^2}{6D}\right) \qquad (23)$$

Plotting the left side of the equation versus t, P can be obtained of the slope of the curve.

3.3.1 FT-IR Spectroscopy Technique

An FT-IR (Fourier Transform Infrared) is a method of obtaining infrared spectra by first collecting an interferogram of a sample signal using an interferometer, and then performing a Fourier Transform (FT) on the interferogram to obtain the spectrum. In this investigation, the FT-IR spectroscopy is used to obtain a series of spectra of the methanol concentration through the Nafion® membrane at various times. The membrane is maintained wetted with liquid methanol and the spectra are recorded to determine the methanol concentration with the time (Figure 3.5).

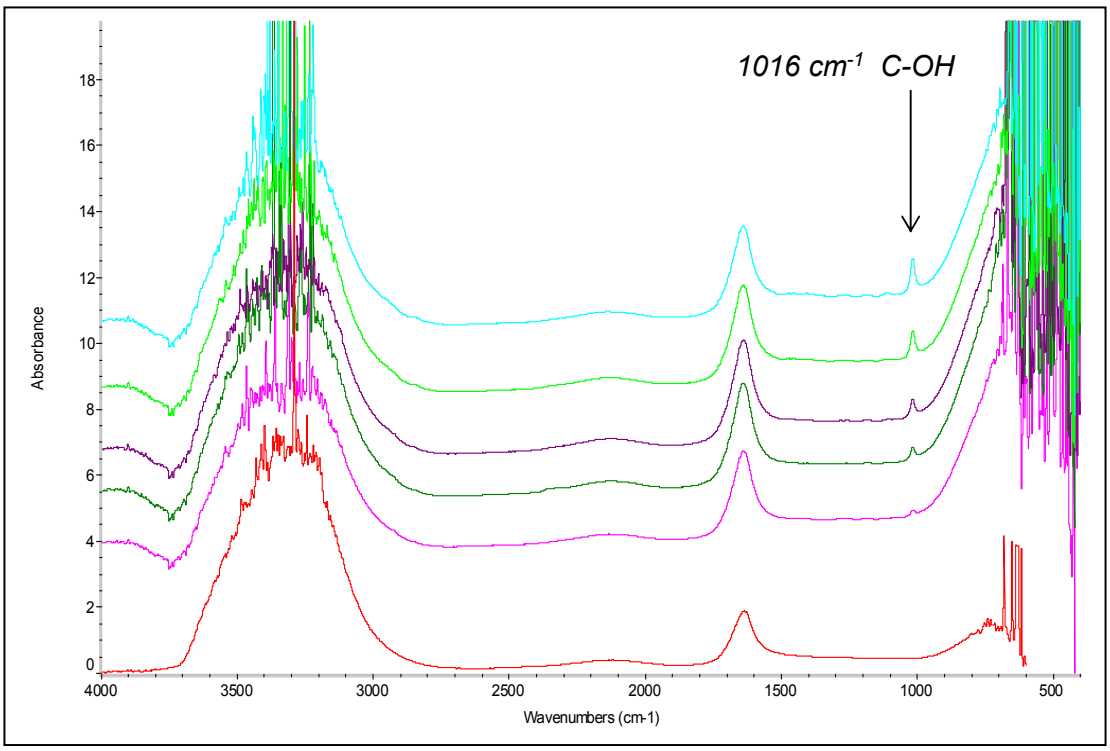

Figure 3.5 FT-IR spectra to different times

Previously, a methanol calibration curve was made to calculate the methanol concentration as a function of the absorbance. The methanol peak was identified at 1016 cm^{-1}. The methanol peak height for the spectra was determined with the software of the equipment (IR 300 Spectrometer). The methanol concentration was obtained from the calibration curve. The

results for the permeabilities of the membranes processed with different co-solvents and SCF are shown in the Figure 3.6

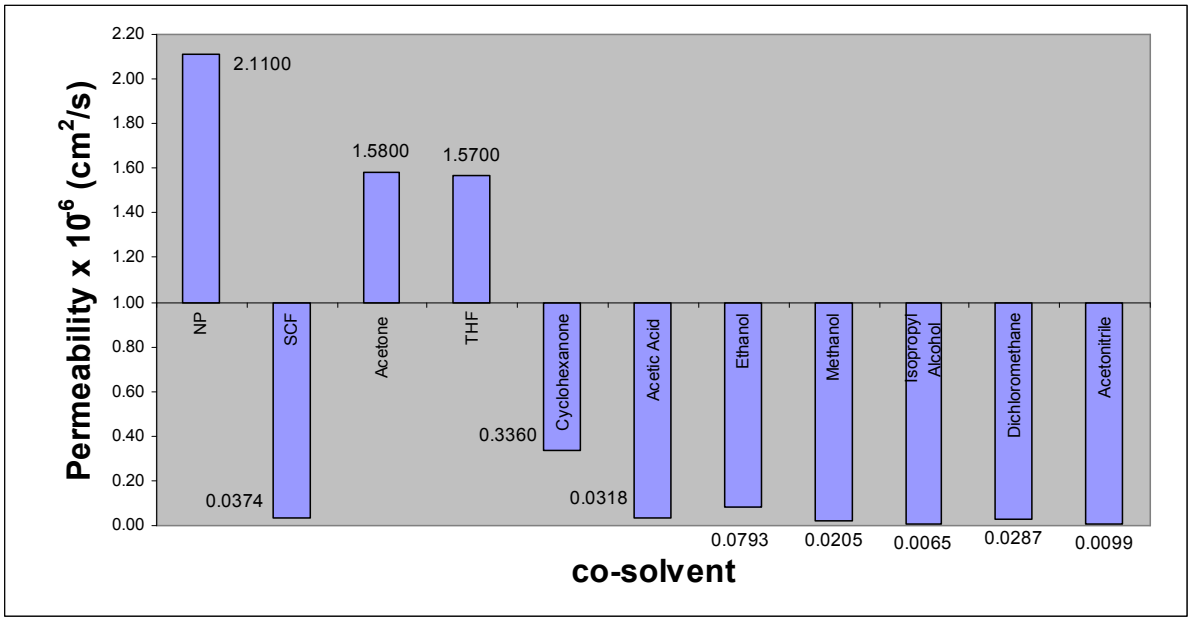

Figure 3.6 Methanol permeabilities in liquid phase of Nafion® membranes

3.4 Permeation in Vapor Phase

Measurements of the methanol vapor permeability were made using a fiber glass cell by a gravimetric technique. A schematic of the diffusion cell used for these measurements is shown in Figure 3.7. In this experiment, the membrane sample separates two chambers, which are the reservoir (methanol vapor) and diffusate. As methanol vapor permeated across the membrane, the weight of the cell was monitored and used to determine the steady-state flux and the permeability coefficient. Figure 3.8 shows the plot of the mass of methanol (*dm*) that diffused across the Nafion® membrane as a function of the time. The molar flux (*J*) was obtained by dividing the slope of this plot by the area normal to the flux. These measurements were made for the membranes treated with the different co-solvents and the SCFs. All the measurements were made at 26ºC.

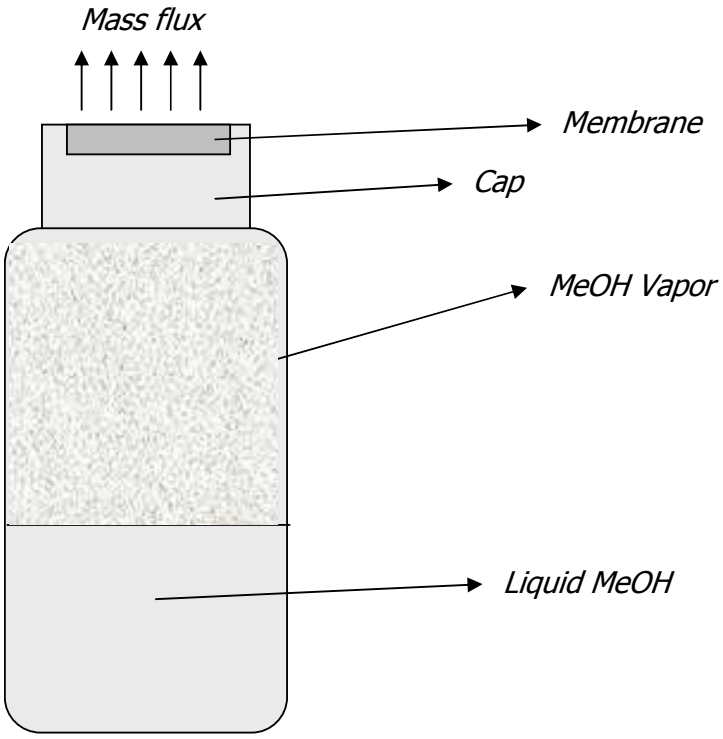

Figure 3.7 Permeation cell for vapor phase

Assuming that D is independent of the concentration and that the Henry's law is applied (both assumptions are valid at low concentrations of permeate), the permeation rate after the establishment of steady state flux can be written as:

$$\frac{LQ}{P_V - P_{EXT}} = DH\left(t - \frac{L^2}{6D}\right) \qquad (24)$$

In the expression above, Q is the mass flux, H is the Henry's constant, L is the membrane thickness and P_V and P_{EXT} are the vapor pressure and external pressure of the permeate, respectively (in the case of organic vapors, P_{EXT} is assumed to be zero) The product DH defines the permeability coefficient (P). Therefore the slope of the plots of the permeate mass versus time, at steady state conditions, provides the permeability coefficient [18].

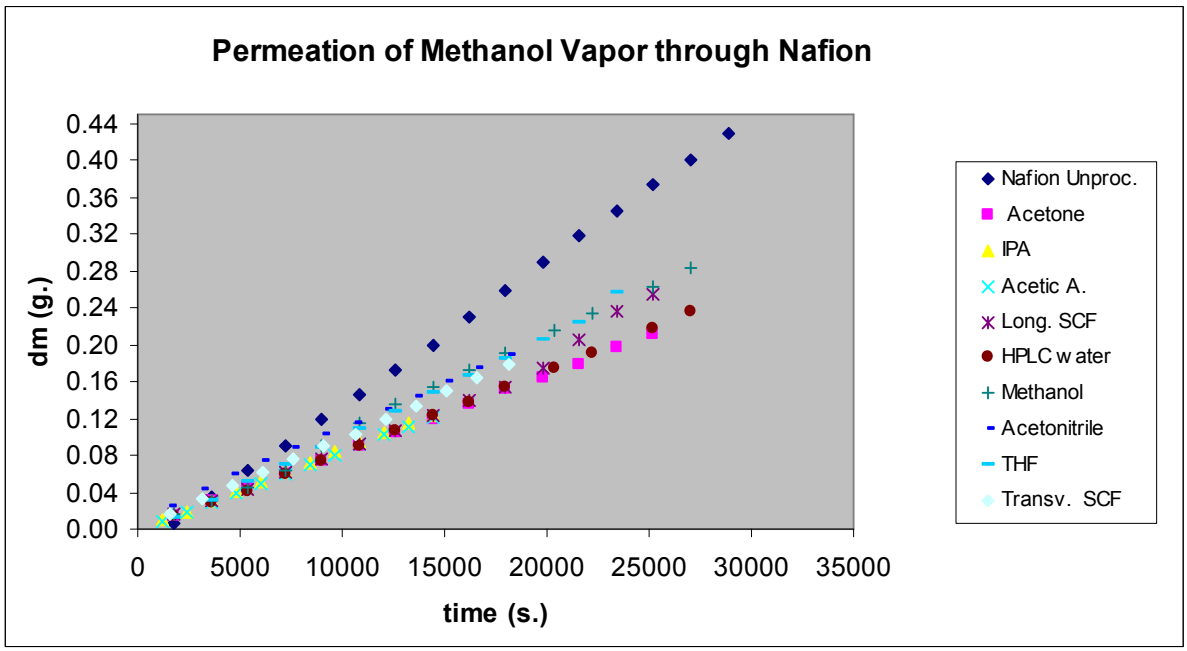

Figure 3.8 Permeation of methanol vapor through Nafion® membrane

3.5 Measurements of Proton Conductivity

The proton conductivity of the samples (Nafion® processed with SCFs and cosolvent) was measured normal to the plane by AC Electrochemical Impedance Spectroscopy (IES) using a fuel cell feed of 6 mL/min of hydrogen at 26ºC. The measurements were carried out on a potentiostat/galvanostat (PARSTAT, Model 2263). The range frequency used was from 10 mHz up to 100 kHz. The higher frequencies were used to separate membrane resistance from interfacial capacitance. It was used to collect the impedance data (Nyquist plots) the Powersuite software. All the membranes were humidified passing 250 mL deionized water through the fuel cell prior to measurement. The proton conductivity (σ) was calculated from the impedance data, using the relation:

$$\sigma = \frac{L}{R_{\Omega} A} \qquad (25)$$

where L and A are the thickness and area of the membrane, respectively. R_{Ω} was obtained from the low intersect of the high frequency semicircle (Nyquist plot) on the complex impedance plane with the Re(z) axis (real component of impedance) [19]. Figure 3.9 shows the proton conductivities obtained for the Nafion® membranes processed with the different co-solvents.

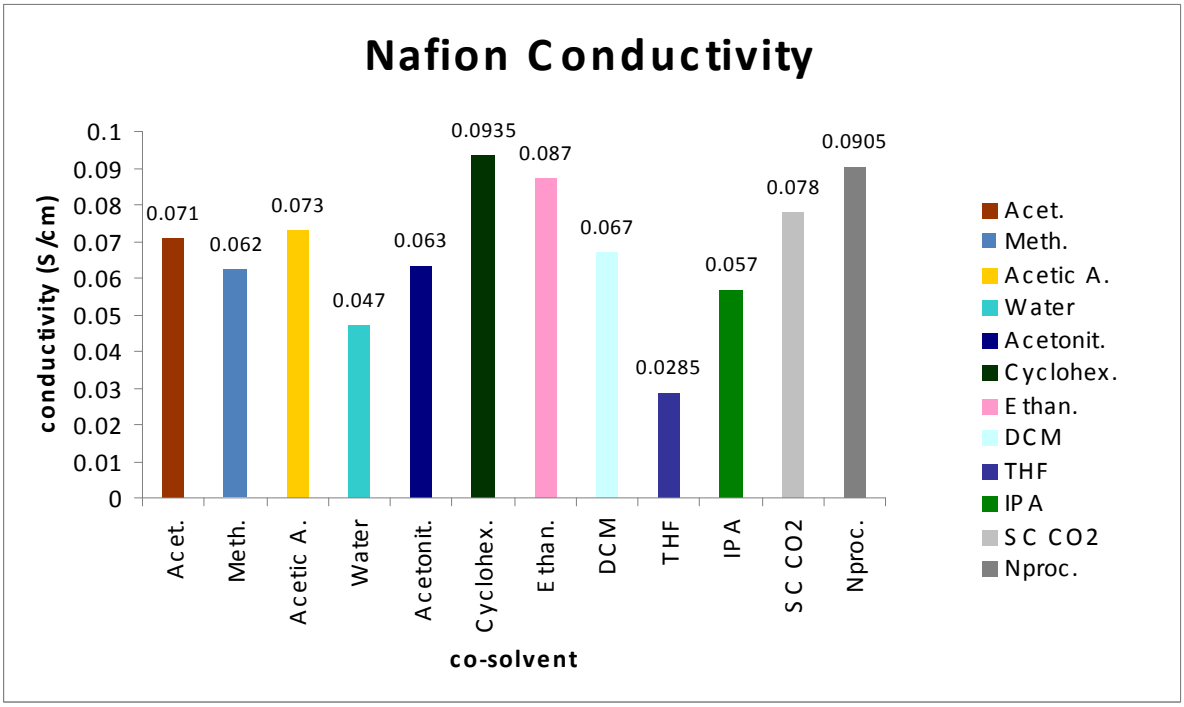

Figure 3.9 Proton conductivities of the Nafion® membrane

3.5.1 Nyquist plots

In the study of the electrochemical systems EIS provides several output formats, such as: Nyquist plots and Bode diagrams. The main advantage of the EIS is that the obtained data can be used to simulate or model the electrochemical cell using a electronic model (equivalent circuit). A technique to evaluate ac impedance data is the Nyquist Plot, which is a complex plane where the imaginary component is plotted versus the real component of the impedance as shown in Figure 3.10.

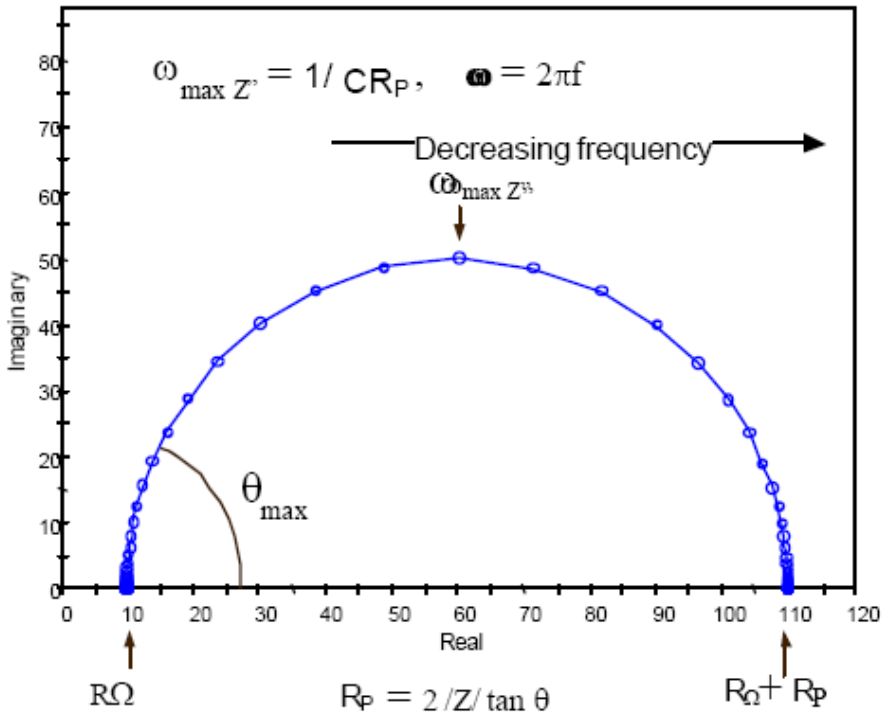

Figure 3.10 Nyquist Plot for an electrochemical system.

This plot represents the expected response of the electrochemical cell and the data can be used to calculate the ohmic resistance (R_Ω), the polarization resistance (R_p) and the double-layer capacitance (C_{dl}). In the plot of the Figure 3.10 the frequency values decrease from left to right. At high frequency values, only the ohmic resistance (R_Ω) contributes to the real

component of the impedance, while at low frequency values the polarization resistance (R_p) or charge transfer resistance (R_{ct}) also contributes to this real component of the impedance.

As shown at the Nyquist Plot in Figure 3.10, at higher frequency values (where the semicircle touches *x* axis) the imaginary component of the impedance (Z_{im}) becomes zero, in this value the impedance is given by the ohmic resistance (R_Ω) also called uncompensated resistance. At lower frequency values the Z_{im} becomes zero again and at this value the resistance is formed by the sum of R_Ω and R_p. Also at an intermediate value of frequency, the Z_{im} value reaches a maximum. This maximum is determined by the double-layer capacitance (C_{dl}) and the polarization resistance (R_p):

$$\omega_{\max} = \frac{1}{C_{dl} R_p} \qquad (26)$$

Nyquist plots of different Nafion® samples processed with co-solvents are shown in Figures 3.11 to 3.13.

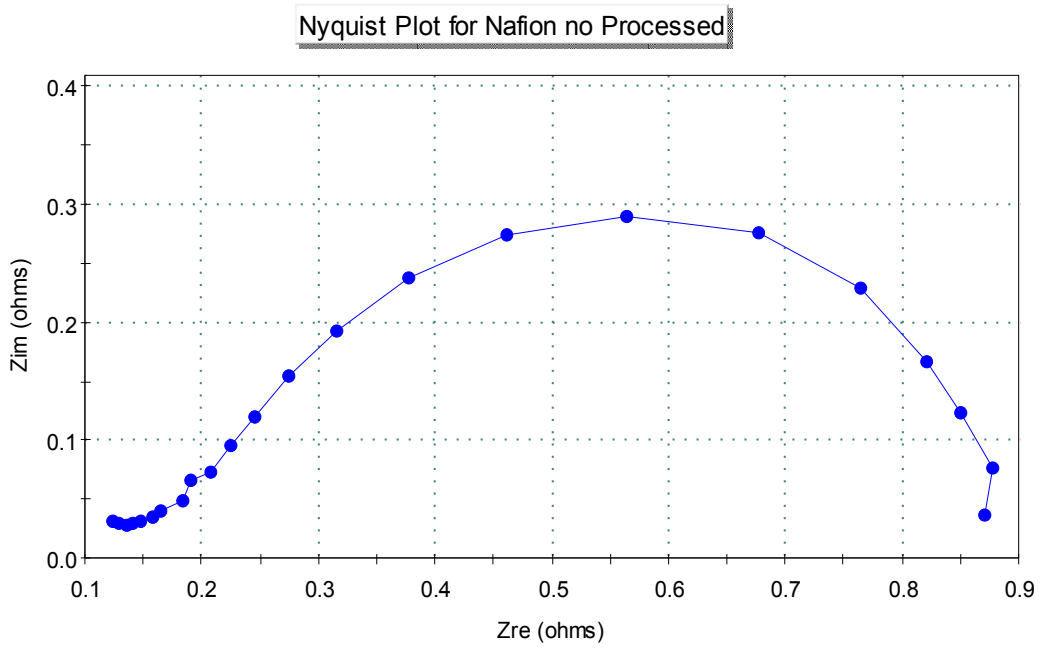

Figure 3.11 Nyquist plot for Nafion® not processed

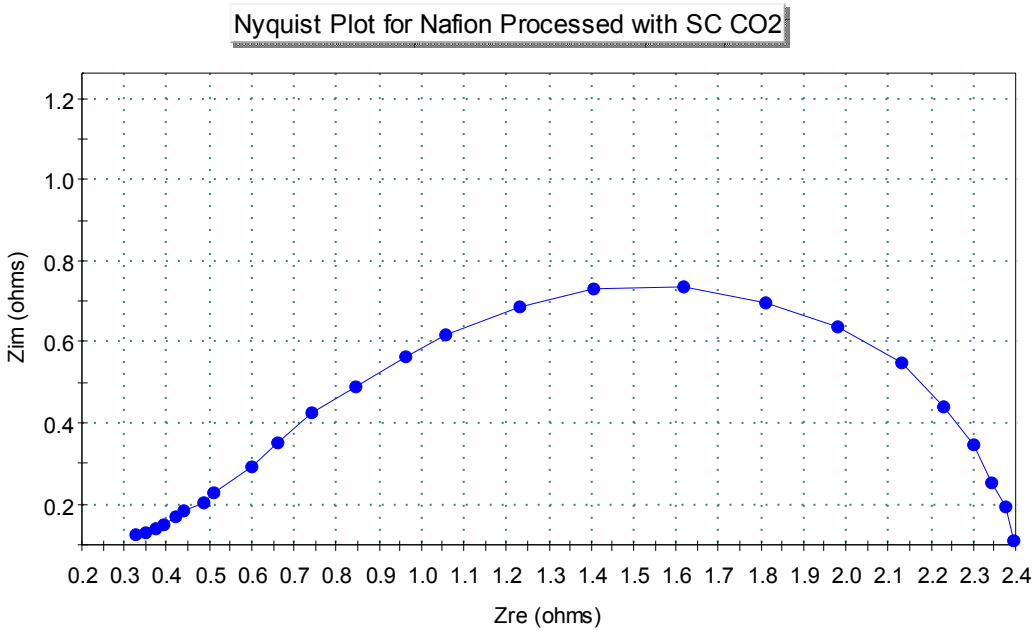

Figure 3.12 Nyquist plot for Nafion® processed with supercritical CO_2.

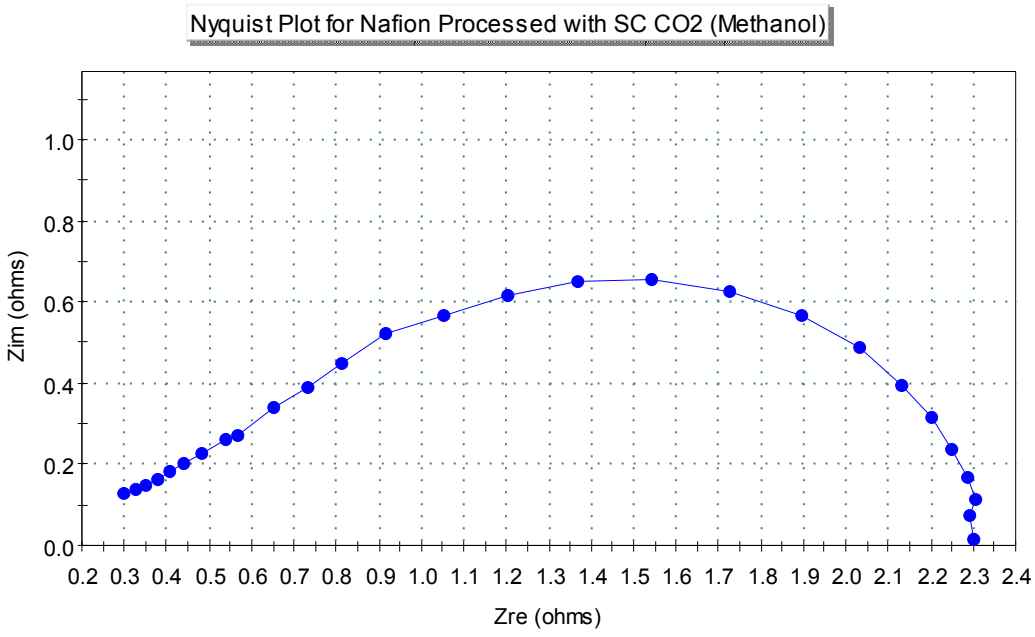

Figure 3.13 Nyquist plot for Nafion® processed with supercritical CO_2 and methanol.

3.6 Selectivity of Nafion®

In order to compare the results, Nafion® selectivities (α) were calculated and compared. The selectivity in PEMs is defined as:

$$\alpha_{p/m} = \frac{\sigma_p}{P_m} \qquad (27)$$

where α is in S. s/cm^3 [13].

S : siemens

s : second

cm : centimeter

σ_p : S/cm

P_m : cm^2/s

$\alpha_{p/m}$: S . s/cm^3

Figure 3.14 presents the selectivities for all the studied cases. Although the processing with SCF reduced the proton conductivity compared with the unprocessed membrane, the obtained results of the permeabilities increased notably the selectivity of the studied samples. There was a significant increasing of the selectivity for the samples processed with acetonitrile and alcohols (methanol and isopropanol).

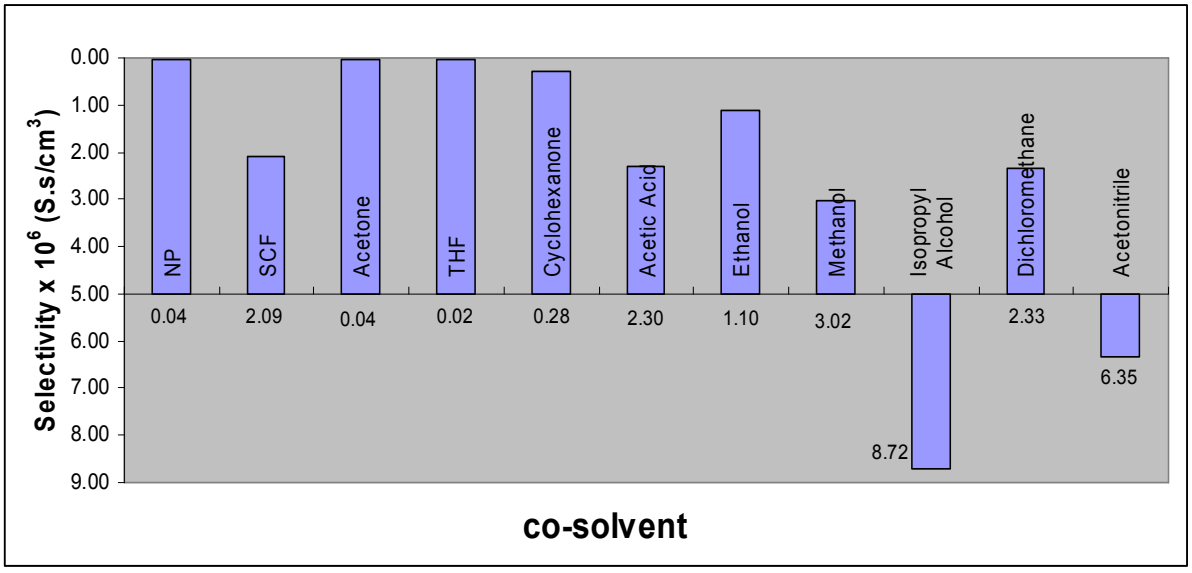

Figure 3.14 Selectivities of the Nafion® membrane

3.7 X-Ray Diffraction Analysis

X-ray diffraction (XRD) analysis was performed to all membranes processed and unprocessed using a X-Ray diffractometer (Siemens, model D500) equipped with a Cu Kα radiaction source, ßNi filter and graphite monochromator. The results of these analyses are included in Appendix I. The XRD analysis of the Nafion membrane processed with SCFs suggest a structural modification which may be due to the decreasing of the cristallinity of the membrane. The results for the samples processed with the SCFs in the direction normal to the plane and the direction parallel to the plane showed significant changes with the unprocessed sample approximately at $2q$=15º. This can be explained by the effect of the processing on the orientation of the polymeric chains in the Nafion® structure. However, an additional instrumental technique is necessary to validate this hypothesis.

3.8 Small-Angle X-Ray Scattering Analysis

Small-angle X-ray scattering (SAXS) was performed on a beamline X27C at the laboratory. Two-dimensional scattering patterns were collected on a pinhole-collimated system using Fujitsu image plates and read by a Fujitsu BAS 200 image plate reader. Specialty software available at the laboratory was used to reduce two dimensional data to one-dimensional intensity versus scattering vector (q) plots after background subtraction by circular averaging. The X-ray wavelength employed was 1.6 Å. The calibration standard was silver behenate and the sample distance to the detector was 210 cm.

SAXS experiments were conducted on the Nafion® membranes processed with SCF to determine polymer structure changes and their possible effects on the transport properties. Since transport is the main interest in this study, the structural characterization was the focus of these analyses. The results are shown in Figure 3.15. This figure shows the intensity profiles (I versus q) for each Nafion® membrane processed with the SCF and the different co-solvents. The samples were characterized in the plane of the film. The scattering vector, q, can be defined as:

$$q^{*} = \frac{4\pi \sin(\theta)}{\lambda} \qquad (28)$$

where 2θ and λ are scattering angle and wavelength, respectively. Figure 3.15 shows a periodic distribution with distinct reflections in the intensity maxima located at the scattering vector positions: 0.45 nm^{-1} and 1.8 nm^{-1} for all the samples analyzed. The maximum scattering pattern specifically corresponds to the sample treated with cyclohexanone and SCF. The processed samples presented a similar scattering pattern, while the sample not processed showed minor intensity of scattering.

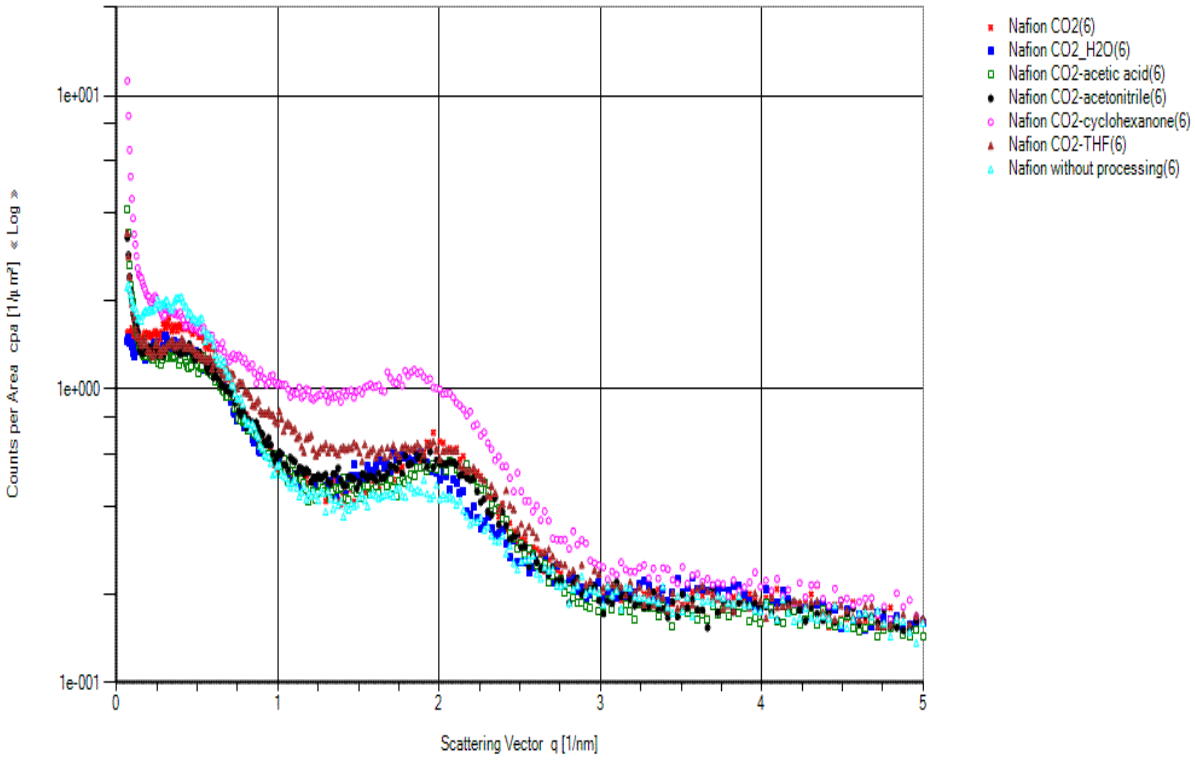

Figure 3.15 SAXS profiles for Nafion® membranes

This scattering pattern specifically corresponds to ordered morphology. The results of the samples treated suggest an anisotropic structure, where the polymer chains are highly

oriented in the plane of the membrane. The interplanar or Bragg spacing, which has been interpreted as an average domain spacing or size, can be calculated from Bragg's law:

$$d_{lam} = \frac{2\pi}{q^*} \qquad (29)$$

The Bragg spacing, d_{lam}, is determined from the maximum in the first order reflection, q^*, in Figure 3.15. In addition, a more accurate domain spacing (a_{lam}) or size, can be calculated from a regression method using all observed peaks (*i.e.* experimental interplanar spacings) using the equations:

$$a_{lam} = d_h(lam)h, \qquad h=1, 2, 3, 4, \ldots \qquad (30)$$

$$d_h(lam) = mh + b \qquad (31)$$

where h is the order of reflection and the y intercept b is ideally zero. The values calculated for d_{lam} are listed in Table 3.1 and are similar for each membrane. These values are from range 12 to 14 nm with no apparent trend in relation with the processing, except for the membrane without processing, which showed the highest value for d_{lam}.

Table 3.1 Bragg spacing for Nafion® membranes treated with SCF

Processing	**d(nm)**
Unprocessed	13.9627
SCF(CO_2)	12.8229
SCF(CO_2)+water	12.9551
SCF(CO_2)+acetic acid	12.8754
SCF(CO_2)+acetonitrile	12.6677
SCF(CO_2)+cyclohexanone	13.0628
SCF(CO_2)+tetrahydrofuran	12.7448

4 TRIBLOCK COPOLYMERS: SIBS AND SEBS

Some thermoplastic elastomers (TPEs) show unique properties capable of separating protons from methanol solutions, which can be used in applications such as fuel cells. A common type of commercial TPE is based on A-B-A triblock copolymers, where the A blocks are polysterene (PS) (minor component) and the B block is a diene-based rubber (major component). These materials are phase-separated due to the immiscibility of the component blocks; however the morphology, mechanical and transport properties of a given triblock copolymer depend on the relative amounts of each component, block molecular weights, molecular weights distribution of each block and the sample preparation [20].

The phase-separated domains are commonly in the form of spheres or cylinders of the minor component dispersed in a continuous matrix of the major component. Sulfonated block copolymers are an example of this phase-segregated, which have a potential application as proton exchange membranes (PEM) for both hydrogen and methanol fuel cells. This application can be used in the making of membranes to conduct protons across the ionic domains (sulfonic groups), while blocking the passage of hydrogen or methanol (fuel) across itself [21].

Recently, sulfonated triblock copolymers such as poly(styrene-isobutylene-styrene) (SIBS) and poly(styrene-ethylene-butylene-styrene) (SEBS) have generated interest by their unique and particular transport properties which are in relation with their morphology [3] (Figure 4.1).

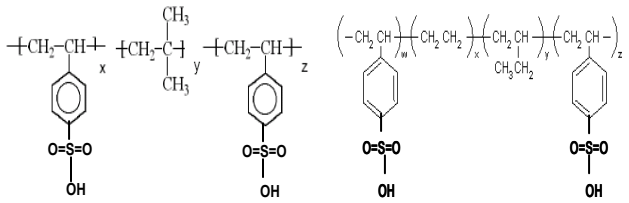

Figure 4.1 SIBS and SEBS structures

In this study, the transport properties (methanol permeability and proton conductivity) of SEBS and SIBS membranes have been investigated with infrared spectroscopy and electrochemical impedance spectroscopy. In addition to the effect of the sulfonation degree on the triblock copolymer, the porous diameter of the membranes was measured using SAXS and SANS to determine the effect on the transport properties of these membranes.

4.1 TRANSPORT THROUGH TRIBLOCK COPOLYMER MEMBRANES

The transport through the triblock copolymer depends on the internal geometry of the membrane, which in many cases has a random fractal-like structure. The major component of the triblock copolymers is polyisobutylene (PIB) 70% by weight. PIB gives flexibility to the material as well as excellent barrier properties due to it has an efficient intermolecular packing. Another component of the triblock copolymers is polystyrene (PS), which comprises up to 30% by weight of the material and forms a glassy region which imparts mechanical strength to the polymer film. The immiscibility of these two components makes up a microphase separation in which PS domains are formed in the rubbery PIB matrix. PS is the controlling phase of the final morphology, which can be in form of cylinder, spheres or lamellar depending on the sulfonation degree [22, 23].

The transport mechanism of the ions through an ion exchange membrane has been described by the Nersnt-Planck equation [13]:

$$-j_p = D_p C_p \left(\frac{\nabla C_p}{C_p} + z_p \frac{F \nabla \psi}{RT} \right) \qquad (31)$$

where:

j_p: proton flux

D_p: Diffusion coefficient C_p: Concentration

F: Faraday's constant R: Gas constant

T: Temperature ψ: Electrostatic potential

In general, the transport of ions through the membrane is controlled by the interaction between the ions and the membrane functional groups, as well as by the internal geometry of the polymer which forms the membrane.

When one block in a block copolymer contains ionic groups, this material can be called a block copolymer ionomer. In this investigation a triblock copolymer ionomer was synthesized by incorporating ionic groups (sulfonic acid) randomly along the backbone of the styrene blocks (sulfonation process).

Ionomer displays a two phase segregate behavior to nanometer scale: ion-rich and ion–poor phases. The ionic phases (ion clusters) are interconnected and allow water transport, while acting as a chemical barrier to organic toxins. The non-ionic phase is constituted of polyisobutylene and unsolfunated polystyrene groups (polymeric matrix) resulting in a lamellar-type structure of water molecules linked to the sulfonate groups [13, 23].

4.2 SULFONATION PROCESS

The sulfonation of the copolymer was made in solution using acetyl sulfate as sulfonating agent. Acetyl sulfate was obtained by reaction of acetic anhydride with sulfuric acid (also is obtained acetic acid by product). After the reaction it is required to remove the water (anhydrous conditions are necessary for the sulfonation) (Figure 4.2).

An amount of 50 g SIBS is dissolved in 500 mL. methylene chloride (10% w/v solution). This solution was mixed with the sulfonating agent and stirred at approximately 40 ºC. After 5 h, the reaction finished by slowly adding 100 mL. methanol. The polymer was precipitated with deionized water. This precipitate was washed with water and methanol, and then dried in an oven at 60 ºC for 24 h [24].

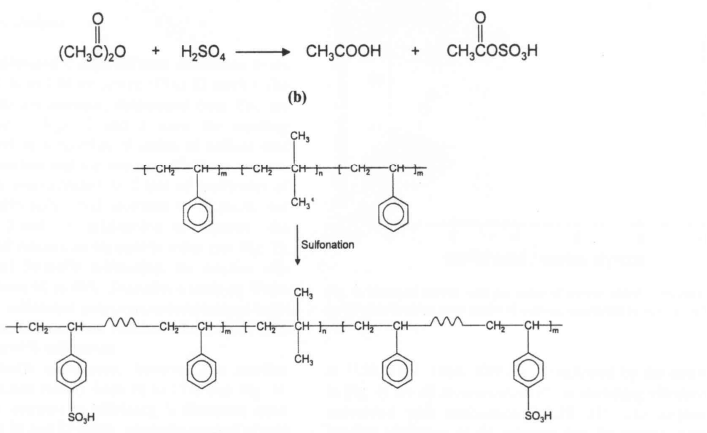

Figure 4.2 Reaction of sulfonation for triblock copolymer SIBS

4.2.1 Casting solvent

After of the sulfonation process the polymer sample obtained was dissolved in a toluene/hexanol solution (85/15 %v/v) and the mix was placed in open Teflon Petri Dishes for approximately 5 days at ambient conditions. The membranes obtained were then annealed in an oven at 60 ºC for 3 days to remove any residual solvent. The unsulfonated

polymer (S-SIBS-0) was processed in a similar way, but using pure toluene as casting solvent. The percentage sulfonation was obtained after elemental analysis (EA), which was conducted by Atlantic Microlab in Norcross, GA

4.2.2 Blends preparation

The preparation procedure of some blends can be described by following form: 120 mg SEBS and 130 mg SIBS were dissolved in a 20 mL solution of toluene/hexanol (85/15 %v/v). The mix was stirred for 48 hours and the solution cast in an open Teflon Petri dish for the membrane to thermodynamically self-assemble. The membrane obtained was annealed at 45 ºC for 48 hours.

For the blends Nafion/SIBS and Nafion/SEBS 250 mg SIBS or SEBS was dissolved in 20 mL of a solution toluene/hexanol (85/15 %v/v). After the membrane was dissolved, then 10 mL of Nafion Solution (5%) was added to the mix. The resulting solution was cast in open Teflon Petri dishes. The membrane was annealed at 45 ºC for 48 hours.

4.3 RESULTS OF PERMEABILITY IN LIQUID PHASE

The permeability was measured for the samples of triblock copolymers using the permeation cell showed in the figure 3.3. Also the permeability in gas phase was determined using a gravimetric technique and the equation 23. The concentration profiles showed a Non-Fickian behavior, which is characteristic of the permeation of a solvent through polymeric material. The following figure 4.3 shows the results obtained for the permeability in liquid phase from the different membranes.

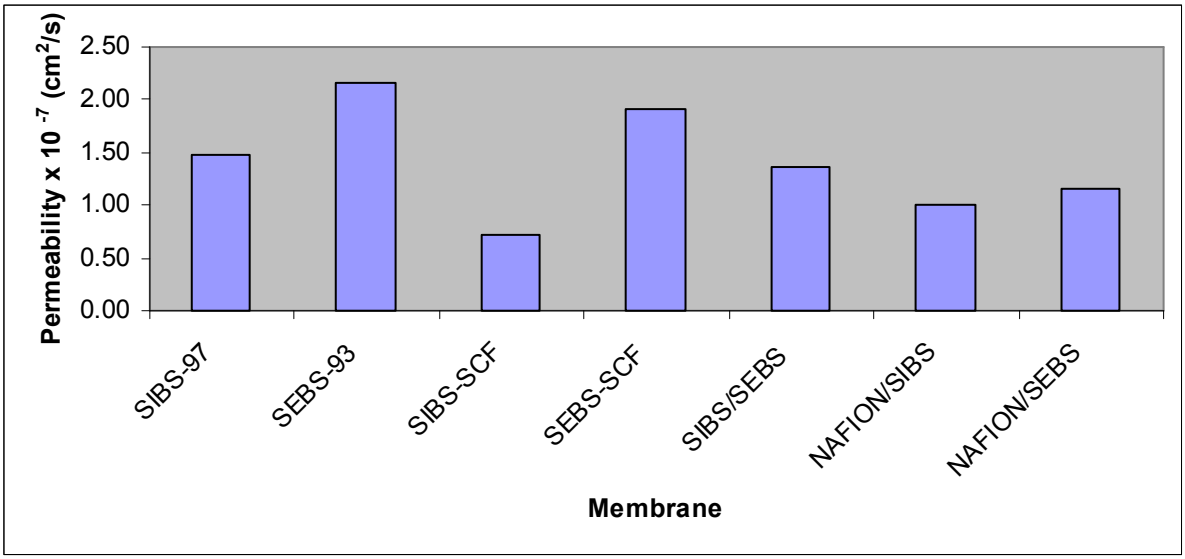

Figure 4.3 Methanol permeability in liquid phase for Blends, SIBS and SEBS membranes.

The triblock copolymer SIBS and SEBS show a lower methanol permeability compared with the Nafion commonly used in fuel cells. However, the proton conductivity of these membranes of triblock copolymer were not high as Nafion. The proton conductivity of these triblock copolymers could be increased by the addition of sulfonic groups to the structure of the triblock copolymer (increase sulfonation level). But when the sulfonation degree increased in these triblocks copolymer, an increase elevated in the swelling of the membrane was detected, which affect the mechanical properties of the membranes. Similarly, the sulfonation process of the triblock copolymer SIBS increased the permeability with the increase of sulfonation in the membrane.

SIBS-97 and SEBS-93 membranes were treated using SCF processing. The methanol permeability of SIBS-97 was reduced by 51% compared with the unprocessed SIBS-97. SCF processed SEBS had a reduced permeability of only 11% compared with unprocessed SEBS-93. The major reduction of the permeability of the SIBS on the SEBS could be attributed to morphological changes generated by the SCF on the isobutylene groups of SIBS, while than the effect of the processing on the ethylene and butylene groups was minor. These changes can be directly related with variations on the free volume of the polymer. A major effect on

the decreasing of the volume free of SIBS could be due to the reordering of the isobutylene groups form the SIBS structure, generating a decrease of the free volume in the polymer and therefore a decrease of the permeability. The effect of decreasing the free volume on the ethylene and butylenes groups seem to be less than the isobutylene. They are both smaller effects than the perfluorinated backbones of Nafion. These results can be explained in terms of the solubility in SCF CO_2.

With the goal of searching a new alternative to proton membranes, the blend synthesis was suggested. A blend of the triblocks SIBS and SEBS was synthetized, but the methanol permeability tests showed only a reduction of the 7.5% compared with SIBS. This low reduction can due to incompatibilities in the intermediate groups (isobutylene, butylene and ethylene) to the mixing the 2 triblock copolymers. Another effect that can generate a major permeability of this blend can be related to the effect of casting-solvent when the membrane is synthesized.

Other blends were synthesized using Nafion in solution mixed with the triblock copolymer SIBS and SEBS, respectively. The permeabilities of these blends are in the order of 10^{-7} similar to the above mentioned. However, on the synthesis processing of the blend using the Nafion solution mixed with the triblock copolymer, a segregation phenomena was noted. This phenomena can be due to the inmiscibility degree of the fluorocarbon matrix of the Nafion with the styrenic groups of the triblock copolymers. This inmiscibility of these groups could be the explanation of the formation of "regions" formed by fluorocarbons chains and another formed by styrenic groups. These "regions" have effect on the transport of methanol and water through them, blocking it or faciliting it. This effect can be revealed on the permeability of these membranes. A major study varying the composition of these blends could be done to determine how to reduce more the permeation to solvents like methanol and water.

4.4 RESULTS OF PROTON CONDUCTIVITY AND SELECTIVITY

Figure 4.4 shows the obtained selectivities for the SIBS and SEBS membranes processed with SCF. SIBS membrane processed with SCF had a increasing of the 23% in its selectivity compared with the sulfonated membrane. A morphological changes in the membrane structure may be the reason for the increased selectivity. The membrane processed SEBS was not affected by the SCF processing.

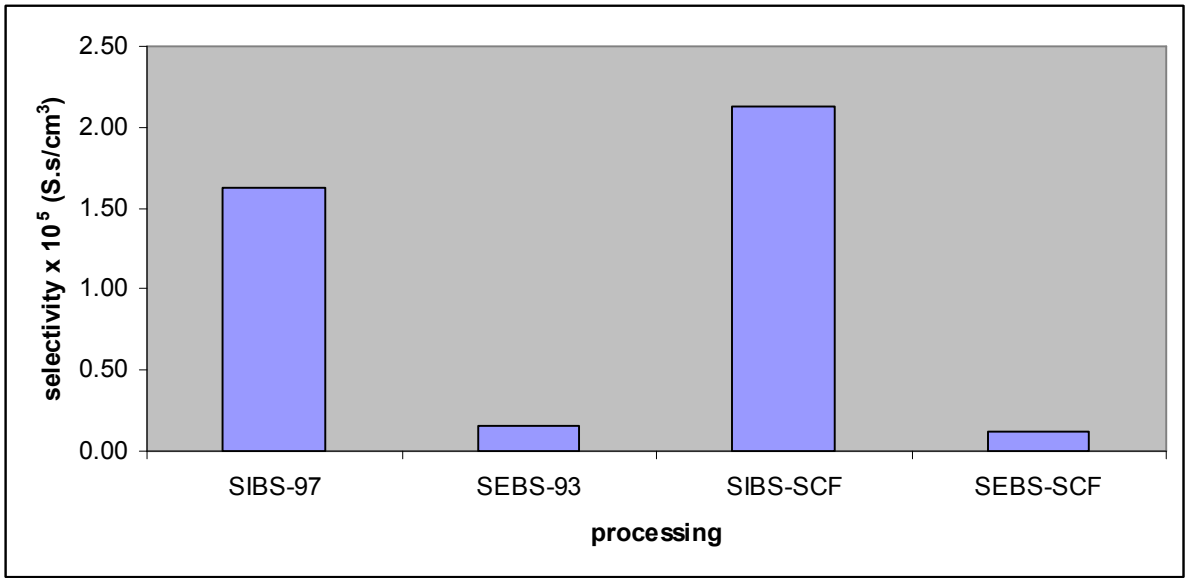

Figure 4.4 Selectivity for SIBS and SEBS membranes.

4.5 PERMEATION IN VAPOR PHASE

The permeation of methanol in vapor phase using the membranes SEBS was investigated. Figure 4.4 shows the permeation profiles obtained using a permeation cell and pure methanol in the vapor phase. Unsulfonated SEBS present the lowest permeation of methanol vapor, however it also has the lowest proton conductivity, which make inefficiency to fuel cell applications. The membranes SEBS processed with the supercritical fluid did not reduce at major grade the permeation of methanol vapor. This can be explained by the effect of the supercritical fluid on the ethylene and buthylene, which did not decrease the free volume of

the polymer enoughly to decrease the permeation of methanol vapor. While the sulfonation of the triblock SEBS had an effect to increase the permeation due to addition of the sulfonic groups. The sulfonic groups are responsible of the transport of the methanol molecules through of the membrane.

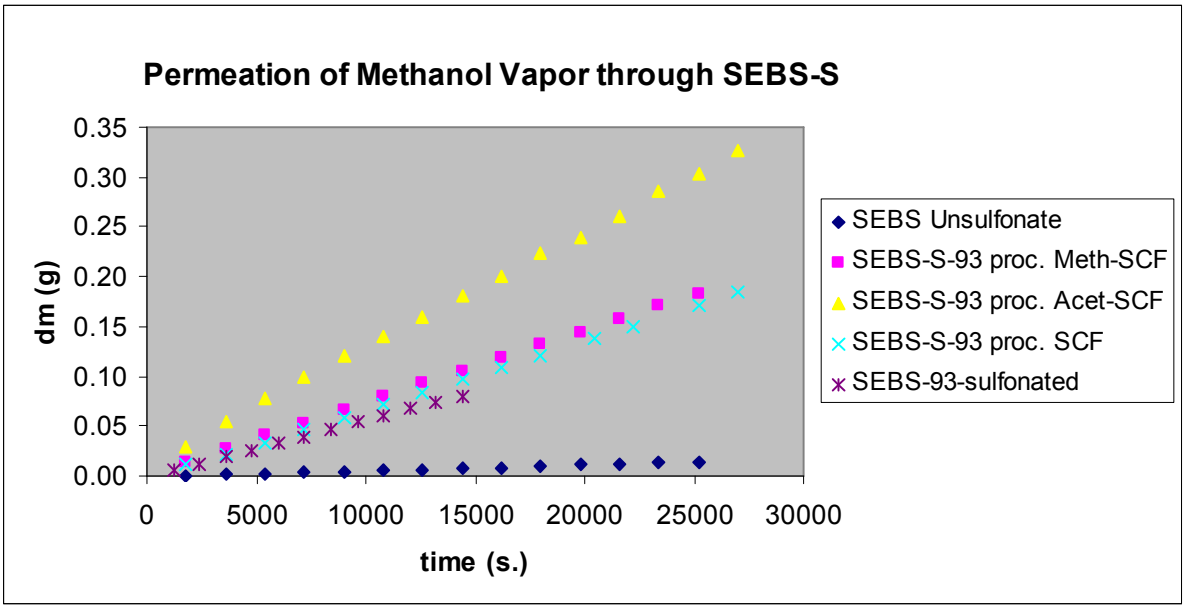

Figure 4.5 Methanol permeation in vapor phase for SEBS membranes.

5 SIBS MEMBRANES WITH METALIC CATIONS

Recently, our laboratory has focused on the synthesis (via ion exchange) and characterization of SIBS membranes with different cations for application to DMFC as a possible alternative PEM to Nafion, the most frequently used PEM in the fuel cells. These ionomer membranes are of interest because they conjoin the concepts of two different materials: block copolymers and ionomers, in which only one of the blocks is sulfonated or ionic. In theory, a sulfonated block copolymer should self assemble into a three-phase morphology in the solid state. In this state, different blocks phase segregate as result of thermodynamic incompatibilities, while phase segregation will occur within the ionic block as a result of electrostatic interactions among ion pairs [24]. These ionomer membranes are intriguing materials because of the combination of their different block (ionic and non-ionic) properties and their ordered ionic structures.

In this work, we have evaluated the effect of utilizing inorganic counter ions to neutralize the sulfonic acid groups. The goal of this process is to minimize the amount of swelling that the acid polymers exhibit. We have selected to study metallic cation-exchanged S-SIBS (Mg^{2+}, Ca^{2+}, Ba^{2+}, Zn^{+}, Fe^{3+}, Ag^{+}, Cu^{2+}, Al^{3+}) to create highly cross-linked membranes. In this research we have examined the thermal stability of these ionomer membranes, their transport properties: proton conductivity and permeability.

5.1 PROCESSING CONDITIONS

The sulfonation of poly(styrene-isobutylene-styrene) was performed previously with acetyl sulfate as the sulfonating agent, described in more detail elsewhere [24]. The mole percent of styrene sulfonated in each polymer was controlled by the amount of acetyl sulfate used in each reaction and its exact amount was determined by elemental analysis (EA). After sulfonation, the S-SIBS samples were solvent casted in a toluene/hexanol (85/15 wt%) solution in an open Teflon Petri dish for several days at ambient conditions. For S-SIBS-0,

pure toluene was used to cast the membranes. The films were then annealed under vacuum at 50 ºC for an additional 2 weeks to remove any residual solvent [22].

The cations selected for cross-linking the membranes were: Mg^{2+}, Ca^{2+}, Ba^{2+}, Zn^{2+}, Fe^{3+}, Ag^{+}, Cu^{2+} and Al^{3+}. They were selected to allow ionic interactions to occur between two individual sulfonic acid groups. The sulfonated polymers were irreversibly cross-linked by immersing them for several hours in a 1.0 M solution of the salt (magnesium perchlorate, $Mg(ClO_4)_2$; calcium chloride, $CaCl_2$ or barium chloride $BaCl_2$, magnesium chloride, Iron sulfate) depending on the desired cation. The cross-linked membranes were washed with de-ionized water and left to dry for at least 24 hours in a vacuum oven at 50 ºC.

5.2 THERMAL CHARACTERIZATION

A thermal characterization was made to all membranes with metallic cations using techniques as DSC and TGA. The DSC results did not show any appreciable change. The TGA results are showed in Appendix H.

5.2.1 Differential Scanning Calorimetry (DSC)

The samples were analyzed in a calorimeter TA Instruments DSC Q2000. Each sample (SIBS with cations) was scanned from 0°C to 120°C at scanning rate of 3°C/min under dry nitrogen purge (50 mL/min.). Sample weights were in the range of 5-8 mg and the cations analyzed were Mg^{2+}, Ba^{2+}, Ca^{2+}, Fe^{3+}, Cu^{2+}, Zn^{2+}, Ag^{+}, Al^{3+} and a sample without cation with 88% sulfonation (SIBS-88).

All samples did not show any significant change. Only a thermal variation at 75 ºC (endothermic transition) for the sulfonated membrane, which could be attributed to vaporization of some residual solvent inside the sample. For the other membranes with the cations the temperature was approximately 60 ºC. However the membrane containing the Ag

cation showed the lowest quantity of residual solvent inside it. The following are some of scanning realized to the samples.

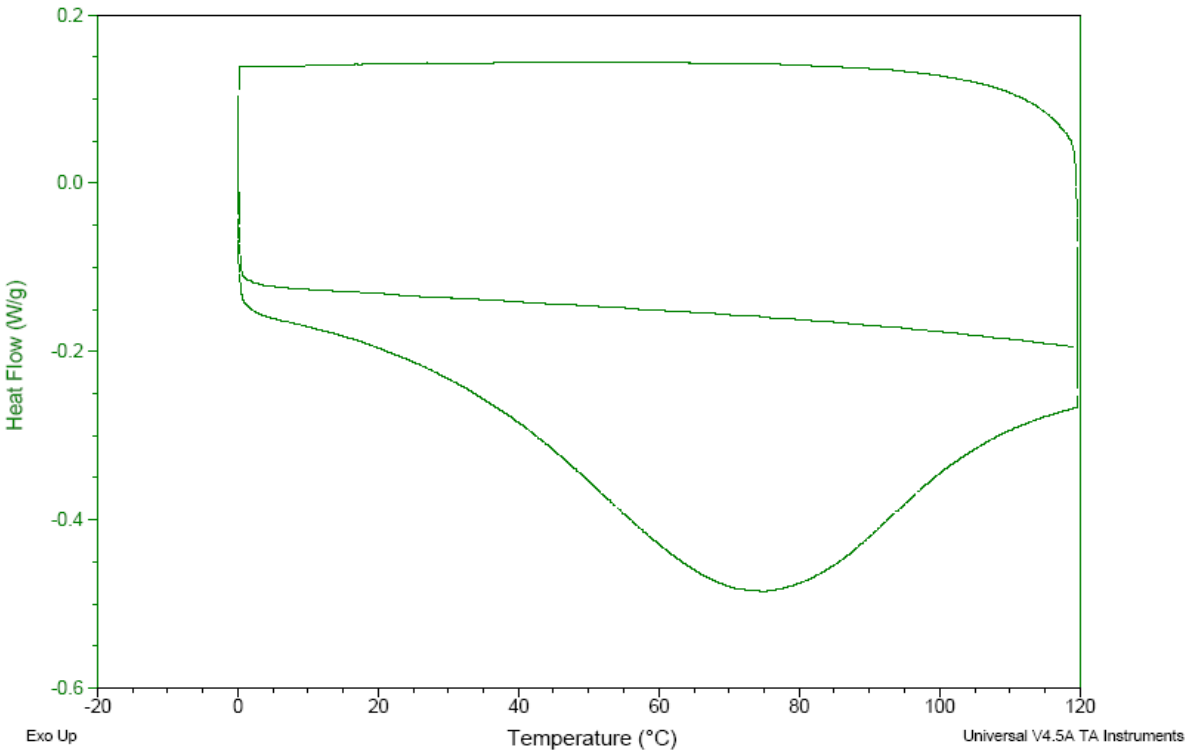

Figure 5.1 Thermogram realized to SIBS-88 membrane

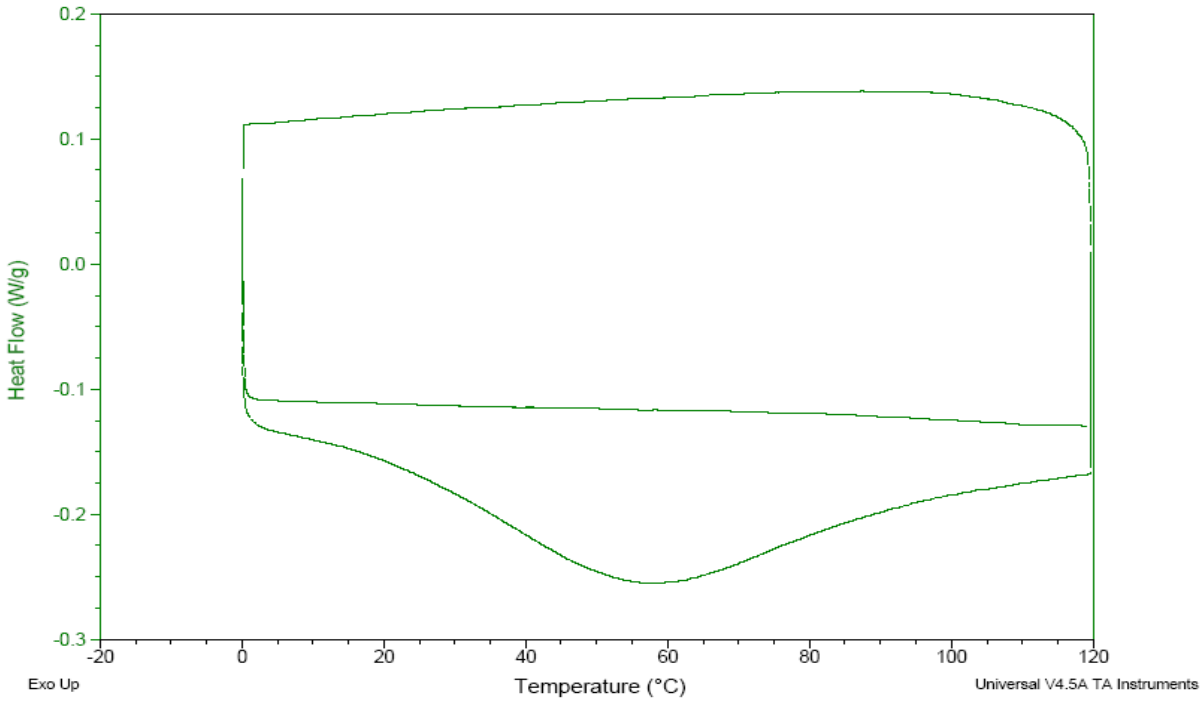

Figure 5.2 Thermogram realized to SIBS-Ba^{2+} membrane

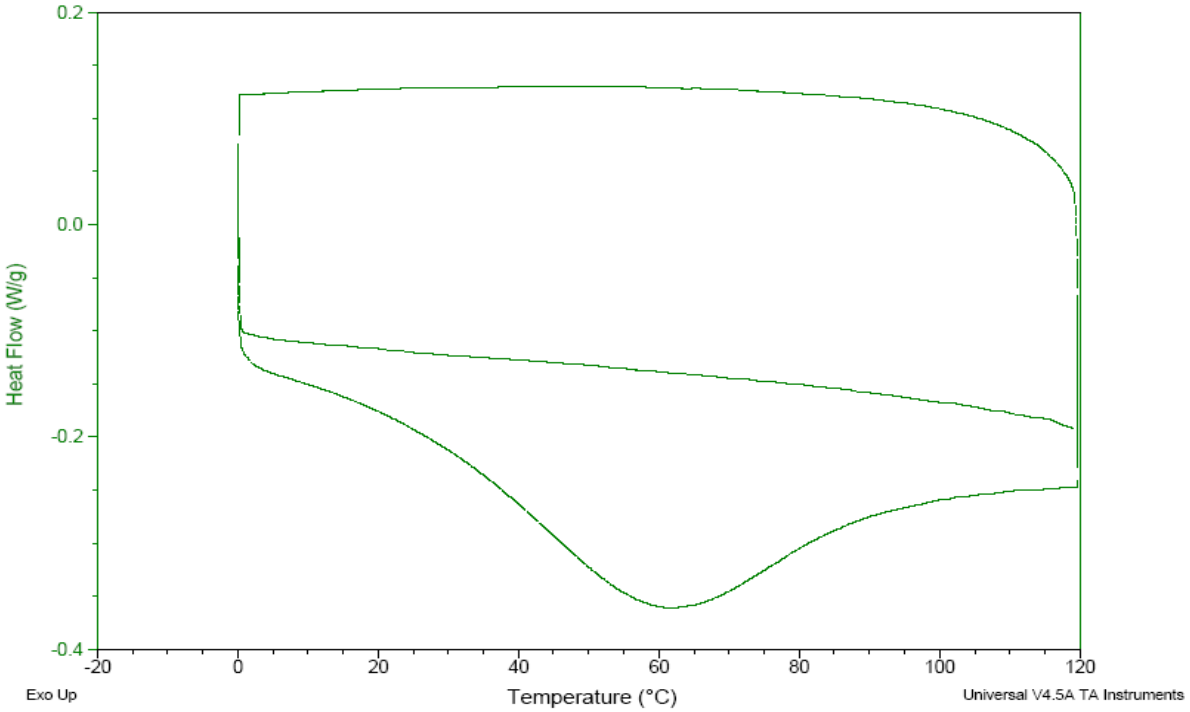

Figure 5.3 Thermogram realized to SIBS-Ca^{2+} membrane

The samples were scanned in heating and cooling cycles. Endothermic transitions were observed in the following samples: SIBS-88 at 74°C, SIBS-Ba at 58°C, SIBS-Ca at 61°C, SIBS-Cu at 60°C, SIBS-Al at 63°C, for this last membrane the energy change was ten times lower than the others. SIBS-Fe, SIBS-Ag, did not show considerable energy changes at the temperature range studied, the same behavior is observed for SIBS-Mg and SIBS-Zn. Some samples showed appreciable energy change on the heating cycle. Other thermograms for the cations are showed in the Appendix G.

5.2.2 Thermogravimetric Analysis (TGA)

The thermal history and solvent loss (sorption) of the S-SIBS block copolymers with the metallic cations were determined using a TGA 2950 Thermogravimetric Analyzer (TA Instruments). In each experiment, a polymer sample weighting approximately 5-10 mg was used. Degradation temperatures were determined by heating the polymer samples to 600 ºC at 5 ºC/min under nitrogen and observing regions of significant weight loss. The degradation temperatures for the different metallic cations are reported in the table 5.1.

Table 5.1. Degradation temperatures for SIBS membranes containing metallic cations

Cation	1st Deg. Temp. (ºC)	2nd Deg. Temp. (ºC)	3rd Deg. Temp. (ºC)	4th Deg. Temp. (ºC)
Ca^{2+}	--	±412	488	540
Ba^{2+}	--	411	479	543
Mg^{2+}	175	396	498	557
Zn^{2+}	151	399	483	524
Ag^{+}	--	355	388	--
Al^{3+}	--	370	425	490
Cu^{2+}	--	365	398	--
H^{+}	275	421	495	--

The sulfonation process of SIBS increases its degradation temperature compared with the polymer without sulfonation. This variation in temperature is related to the chemical change occurred in the polymer due to the substitution (in *para* position) of sulfonic groups in the styrene rings. It is clear that an increase in the amount of these hydrophilic sulfonic groups in the structure of the polymer generate an increase in the water sorption. In the same way the cation substitution in the sulfonic group can decrease the capacity of water sorption or some other solvent with hydrophilic affinity.

All the TGA curves for SIBS with metallic cations appear similar in shape, except the curve for SIBS in acid form (Appendix H). Four weight loss stages can be clearly identified for the forms containing cations and three stages for the acid form. The weight loss in the 25-250ºC range can be attributed to the evaporation of moisture and residual solvent of the synthesis process. The sulfonic groups have a high affinity by the water molecules, which denote a wide range of temperature to liberate the water inside the membrane. The forms with cations Ba^{2+} and Mg^{2+} showed the lowest amount of moisture, 8% and 12% respectively. The weight loss occurring in the 250-425ºC range is caused by the breakdown of the sulfonated groups linked to the styrene rings. The third weight loss region occurs at 425-490ºC, which can be due to degradation of the polystyrene and polyisobutylene segments. Using the derivative TGA in the sample of the acid form (without cation) one peak located at approximately 421ºC is showed, which is due to polystyrene block decomposition. For the samples containing cations the peak is more or less between 399 to 413ºC range. For cation Mg^{2+} the peak is at 396ºC, for Ca^{2+} at 413ºC, Ba^{2+} at 411 and Zn^{2+} at 399ºC. The forth and last weight loss region showed only at the samples containing cations occurs at 475-580ºC range. This weight loss has been observed in all the samples containing cations, except in the acid form. This weight loss can be associated to the degradation of the complex formed by the metallic cation linked to the sulfonic groups at the styrenic rings. Figure 5.4. This metal ion complex has the ability of act like cross-linking and stabilize the polymer varying the decomposition temperature.

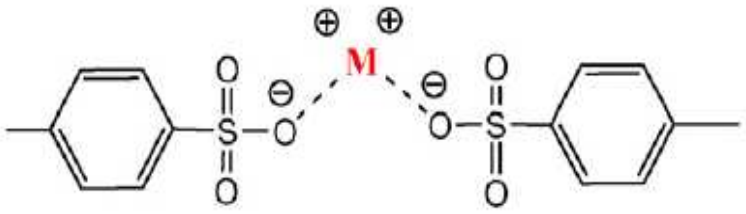

Figure 5.4 Structure of the metal ion complex in the SIBS membranes

5.3 RESULTS OF PERMEABILITY

The permeability was measured for the samples of the cation ionomers using the permeation cell showed in Figure 3.3. Also the permeability in gas phase was determined using a gravimetric technique and the equation 24. The concentration profiles in liquid phase showed a Non-Fickian behavior, which is characteristic of the permeation of a solvent through polymeric material. The following figure 5.5 shows the results obtained for the permeability in liquid phase from the different membranes containing the cations above mentioned.

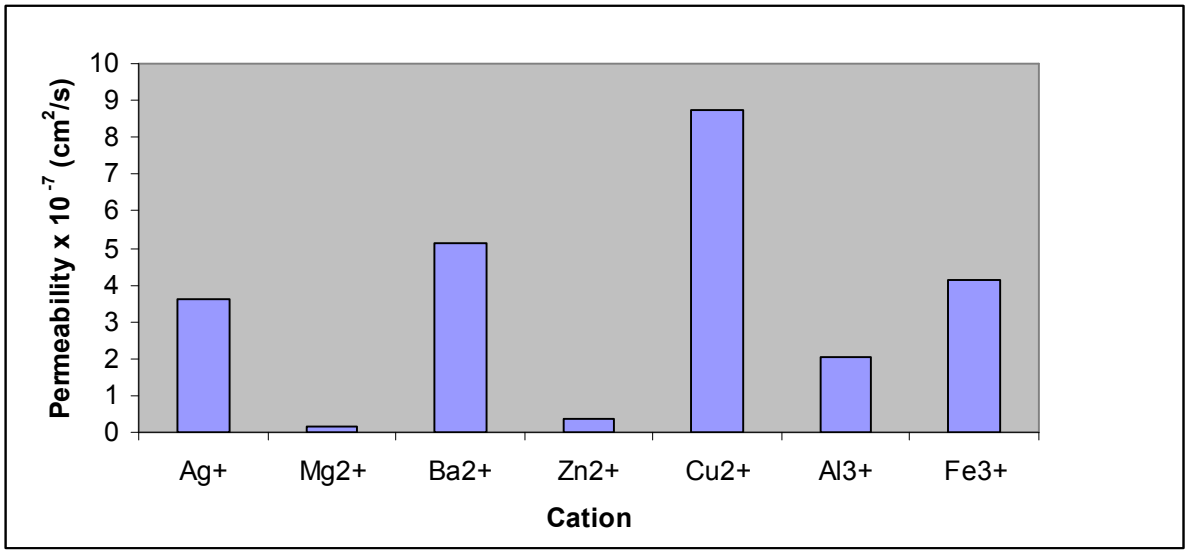

Figure 5.5 Methanol permeability in liquid phase for SIBS membrane containing cations.

The effect of the cation substitution on the permeability of the membranes SIBS showed a decreasing for those containing cations like Mg^{2+}, Zn^{2+}, Al^{3+} and Ba^{2+}. The same way this

ionic substitution is the responsible in the reduction of the solvent uptake of the membrane, which affect directly the swelling and the transport of solvents like methanol and water through the membrane. The decreasing in permeability was up to 2 orders of magnitude compared with the SIBS only sulfonated. The SIBS sulfonated has a major affinity by some cations than others. This major affinity can due to these cations are more electropositive than the others, which permit to link to the terminal sulfonic groups. The cation substituted can form a metallic complex (Figure 5.4) with 2 sulfonic groups adjacent, reducing of this way the available sites to transport solvent molecules through of the membrane. This effect can be noted in the reduction of the permeability of the SIBS samples substituted with cations compared with the membrane only sulfonated. The TGA analyses prove the presence of this metallic complex in the last weigh loss region, which is not present in the sample sulfonated. At the same way the TGA analyses evidence a major ionic density for this cations, which can suggest that it constitute a barrier to the transport of solvents through the membrane.

5.4 PERMEATION IN VAPOR PHASE

The permeation of methanol in vapor phase using the membranes SIBS functionalized with metallic cations was investigated. The figure 5.6 shows the permeation profiles obtained using a permeation cell and pure methanol in vapor phase. SIBS functionalized with cations Ba^{2+}, Ca^{2+} and Zn^{2+} presented the lowest permeation of methanol vapor. This can be explained by the effect of adding to the sulfonic groups bivalent cations to reduce the sites that transport the methanol molecules. While the sulfonation of SIBS had an effect of increase the permeation due to the addition of the sulfonic groups. The sulfonic groups are responsible of the transport of the methanol molecules through of the membrane. The formation of the metallic complex with sulfonic groups (Figure 5.4) reduced the hidrophilic sites to conduct the polar molecules as methanol. Decreasing of these sites caused a decreasing of the permeability of the methanol through of the membrane.

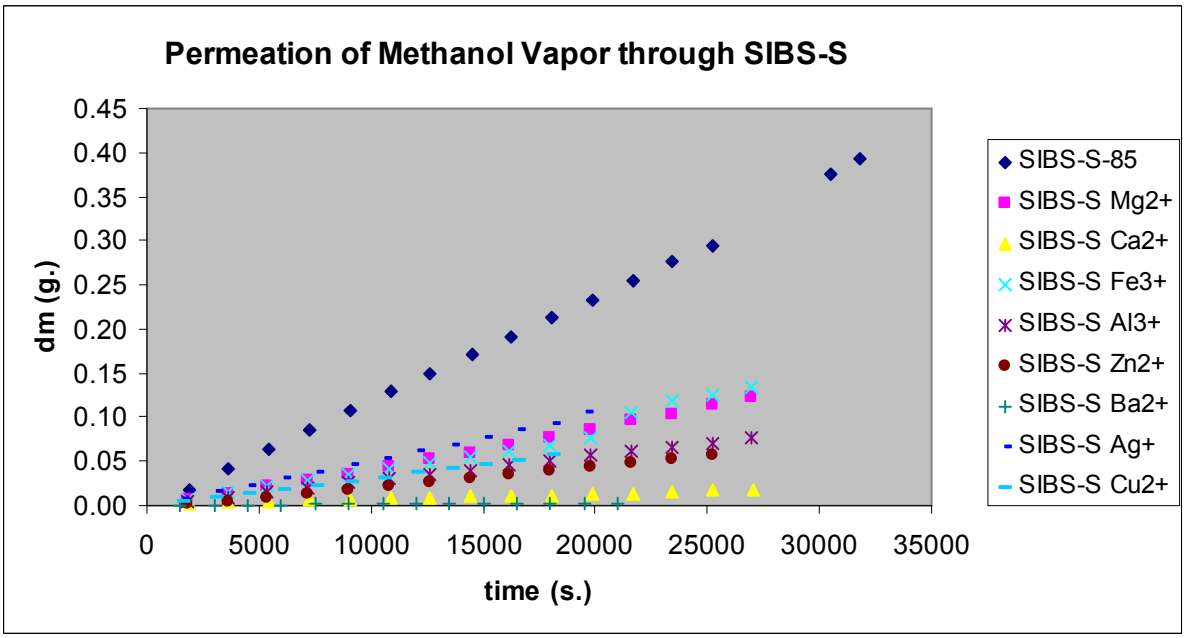

Figure 5.6 Methanol permeation in vapor phase through SIBS membranes functionalized with metal cations

5.5 RESULTS OF PROTON CONDUCTIVITY

The proton conductivity of the samples of SIBS functionalized with metallic cations was measured normal to the plane by AC Electrochemical Impedance Spectroscopy (IES) using a Fuel cell feed of 6 mL/min of hydrogen at 26ºC. The measurements were carried out on a potentiostat/galvanostat (PARSTAT, Model 2263). The range of frequency used was from 10 mHz up to 100 kHz. Higher frequencies were used to separate membrane resistance from interfacial capacitance. It was used to collect the impedance data (Nyquist plots) the Powersuite software. All the membranes were humidified passing 250 mL deionized water through the fuel cell prior to measurement. The proton conductivity (σ) was calculated from the impedance data, using the relation showed by the equation 25 of the chapter 3. The figure 5.7 shows the values of proton conductivity for the membranes SIBS functionalized with the different cations.

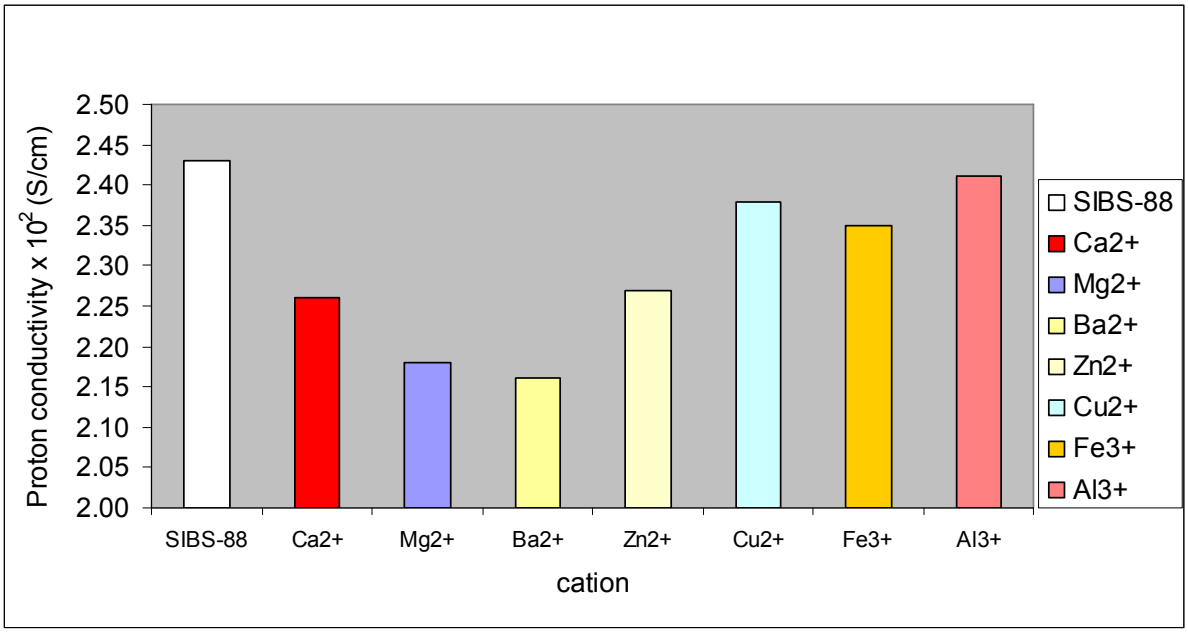

Figure 5.7 Proton conductivity for SIBS membrane containing metal cations.

The sulfonation of the triblock copolymers permits an increasing of the proton conductivity compared with the unsulfonated samples. This is explained because the transport of protons is realized through of the sulfonic groups present on the membrane. However, the cation substitution of the SIBS membranes revealed a decreasing of the proton conductivity of some SIBS samples, but others maintain this parameter more or less constant. The effect of the cation substitution can be explained like competence by the ionic sites to transport the protons through the membrane. The cation substitution and the metallic complex formation with the sulfonic groups reduced the available ionic sites to transport the cations, which it has effect direct on the proton conductivity. However, the decreasing of the permeability compensate this decreasing of conductivity, which has incidence on the selectivity of the membrane.

The major effect on the proton conductivity was generated by the cations Ba^{2+}, Mg^{2+} and Ca^{2+}, these cations have major effect due to its affinity by the sulfonic groups. XRD analyses

show a decreasing of the crystalline region of the SIBS membranes, which can evidence the diminution of the transport of protons through the membrane. The measurements were made normal to the plane of the membrane, which affect a minor degree the transport of the protons. A study of the conductivity in the plane of the membrane could be of interest to determine what effect has the orientation of the sulfonic groups on the transport of the protons.

5.6 RESULTS OF SELECTIVITY

Figure 5.8 presents the obtained selectivity for the SIBS membrane with the different cations. The membranes SIBS with cations Ca^{2+} and Mg^{2+} showed an increasing of the selectivity of the 88% compared with SIBS membrane sulfonated. This increasing can be attributed not only to the reduction in permeability else to an effect of the formation of the metallic complex of the cation with the sulfonic groups.

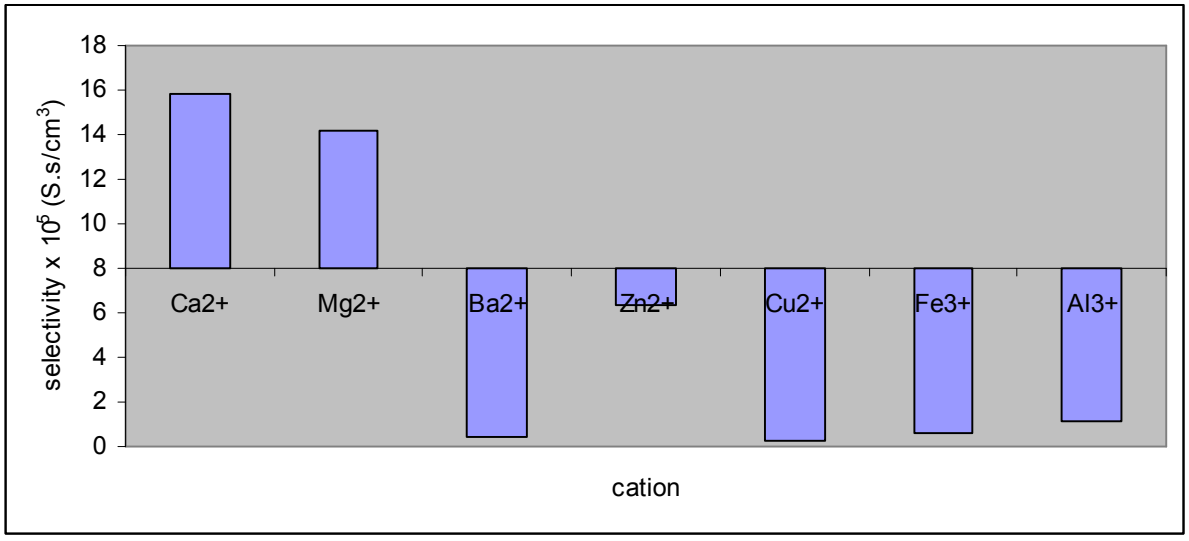

Figure 5.8 Selectivity for SIBS membrane containing metal cations.

6 CONCLUSIONS

This investigation studied the transport properties (*i.e.*, methanol permeability and proton conductivity) of proton exchange membranes after a careful functionalized and SCF processing. Transport properties results were explained in terms of the materials characterization techniques such as: DSC, TGA, XRD and SAXS.

Nafion® membranes processed with SCF CO_2 showed a significant reduction in the methanol permeability both in the liquid and vapor phase. This processing was made using a previously saturated membrane with diverse co-solvents and then flowing with SCF CO_2. The best result was obtained by the combination of supercritical carbon dioxide and acetonitrile, showing a permeability order of 10^{-9} cm^2/s (three orders of magnitude below the unprocessed Nafion®). The use of some alcohols as co-solvents and supercritical carbon dioxide decreased the permeability to 10^{-8} cm^2/s, which is very significant compared to the value of 10^{-6} for unprocessed Nafion®. These solvents used as additives in the SCF processing are highly polar, however no specific parameter (dielectric constant, solubility parameter, dipolar moment) was found to relate to this behavior. One probable explanation to this observed behavior is that aided by the high diffusivity of the SCF CO_2 the co-solvents are penetrating the membrane and re-structuring the functional groups more easily. The removal with SCF of the co-solvent absorbed by the membrane could generate morphological changes in the structure of the polymer, affecting the way the methanol and the protons are transported through the membrane.

The proton conductivities of the Nafion® membranes were affected by the SCF processing, but they maintained an acceptable range compared with the Nafion® without processing. The co-solvent that affected more significantly the proton conductivity of the Nafion® were the samples treated with methanol, water and tetrahydrofuran. The proton conductivity was

maintained constant since Nafion® is composed by hydrophobic (backbone) and hydrophilic domains constituted by the sulfonic groups, which are the responsible for the proton transfer. Theses hydrophilic sulfonic groups aggregate to form ion clusters to facilitate the transport of protons. These ionic clusters do not seem to be affected during the processing with the SCFs. While the sample processed with cyclohexanone did not show variation in the proton conductivity presenting a similar value to the Nafion® not processed.

After the SCF CO_2 processing of Nafion® membranes several material characterization techniques were performed like X-Ray diffraction (XRD) and SAXS, with the goal to determine if there were some changes in the structure or morphology of the polymer. The XRD analysis of the membranes before and after the processing allowed detect a vanishing pattern in the crystalline region caused by the SCF processing, which affected the liquid and vapor permeation through out them. This can be explained by the effect of the processing on the orientation of the polymeric chains in the Nafion® structure. At the SAXS profile the scattering curve related to the processing with cyclohexanone showed a variation over the other samples, which can be attributed to the high interfacial energy between the co-solvent molecules (cyclohexanone) and the perfluorinated matrix. Co-solvents like cyclohexanone less polar than alcohols can affect the behavior of the perfluorinated matrix of Nafion®, which would indicate the difference of Nafion® scattering profile treated with this co-solvent. The membranes processed with cyclohexanone presented a similar value of proton conductivity to the sample not processed, which seem to indicate no effect over the sulfonic groups responsible for the transport of protons.

Most of the Nafion® samples were processed in the supercritical fluid extractor in the direction *in the plane* of the membrane, while only one sample of Nafion® was processed *normal to the plane*. The sample processed normal to the plane did not show a notable change in its transport properties as the processed in the direction *in the plane*.
SAXS profiles showed two peaks, the first peak, at the lowest scattering vector, can be attributed to the ion segregation in the hydrophobic polymer matrix (perfluorinated groups)

of the Nafion® membrane. The ionic groups aggregate to form clusters and the dimension of these is controlled by the polymer chain rigidity and the distance between ionic groups along the polymer chain and the steric hindrance of the latter, creating some geometrical packing constraints. The second peak of the profiles SAXS, which are showed at higher values of the scattering vector could be related with the sulfonated groups present in the Nafion® membrane, which play an important role in the transport of the protons through the membrane. The processing with SCF minimized the interfacial energy of these, taking into account the geometrical packing constraints induced by the residual co-solvent located at the interface. A lamellar structure for the Nafion® could generate the formation complex channel structures that influence in the methanol transport.

Triblock copolymer SIBS showed a reduction of the permeability with the SCF CO_2 processing; however SEBS present a high level of swelling in the presence of solvents like water and methanol, which affect its mechanical properties. The synthesis of blends using SIBS and SEBS reduced the permeation of methanol, but blends produced using the Nafion® solution and a triblock copolymer like SIBS or SEBS did not prove to be stable since they are thermodynamically immiscible. This behavior is due to the segregation phenomena of the polymers when they are combined or mixed.

The functionalization of the triblock copolymer SIBS with metallic cations suggest the formation of a cross-link complex between the terminal sulfonic groups and the metallic cation, which derived in a minor capacity of the membrane to sorption of solvents like water or methanol. This way the permeation through the membrane was reduced using cations like Ca^{2+}, Zn^{2+} and Ba^{2+}. This cross-linking can affect the transport of protons through the membrane, which was noted by the decreasing of the membranes containing Ca^{2+}, Mg^{2+} and Ba^{2+}.

The permeation profiles were determined both vapor and liquid phase using diffusion cells. The permeation of methanol vapor through the membranes followed a behavior that fited to the pattern of Fick's First Law, meanwhile the behavior showed by the methanol permeation

in liquid phase was non-Fickian due to the complex interactions within the membrane. This difference in patterns indicates that the permeation of the vapor phase is independent on the concentration of the solvent that permeate, while in the liquid phase is strongly dependent on the concentration.

7 RECOMMENDATIONS

The experimental procedures carried out to determine both permeabilities and proton conductivities can be enhanced or optimized by the execution of some experimental changes, such as:

- Adapt an FT-IR probe to the permeation cell to measure permeability in liquid phase and execute the concentration measurements in-line.
- Carry-out the measurements of proton conductivity with a fuel cell that uses a methanol solution as the fuel (instead of H_2).
- The thermal characterization could be done at temperatures below 0ºC to determine if there are changes in the glass transition temperature of the individual polymer block of the membranes studied.
- Execute positron annihilation lifetime spectroscopy (PALS) to the membranes to study the variations experimented in the free volume of the polymer membrane after the supercritical processing.
- Determine the sorption profiles of liquid methanol at different concentration levels for the Nafion® and triblock copolymer membranes.
- Measure the effect of the feed concentration at different levels of the permeation cell.
- Determine the influence of the composition on the blends synthesis using the triblock copolymers SIBS and SEBS and the relation with the transport properties.

Other membranes can be studied in the search of new alternative to proton exchanges membranes. Investigate the use of additives such as silica oxide to increase the proton conductive of Nafion® membranes, and reduce the swelling of this membrane in the

presence of solvents such as methanol. An alternative to proton exchange membrane would be using polyurethanes membranes, modifying its structure by the addition of unique functional chains to improve the proton conductivity and reduce the permeability to the methanol.

Finally, it is recommended to study new blends with polymers such as polyvinyl alcohols and poly ether ketones, which there is evidence to be easily manageable and cheaper than Nafion. Also, to understand more about the transport mechanism of the membranes a computer simulation study could be made on the permeation phenomena of a model molecule (*i.e.,* methanol) through studied polymers using molecular dynamic (MD) simulations, which could be very useful in the determination of the diffusion coefficients, the understanding of property-structure relations and the transport properties for specialty separations.

REFERENCES

1. Sata, T., Tanimoto, M., Kawamura, K., Matsusaki, K. , *Transport Properties of Cation Exchange Membranes in the presence of Ether Compounds in Electrodialysis.* Journal of Colloidal interface science, 1999. **219**: p. 310-319.
2. Sproule, T., Lee, A. J., Li, H., Lannuti, J., Tomasko, D., *Bioactive Polymer Surfaces Via Supercritical Fluids.* Journal of Supercritical Fluids, 2004. **28**: p. 241-248.
3. Suleiman, D., et al., *Thermogravimetric characterization of highly sulfonated poly(styrene-isobutylene-styrene) block copolymers: Effects of sulfonation and counter-ion substitution.* Thermochimica Acta, 2007. **460**(1-2): p. 35-40.
4. Okada, T., et al., *Ion and water transport characteristics of Nafion membranes as electrolytes.* Electrochimica Acta, 1998. **43**(24): p. 3741-3747.
5. Ramirez, C., *Supercritical Fluid Processing of Sulfonated Styrenic Tri-Block Copolymers*, in *Chemical Engineering*. 2005, Puerto Rico: Mayaguez.
6. Ocasio, M., *Supercritical Fluid Processing of Perfluorinated and Sulfonated Membranes*, in *Chemical Engineering*. 2004, Puerto Rico: Mayaguez.
7. Marrero, A., *Perfluorinated and Sulfonated Proton Exchange Membranes: Effect of Supercritical Fluid Processing on Ion Exchange Capacity and Proton Conductivity*, in *Chemical Engineering Thesis*. 2005, Puerto Rico: Mayaguez.
8. Kazarian, S., *Polymers and Supercritical Fluids: Opportunities for Vibrational Spectroscopy.* Macromolecules Symp., 2002. **184**: p. 215-228.
9. Kojima, M., Tosaka, M., Funami, E., Nitta, K., Ohshima, M., Kohjiya, E. , *Phase Behavior of Crosslinked Polyisoprene Rubber and Supercritical Carbon Dioxide.* J. Supercrit. Fluids, 2005: p. 1-7.
10. Crank, J., *The Mathematics of Difussion*. 1975, Oxford: Oxford University Press.
11. Wilhelm, F., Punt, I., van der vegt, N., Strathmann, H., Wessling, M., *Cation permeable membranes from blends of sulfonated poly(ether ether ketone) and poly(ether sulfone).* Journal of Membrane Science, 2002. **199**: p. 167-176.
12. Arimura, T., Ostrovskii, D., Okada, T., Xie, G. , *The effect of additives on the ionic conductivity performances of perfluoroalkyl sulfonated ionomer membranes* Solid State Ionics, 1999. **118**: p. 1-10.
13. Elabd, Y.A., et al., *Triblock copolymer ionomer membranes: Part I. Methanol and proton transport.* Journal of Membrane Science, 2003. **217**(1-2): p. 227-242.
14. Sing Dhingra, S., *Mixed Gas Transport Study through Polymeric Membranes a Novel Technique*, in *Chemical Engineering*. 1997, Virginia Polytechnic Institute and State University.
15. H. S. Sodaye, P.K.P., A. Goswami, S. B. Manohar, *Measurement of Free-Volume Hole Size Distribution in Nafion-117 Using Positron Annihilation Spectroscopy.* Journal of Polymer Science, 1998. **36**: p. 983-989.
16. C. Nagel, E.S., K. Gunther-Schade, D. Hofmann, D. Fritsch, T. Strunskus and F. Faupel, *Free volume distributions in glassy polymers membranes: comparison*

between molecular modeling and experiments. Macromolecules, 2000. **33**: p. 2242-2248.

17. J. Y. Park, D.R.P., *Correlation and prediction of gas permeability in glassy polymer membrane materials via a modified free volume based group contribution method.* Journal of Membrane Science, 1997. **125**: p. 23-29.
18. Gasa, J.V., et al., *Proton-exchange membranes composed of slightly sulfonated poly(ether ketone ketone) and highly sulfonated crosslinked polystyrene particles.* Journal of Membrane Science, 2006. **269**(1-2): p. 177-186.
19. Luis H. Poley, M.G.d.S., Helion Vargas. Laboratorio de Ciencias Fisica, UENF and R.S.L.d.M.A. Marcelo O. Siqueira, UENF, *Water and Vapor Permeability at Different Temperatures of Poly(3-Hydroxybutyrate) Dense Membranes.* Polimeros: Ciencia e Tecnologia, 2005. **15**(1): p. 22-26.
20. Li, C., et al., *Casting Nafion-sulfonated organosilica nano-composite membranes used in direct methanol fuel cells.* Journal of Membrane Science, 2006. **272**(1-2): p. 50-57.
21. R. F. Storey, D.W.B., *Poly(styrene-b-isobutylene-b-styrene) block copolymers produced by living cationic polymerization. Part III. Dynamic mechanical and tensile properties of block copolymers and ionomers therefrom.* Polymer, 2001. **42**: p. 2321-2330.
22. R. F. Storey, D.W.B.I., *Poly(styrene-b-isobutylene-b-styrene) block copolymers and ionomers therefrom: morphology as determined by small-angle X-ray scattering and transmission electron microscopy.* Polymer, 2000. **41**: p. 3205-3211.
23. Suleiman, D., et al., *Thermogravimetric characterization of sulfonated poly(styrene-isobutylene-styrene) block copolymers: Effects of processing conditions.* Thermochimica Acta, 2005. **430**(1-2): p. 149-154.
24. Elabd, Y.A., C.W. Walker, and F.L. Beyer, *Triblock copolymer ionomer membranes: Part II. Structure characterization and its effects on transport properties and direct methanol fuel cell performance.* Journal of Membrane Science, 2004. **231**(1-2): p. 181-188.
25. Elabd, Y.A. and E. Napadensky, *Sulfonation and characterization of poly(styrene-isobutylene-styrene) triblock copolymers at high ion-exchange capacities.* Polymer, 2004. **45**(9): p. 3037-3043.

APPENDIX A

METHANOL CONCENTRATION PROFILES IN LIQUID PHASE THROUGH NAFION MEMBRANES

Table A.1 Concentration data for Nafion membrane without processing

Run	Peak Height (a.u.)	Conc. (%v/v)	Time (s.)
1	0.5620	4.1876	2549
2	0.6390	5.8631	4352
3	0.6772	6.6944	6154
4	0.7259	7.7541	7933
5	0.7526	8.3351	9666
6	0.7694	8.7006	11487
7	0.7858	9.0575	13304
8	0.7935	9.2251	15130
9	0.8013	9.3948	16936
10	0.8071	9.5210	18739
11	0.8074	9.5275	20581
12	0.7962	9.2838	22279
13	0.8005	9.3774	24052
14	0.8026	9.4231	25949
15	0.8039	9.4514	27878

Table A.2 Concentration data for Nafion membrane processed with SCF

Run	Peak Height (a.u.)	Conc. (%v/v)	Time (s.)
1	0.4684	2.1509	1897
2	0.5351	3.6023	3605
3	0.6045	5.1124	5403
4	0.6456	6.0068	7376
5	0.6822	6.8032	9080
6	0.6988	7.1644	10912
7	0.7488	8.2524	12710
8	0.7657	8.6201	14508
9	0.7755	8.8334	16309
10	0.7826	8.9879	18085
11	0.7850	9.0401	19716
12	0.7867	9.0771	21570

Table A.3 Concentration data for Nafion membrane processed with SCF and THF

Run	Peak Height (a.u.)	Conc. (%v/v)	Time (s.)
1	0.4291	1.2957	1373
2	0.5013	2.8668	2558
3	0.5486	3.8960	3756
4	0.5973	4.9557	4886
5	0.6326	5.7239	6164
6	0.6591	6.3005	7412
7	0.6976	7.1383	10038
8	0.6933	7.0447	11275
9	0.7118	7.4473	13422
10	0.7158	7.5343	15303
11	0.7170	7.5604	17033
12	0.7186	7.5952	18679

Table A.4 Concentration data for Nafion membrane processed with SCF and Acetone

Run	Peak Height (a.u.)	Conc. %vol.	Time (sec.)
1	0.4823	2.4533	1961
2	0.5546	4.0266	3097
3	0.6078	5.1842	4226
4	0.6565	6.2439	5505
5	0.6612	6.3462	6738
6	0.7055	7.3102	7965
7	0.7339	7.9282	9315
8	0.7113	7.4364	10400
9	0.7145	7.5060	11624
10	0.7636	8.5744	13355
11	0.7684	8.6789	15165
12	0.7789	8.9074	16954

Table A.5 Concentration data for Nafion membrane processed with SCF and Acetic Acid

Run	Peak Height (a.u.)	Conc. (%v/v)	Time (s.)
1	0.4054	0.7800	715
2	0.4598	1.9637	1305
3	0.5197	3.2672	2135
4	0.5889	4.7730	3401
5	0.6460	6.0155	4697
6	0.6679	6.4920	5741
7	0.6909	6.9925	6897
8	0.6999	7.1883	8302
9	0.7113	7.4364	9434
10	0.7279	7.7976	11252
11	0.7316	7.8781	12998
12	0.7304	7.8520	14694

Table A.6 Concentration data for Nafion membrane processed with SCF and HPLC Water

Run	Peak Height (a.u.)	Conc. (%v/v)	Time (s.)
1	0.4667	2.1139	1247
2	0.5383	3.6719	2523
3	0.5877	4.7469	3683
4	0.6251	5.5607	4881
5	0.6568	6.2505	6082
6	0.6747	6.6400	7575
7	0.6968	7.1209	9093
8	0.7082	7.3689	10587
9	0.7204	7.6344	11972
10	0.7130	7.4734	13633
11	0.7274	7.7867	15108
12	0.7220	7.6692	16600

Table A.7 Concentration data for Nafion membrane processed with SCF and Isopropyl Alcohol (IPA)

Run	Peak Height (a.u.)	Conc. (%v/v)	Time (s.)
1	0.4895	2.6100	1747
2	0.5551	4.0375	3030
3	0.5996	5.0058	4130
4	0.6304	5.6760	5388
5	0.6509	6.1221	6583
6	0.6684	6.5029	7819
7	0.6800	6.7553	8927
8	0.6874	6.9163	10078
9	0.6887	6.9446	11488
10	0.6918	7.0121	12654
11	0.7005	7.2014	13834
12	0.7016	7.2253	15024

Table A.8 Concentration data for Nafion membrane processed with SCF and acetonitrile

Run	Peak Height (a.u.)	Conc. (%v/v)	Time (s.)
1	0.1750	3.9571	1861
2	0.1787	4.0408	3751
3	0.1804	4.0793	5430
4	0.1819	4.1132	7323
5	0.1829	4.1358	9086
6	0.1855	4.1946	10868
7	0.1882	4.2557	12716
8	0.1918	4.3372	14443
9	0.2004	4.5318	16371
10	0.2026	4.5815	18221
11	0.2118	4.7897	20131
12	0.2133	4.8236	21658
13	0.2139	4.8372	23513
14	0.2152	4.8666	25214

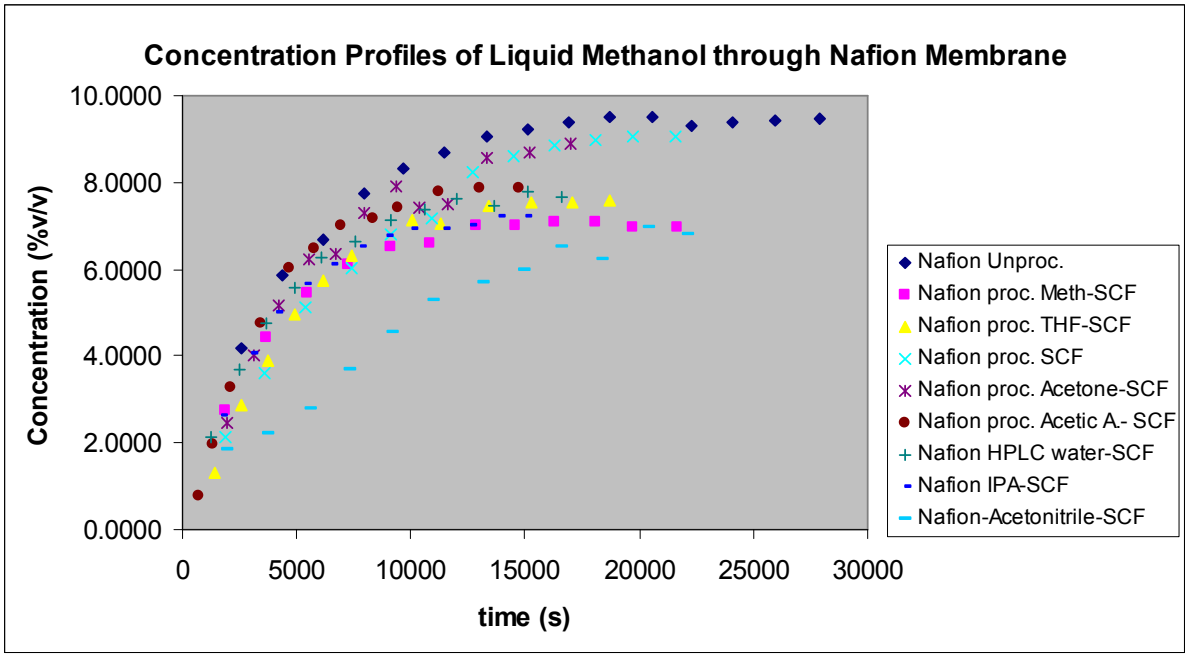

Figure A.1 Methanol Concentration Profiles through Nafion membranes

APPENDIX B

METHANOL CONCENTRATION PROFILES IN LIQUID PHASE THROUGH SIBS AND SEBS MEMBRANES

Table B.1 Concentration data of methanol permeation through SIBS-85 membrane

Run	Peak Height (a.u.)	Conc. (%v/v)	Time (s.)
1	0.5852	4.69	734
2	0.6368	5.82	1305
3	0.6567	6.25	1945
4	0.6881	6.93	2506
5	0.6933	7.04	3403
6	0.6958	7.10	4612
7	0.6989	7.17	5810
8	0.7026	7.25	6987
9	0.6976	7.14	8187
10	0.696	7.10	9386
11	0.6966	7.12	10598
12	0.6982	7.15	11790
13	0.6971	7.13	12984
14	0.6917	7.16	14192

Table B.2 Concentration data of methanol permeation through SIBS-85 membrane treated with SCF

Run	Peak Height (a.u.)	Conc. (%v/v)	Time (s.)
1	0.5741	4.45	732
2	0.6136	5.31	1310
3	0.6366	5.81	1945
4	0.6549	6.21	2510
5	0.6696	6.53	3405
6	0.6752	6.65	4615
7	0.6779	6.71	5812
8	0.6807	6.77	6990
9	0.6793	6.74	8188
10	0.6825	6.81	9386
11	0.6821	6.80	10600
12	0.6811	6.78	11790
13	0.6830	6.82	12985
14	0.6816	6.79	14192

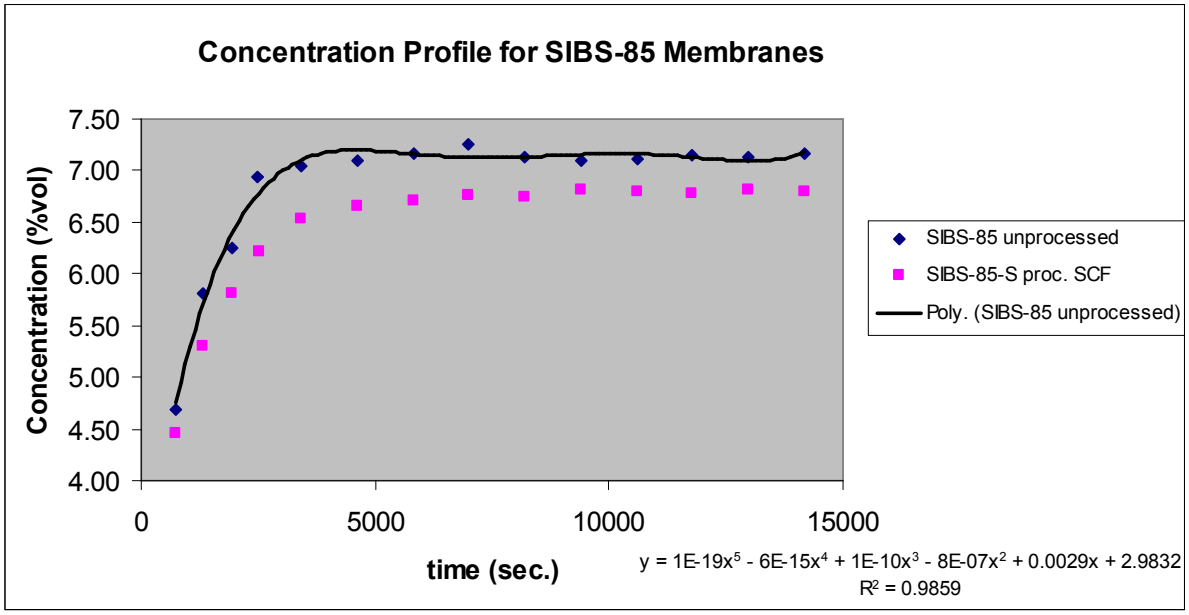

Figure B.1 Methanol Concentration Profiles through SIBS-85 membranes

Table B.3 Concentration data of methanol permeation through SEBS-83 membrane

Run	Peak Height (a.u.)	Conc. (%v/v)	Time (s.)
1	0.4181	1.06	1965
2	0.4462	1.67	3767
3	0.4559	1.88	5659
4	0.4717	2.22	7407
5	0.4778	2.36	9262
6	0.4895	2.61	11182
7	0.5152	3.17	12768
8	0.5305	3.50	14569
9	0.5342	3.58	16369
10	0.5425	3.76	18170
11	0.5428	3.77	19971
12	0.5878	4.75	21766

Table B.4 Concentration data of methanol permeation through SEBS-83 membrane treated with SCF

Run	Peak Height (a.u.)	Conc. (%v/v)	Time (s.)
1	0.1010	0.46	1973
2	0.1815	0.84	3768
3	0.3310	1.55	5778
4	0.4020	1.89	7732
5	0.4080	1.92	9165
6	0.4930	2.33	10969
7	0.5380	2.54	12760
8	0.6030	2.85	14570
9	0.6100	2.88	16512
10	0.6270	2.96	18178
11	0.6670	3.15	20011
12	0.7250	3.43	21902

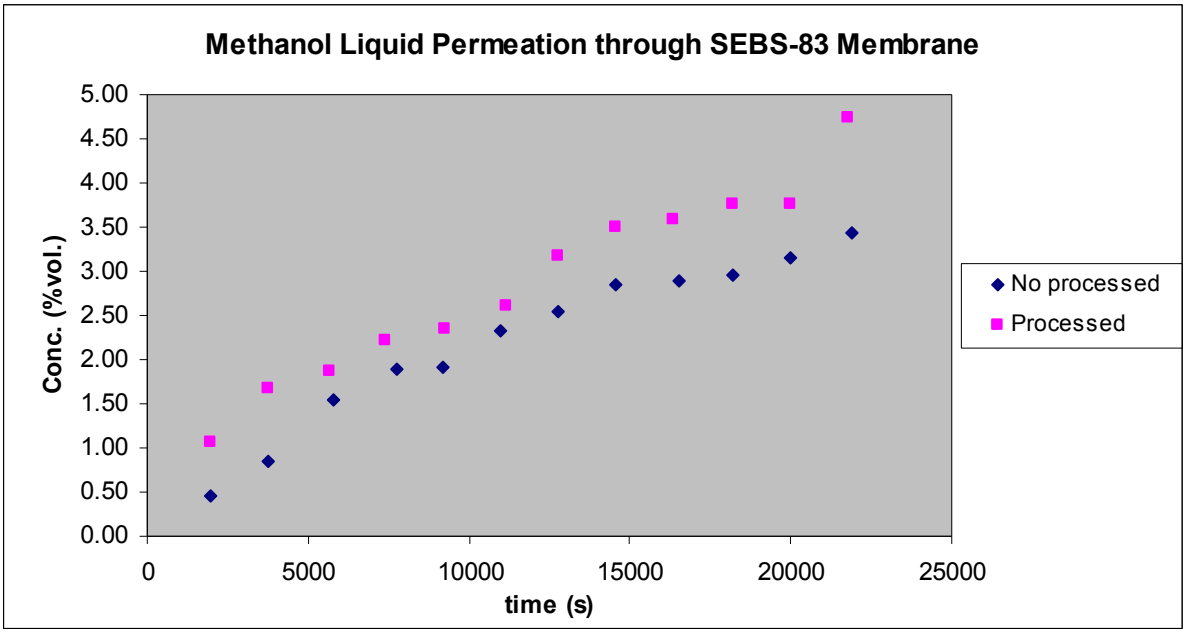

Figure B.2 Methanol Concentration Profiles through SEBS-83 membranes

APPENDIX C

METHANOL CONCENTRATION PROFILES IN LIQUID PHASE THROUGH SIBS MEMBRANES FUNCTIONALIZED WITH METALLIC CATIONS

Table C.1 Concentration data of methanol permeation through SIBS-88 membrane with Ba^{2+}.

Run	Peak Height (a.u.)	Conc. %vol.	Time (sec.)
1	0.2814	0.08	2036
2	0.2929	0.33	3079
3	0.3122	0.75	4699
4	0.3181	0.88	6123
5	0.3264	1.06	8166
6	0.3317	1.18	9299
7	0.3326	1.20	11574
8	0.3333	1.21	12486
9	0.3340	1.23	13218
10	0.3344	1.24	14394
11	0.3347	1.24	15583
12	0.3352	1.25	17055

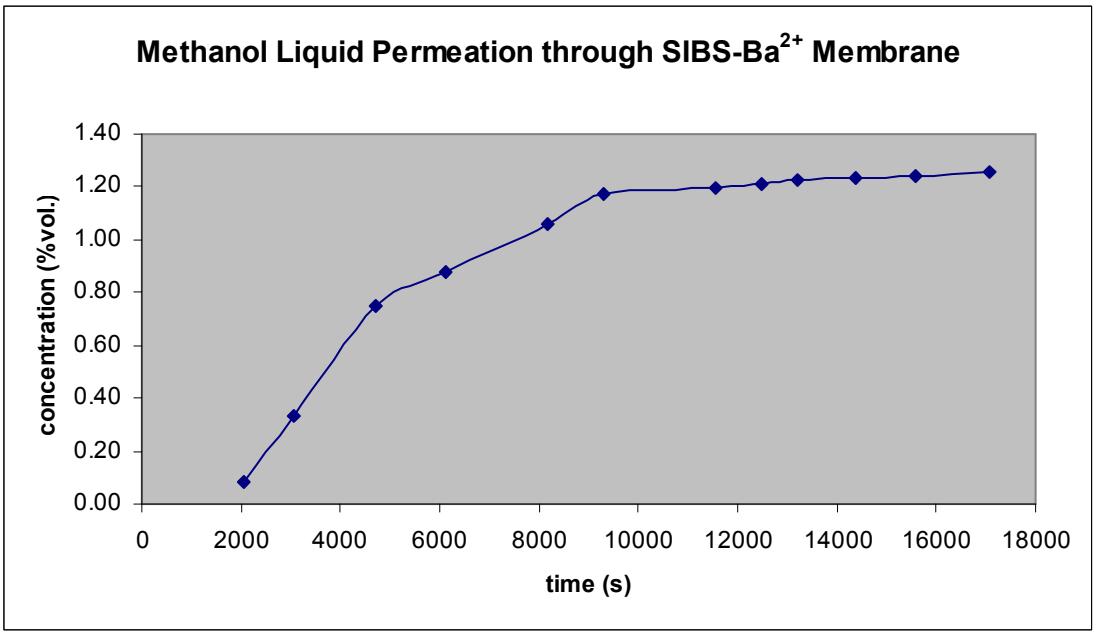

Figure C.1 Methanol Concentration Profile through SIBS-Ba^{2+} membrane

Table C.2 Concentration data of methanol permeation through SIBS-88 membrane with Mg^{2+}.

Run	Peak Height (a.u.)	Conc. %vol.	Time (sec.)
1	0.3040	0.57	1666
2	0.3577	1.74	3144
3	0.3651	1.90	4642
4	0.3691	1.99	6141
5	0.3751	2.12	7755
6	0.3805	2.24	9482
7	0.3815	2.26	11002
8	0.3832	2.30	12566
9	0.4039	2.75	13966
10	0.4051	2.77	15692
11	0.4411	3.56	17000
12	0.4595	3.96	18977

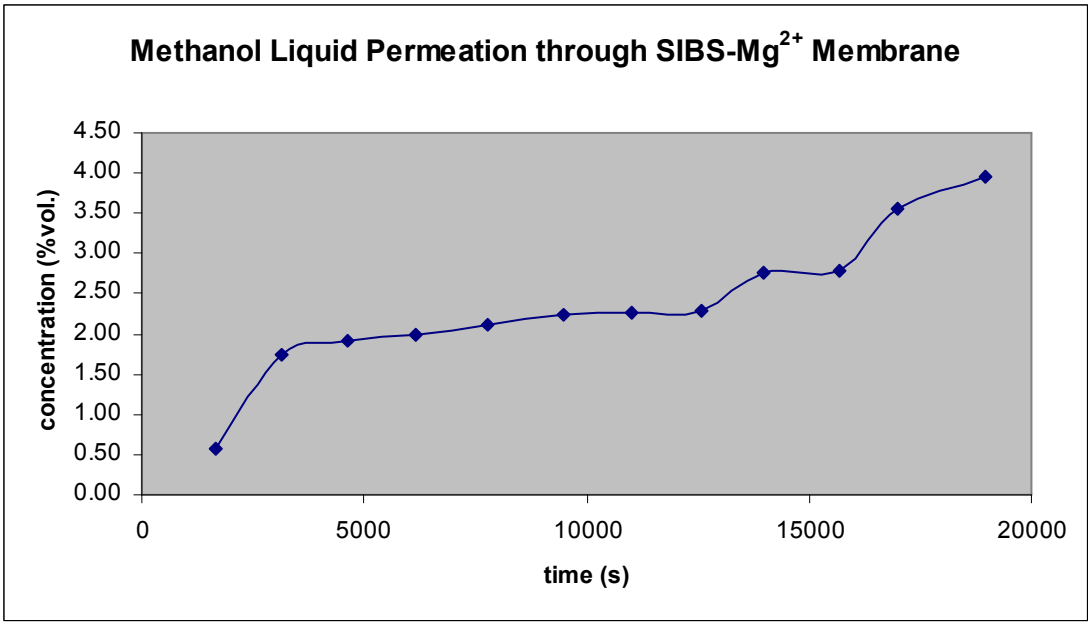

Figure C.2 Methanol Concentration Profile through SIBS-Mg^{2+} membrane

Table C.3 Concentration data of methanol permeation through SIBS-88 membrane with Fe^{3+}.

Run	Peak Height (a.u.)	Conc. %vol.	Time (sec.)
1	0.4008	2.68	519
2	0.4289	3.29	1918
3	0.4357	3.44	3427
4	0.4466	3.68	4948
5	0.4615	4.00	6445
6	0.4737	4.27	7865
7	0.4817	4.44	9825
8	0.4877	4.57	10989
9	0.5133	5.13	12683
10	0.5251	5.38	14200
11	0.5308	5.51	15703
12	0.5339	5.58	17181
13	0.5431	5.78	18685

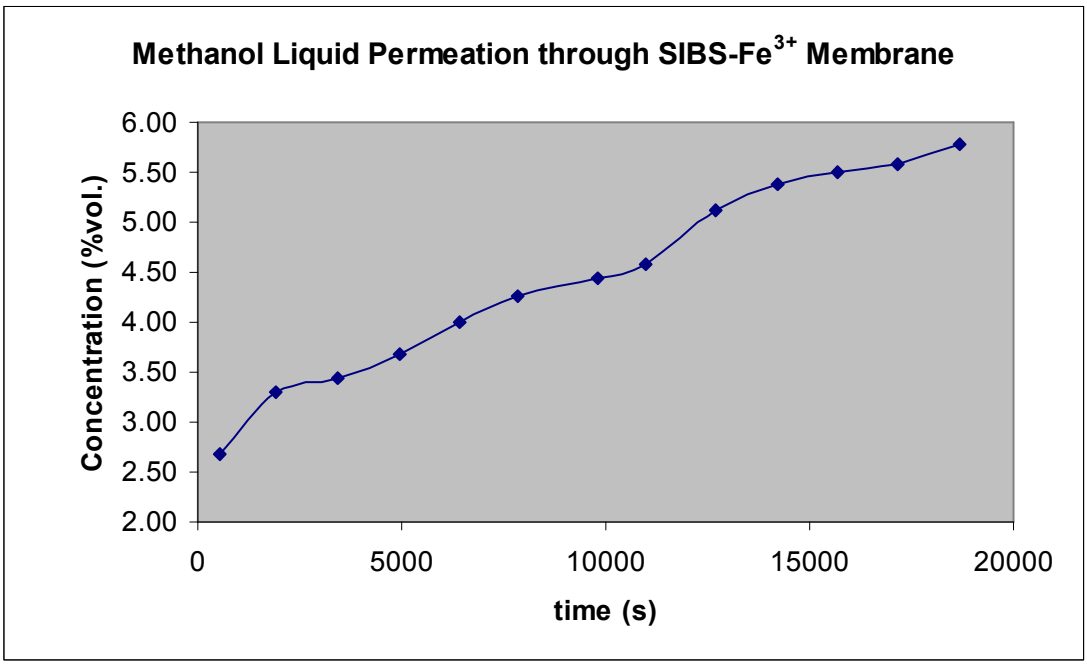

Figure C.3 Methanol Concentration Profile through SIBS-Fe^{3+} membrane

Table C.4 Concentration data of methanol permeation through SIBS-88 membrane with Cu^{2+}.

Run	Peak Height (a.u.)	Conc. %vol.	Time (sec.)
1	0.4416	3.57	1594
2	0.4449	3.64	3172
3	0.4573	3.91	4598
4	0.4629	4.03	6112
5	0.4834	4.48	7592
6	0.4851	4.51	9106
7	0.5025	4.89	11183
8	0.5063	4.98	12693
9	0.5146	5.16	15225
10	0.5161	5.19	16898
11	0.5164	5.20	18401
12	0.5190	5.25	19892

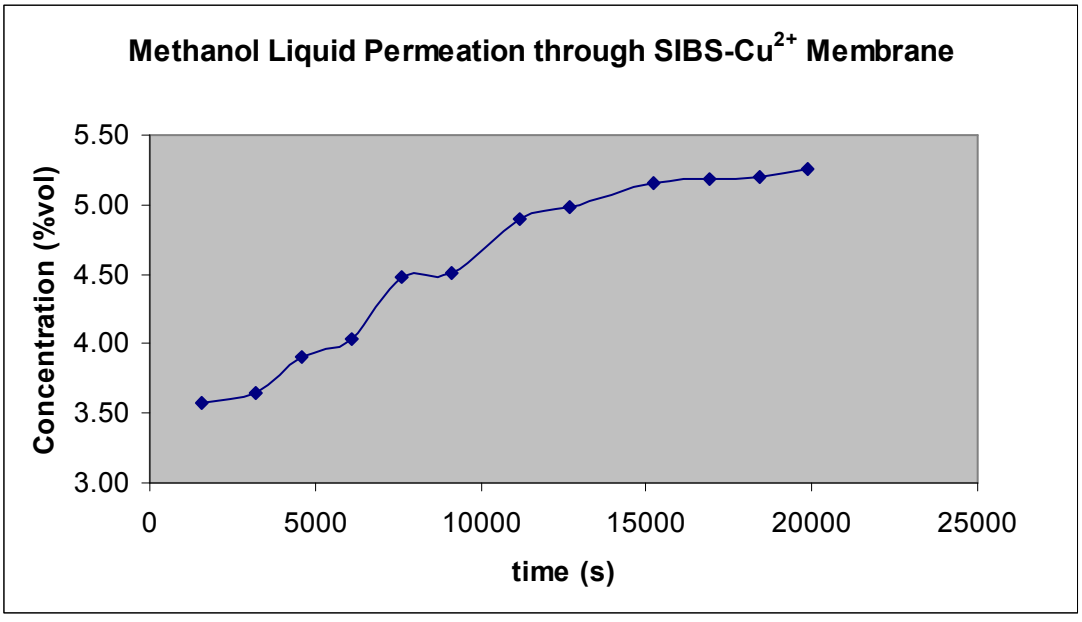

Figure C.4 Methanol Concentration Profile through SIBS-Cu^{2+} membrane

Table C.5 Concentration data of methanol permeation through SIBS-88 membrane with Al^{3+}.

Run	Peak Height (a.u.)	Conc. %vol.	Time (sec.)
1	0.3888	2.42	1710
2	0.4129	2.94	3148
3	0.4387	3.50	4669
4	0.4546	3.85	6245
5	0.4780	4.36	7722
6	0.4942	4.71	9226
7	0.5054	4.96	10666
8	0.5243	5.37	12804
9	0.5295	5.48	13851
10	0.5349	5.60	15254
11	0.5379	5.66	16711
12	0.5393	5.69	18213

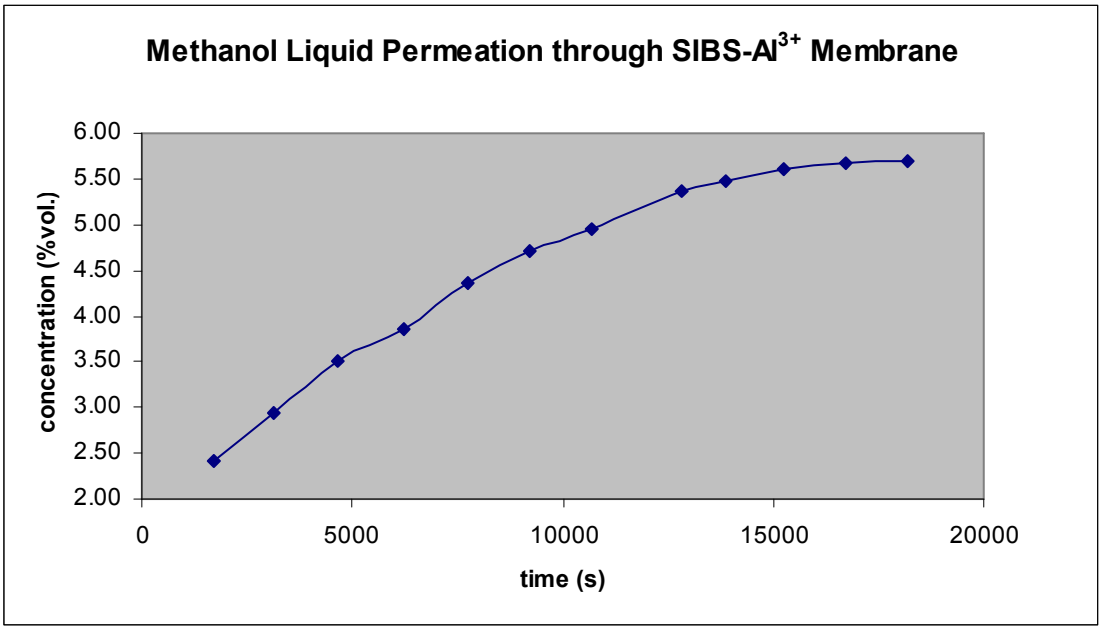

Figure C.5 Methanol Concentration Profile through SIBS-Al^{3+} membrane

Table C.6 Concentration data of methanol permeation through SIBS-88 membrane with Zn^{+}.

Run	Peak Height (a.u.)	Conc. %vol.	Time (sec.)
1	0.3815	2.26	1663
2	0.4264	3.24	3086
3	0.4446	3.63	4597
4	0.4902	4.63	6092
5	0.5225	5.33	7619
6	0.5312	5.52	9142
7	0.5462	5.84	10802
8	0.5567	6.07	12112
9	0.5643	6.24	13644
10	0.5663	6.28	15017
11	0.5720	6.41	16529
12	0.5895	6.79	18026

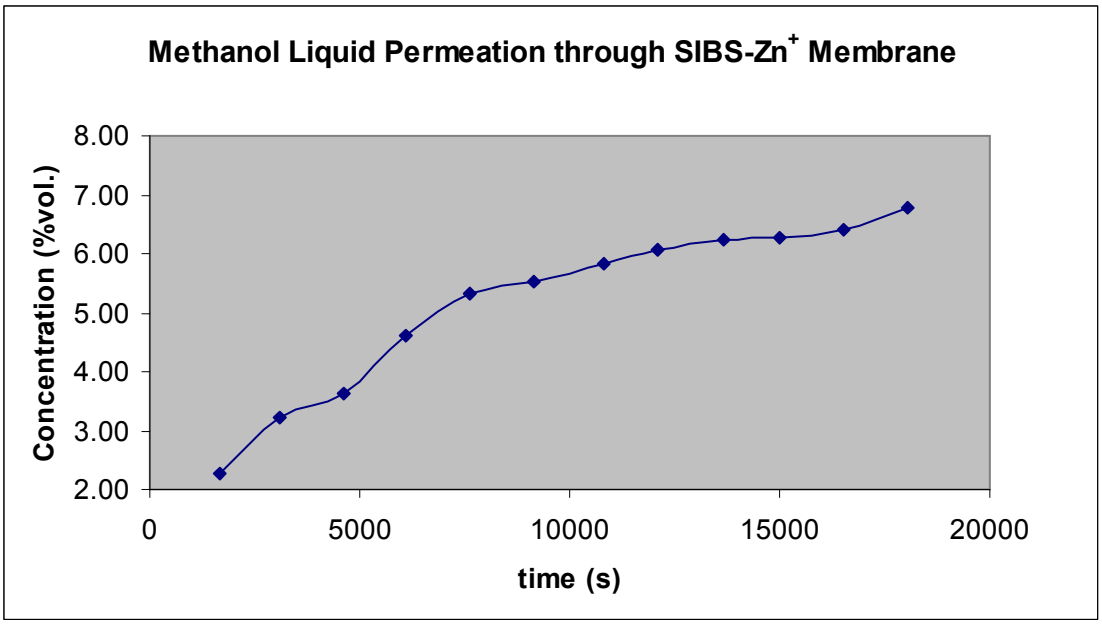

Figure C.6 Methanol Concentration Profile through SIBS-Zn^{+} membrane

Table C.7 Concentration data of methanol permeation through SIBS-88 membrane with Ag^+.

Run	Peak Height (a.u.)	Conc. %vol.	Time (sec.)
1	0.4891	4.60	1674
2	0.5226	5.33	3049
3	0.5450	5.82	4665
4	0.5483	5.89	6125
5	0.5519	5.97	7422
6	0.5542	6.02	9183
7	0.5577	6.09	10763
8	0.5603	6.15	12142
9	0.5661	6.28	13588
10	0.5693	6.35	15047
11	0.5709	6.38	16612
12	0.5732	6.43	18035

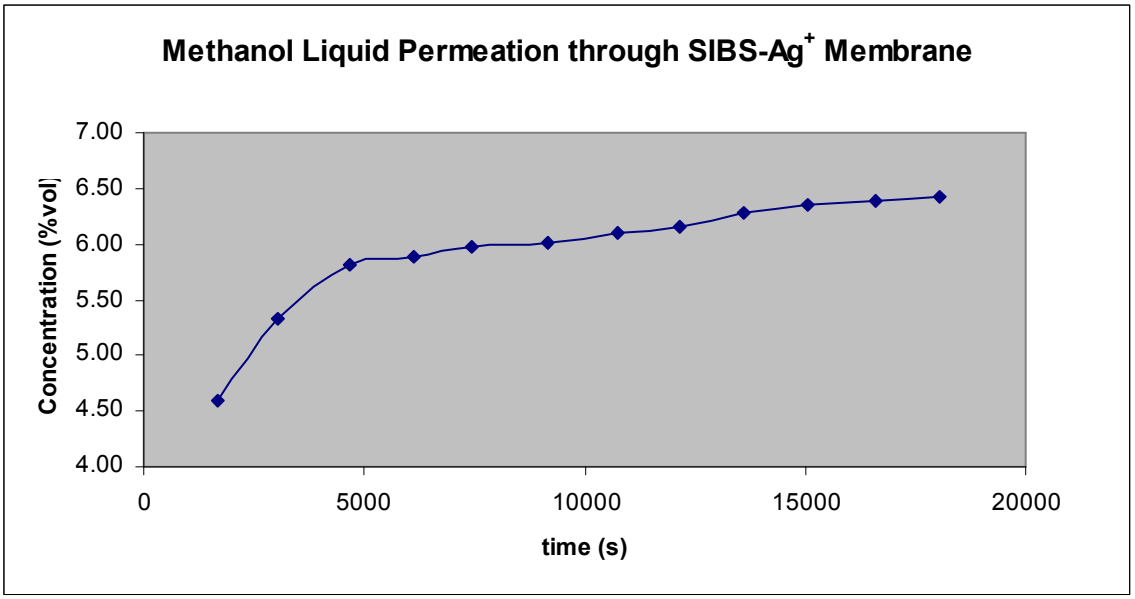

Figure C.7 Methanol Concentration Profile through SIBS-Ag^+ membrane

APPENDIX D

METHANOL CONCENTRATION PROFILES IN VAPOR PHASE THROUGH NAFION MEMBRANES

Table D.1 Methanol permeation in vapor phase through Nafion no processed

m (g.)	dm (g)	time (s.)
21.0054	…	0
21.0000	0.0054	1800
20.9708	0.0346	3600
20.9415	0.0639	5400
20.9145	0.0909	7200
20.8861	0.1193	9000
20.8589	0.1465	10800
20.8328	0.1726	12600
20.8053	0.2001	14400
20.7756	0.2298	16200
20.7462	0.2592	18000
20.7160	0.2894	19800
20.6865	0.3189	21600
20.6592	0.3462	23400
20.6315	0.3739	25200
20.6040	0.4014	27000
20.5757	0.4297	28860

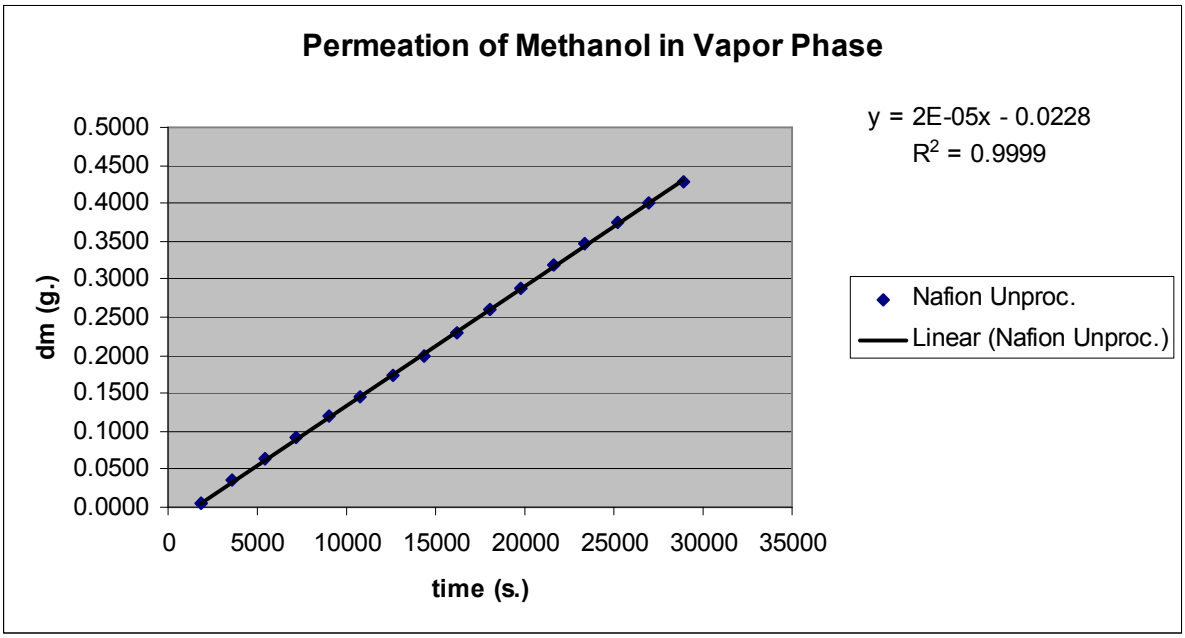

Figure D.1 Methanol permeation profile in vapor phase through Nafion no processed

Table D.2 Methanol permeation in vapor phase through processed Nafion (Longitudinally)

m (g.)	dm (g)	time (s.)
12.0029	…	0
11.9858	0.0171	1800
11.9721	0.0308	3600
11.9590	0.0439	5400
11.9408	0.0621	7200
11.9273	0.0756	9000
11.9104	0.0925	10800
11.8958	0.1071	12600
11.8800	0.1229	14400
11.8637	0.1392	16200
11.8486	0.1543	18000
11.8273	0.1756	19800
11.7972	0.2057	21600
11.7668	0.2361	23400
11.7487	0.2542	25200

Table D.3 Methanol permeation in vapor phase through processed Nafion with acetone

m (g.)	dm (g)	time (s.)
12.1923	…	0
12.1775	0.0148	1800
12.1616	0.0307	3600
12.1470	0.0453	5400
12.1325	0.0598	7200
12.1179	0.0744	9000
12.1021	0.0902	10800
12.0865	0.1058	12600
12.0726	0.1197	14400
12.0574	0.1349	16200
12.0412	0.1511	18000
12.0270	0.1653	19800
12.0129	0.1794	21600
11.9950	0.1973	23400
11.9811	0.2112	25200

Table D.4 Methanol permeation in vapor phase through processed Nafion with isopropyl alcohol

m (g.)	dm (g)	time (s.)
12.0808	…	0
12.0715	0.0093	1225
12.0614	0.0194	2431
12.0503	0.0305	3655
12.0396	0.0412	4823
12.0289	0.0519	6015
12.0183	0.0625	7212
12.0087	0.0721	8405
11.9972	0.0836	9633
11.9863	0.0945	10822
11.9759	0.1049	12021
11.9661	0.1147	13200
11.9567	0.1241	14400

Table D.5 Methanol permeation in vapor phase through processed Nafion with acetic acid

m (g.)	dm (g)	time (s.)
11.9715	…	0
11.9638	0.0077	1200
11.9540	0.0175	2400
11.9432	0.0283	3600
11.9328	0.0387	4800
11.9222	0.0493	6000
11.9115	0.0600	7203
11.9022	0.0693	8404
11.8907	0.0808	9612
11.8793	0.0922	10806
11.8696	0.1019	12010
11.8601	0.1114	13220
11.8507	0.1208	14450

Table D.6 Methanol permeation in vapor phase through processed Nafion with HPLC water

m (g.)	dm (g)	time (s.)
12.0508	…	0
12.0363	0.0145	1800
12.0224	0.0284	3600
12.0090	0.0418	5400
11.9906	0.0602	7200
11.9770	0.0738	9000
11.9604	0.0904	10800
11.9449	0.1059	12600
11.9282	0.1226	14400
11.9126	0.1382	16200
11.8968	0.1540	18000
11.8756	0.1752	20400
11.8589	0.1919	22200
11.8326	0.2182	25200
11.8152	0.2356	27000

Table D.7 Methanol permeation in vapor phase through processed Nafion with methanol

m (g.)	dm (g)	time (s.)
11.9981	…	0
11.9826	0.0155	1800
11.9676	0.0305	3600
11.9532	0.0449	5400
11.9334	0.0647	7200
11.9077	0.0904	9000
11.8834	0.1147	10800
11.8634	0.1347	12600
11.8438	0.1543	14400
11.8255	0.1726	16200
11.8074	0.1907	18000
11.7833	0.2148	20400
11.7645	0.2336	22200
11.7342	0.2639	25200
11.7146	0.2835	27000

Table D.8 Methanol permeation in vapor phase through processed Nafion with acetonitrile

m (g.)	dm (g)	time (s.)
12.1337	…	0
12.1086	0.0251	1620
12.0908	0.0429	3120
12.0743	0.0594	4620
12.0603	0.0734	6120
12.0457	0.0880	7620
12.0313	0.1024	9120
12.0196	0.1141	10620
12.0034	0.1303	12120
11.9891	0.1446	13620
11.9730	0.1607	15120
11.9587	0.1750	16620
11.9456	0.1881	18120

Table D.9 Methanol permeation in vapor phase through processed Nafion with THF

m (g.)	dm (g)	time (s.)
18.1936	…	0
18.1815	0.0121	1800
18.1627	0.0309	3600
18.1432	0.0504	5400
18.1243	0.0693	7200
18.1050	0.0886	9000
18.0854	0.1082	10800
18.0659	0.1277	12600
18.0456	0.1480	14400
18.0281	0.1655	16200
18.0089	0.1847	18000
17.9891	0.2045	19800
17.9701	0.2235	21600
17.9375	0.2561	23400

Table D.10 Methanol permeation in vapor phase through processed Nafion transversally

m (g.)	dm (g)	time (s.)
12.0979	…	0
12.0810	0.0169	1620
12.0655	0.0324	3120
12.0502	0.0477	4620
12.0356	0.0623	6120
12.0212	0.0767	7620
12.0066	0.0913	9120
11.9945	0.1034	10620
11.9794	0.1185	12120
11.9647	0.1332	13620
11.9480	0.1499	15120
11.9334	0.1645	16620
11.9186	0.1793	18120

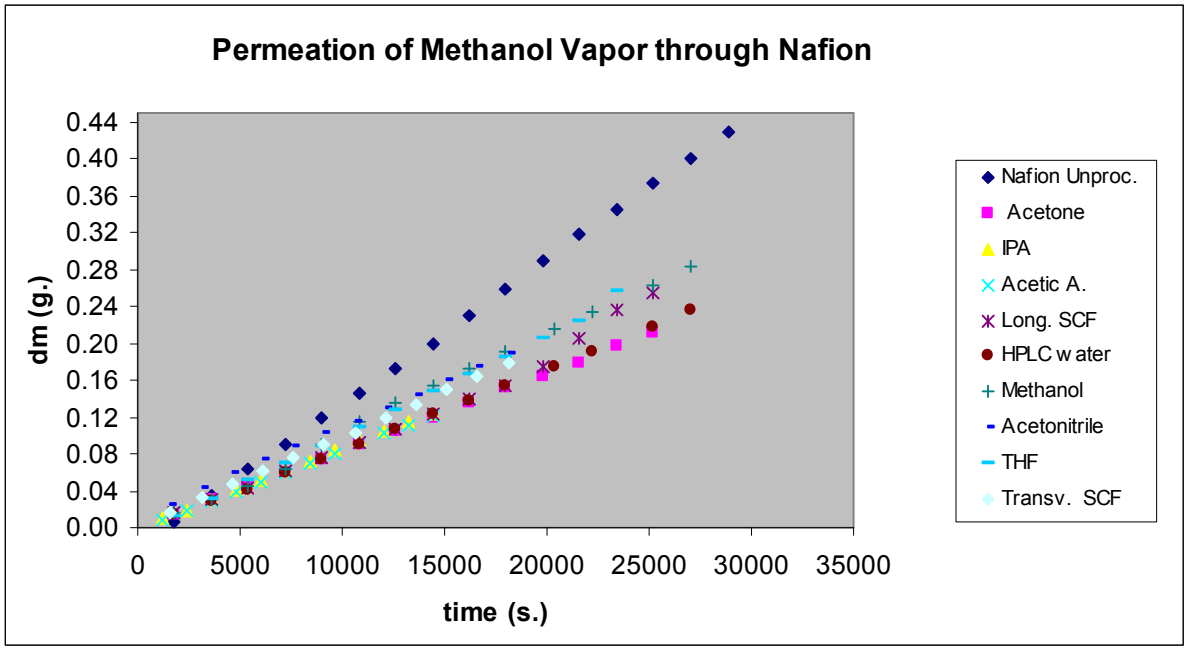

Figure D.2 Methanol permeation profiles in vapor phase through Nafion

APPENDIX E

METHANOL CONCENTRATION PROFILES IN VAPOR PHASE THROUGH SIBS AND SEBS MEMBRANES

Table E.1 Methanol permeation in vapor phase through SIBS-85

m (g.)	dm (g)	time (s.)
20.5347	…	0
20.5164	0.0183	1860
20.4928	0.0419	3660
20.4703	0.0644	5460
20.4486	0.0861	7260
20.4271	0.1076	9060
20.4060	0.1287	10860
20.3853	0.1494	12660
20.3639	0.1708	14520
20.3435	0.1912	16260
20.3223	0.2124	18060
20.3016	0.2331	19860
20.2792	0.2555	21660
20.2587	0.2760	23460
20.2396	0.2951	25260
20.1590	0.3757	30480
20.1413	0.3934	31800

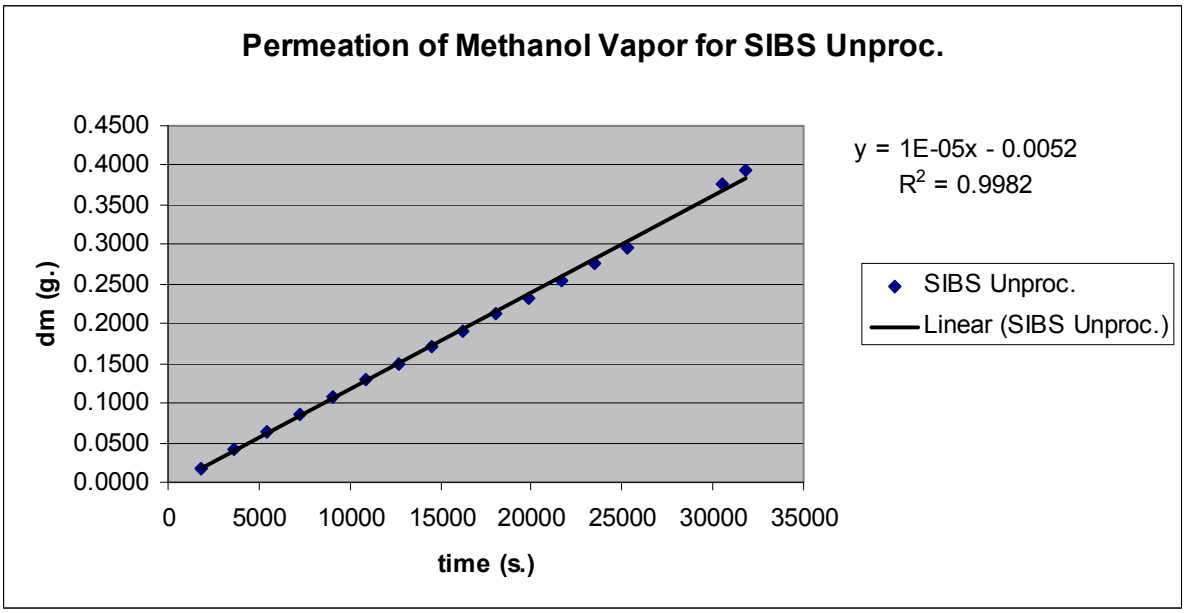

Figure E.1 Methanol permeation in vapor phase through SIBS-85

Table E.2 Methanol permeation in vapor phase through unsulfonated SEBS

m (g.)	dm (g)	time (s.)
19.4786	…	0
19.4783	0.0003	1800
19.4773	0.0013	3600
19.4764	0.0022	5400
19.4752	0.0034	7200
19.4744	0.0042	9000
19.4730	0.0056	10800
19.4720	0.0066	12600
19.4711	0.0075	14400
19.4700	0.0086	16200
19.4689	0.0097	18000
19.4679	0.0107	19800
19.4668	0.0118	21600
19.4652	0.0134	23400
19.4645	0.0141	25200

Table E.3 Methanol permeation in vapor phase through SEBS-93

m (g.)	dm (g)	time (s.)
11.9885	…	0
11.9827	0.0058	1200
11.9762	0.0123	2400
11.9692	0.0193	3600
11.9624	0.0261	4800
11.9554	0.0331	6000
11.9487	0.0398	7203
11.9426	0.0459	8404
11.9350	0.0535	9612
11.9283	0.0602	10806
11.9214	0.0671	12010
11.9152	0.0733	13220
11.9091	0.0794	14450

Table E.4 Methanol permeation in vapor phase through SEBS-93 processed with methanol-SCF

m (g.)	dm (g)	time (s.)
12.4671	…	0
12.4539	0.0132	1800
12.4397	0.0274	3600
12.4269	0.0402	5400
12.4138	0.0533	7200
12.4008	0.0663	9000
12.3870	0.0801	10800
12.3733	0.0938	12600
12.3615	0.1056	14400
12.3487	0.1184	16200
12.3349	0.1322	18000
12.3231	0.1440	19800
12.3105	0.1566	21600
12.2958	0.1713	23400
12.2834	0.1837	25200

Table E.5 Methanol permeation in vapor phase through SEBS-93 processed with acetone-SCF

m (g.)	dm (g)	time (s.)
20.6305	…	0
20.6008	0.0297	1800
20.5758	0.0547	3600
20.5528	0.0777	5400
20.5319	0.0986	7200
20.5104	0.1201	9000
20.4902	0.1403	10800
20.4705	0.1600	12600
20.4506	0.1799	14400
20.4308	0.1997	16200
20.4074	0.2231	18000
20.3908	0.2397	19800
20.3699	0.2606	21600
20.3439	0.2866	23400
20.3271	0.3034	25200
20.3030	0.3275	27000

Table E.6 Methanol permeation in vapor phase through SEBS-93 processed with SCF

m (g.)	dm (g)	time (s.)
12.0320	…	0
12.0209	0.0111	1800
12.0101	0.0219	3600
11.9993	0.0327	5400
11.9846	0.0474	7200
11.9741	0.0579	9000
11.9608	0.0712	10800
11.9484	0.0836	12600
11.9353	0.0967	14400
11.9229	0.1091	16200
11.9107	0.1213	18000
11.8947	0.1373	20400
11.8816	0.1504	22200
11.8613	0.1707	25200
11.8479	0.1841	27000

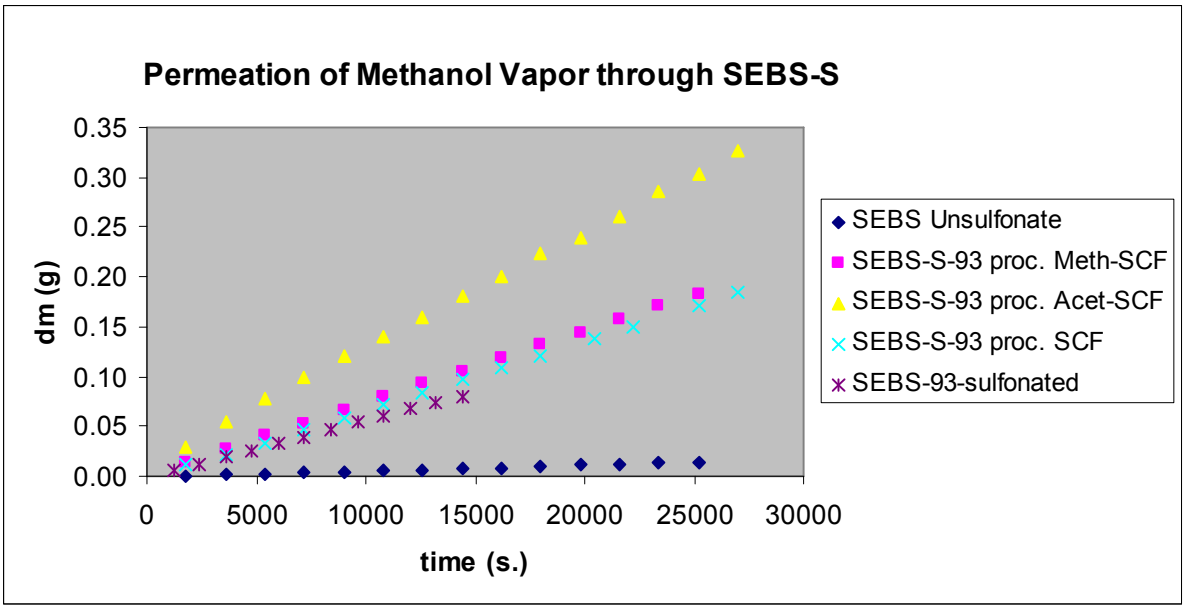

Figure E.2 Methanol permeation in vapor phase through SEBS membranes

APPENDIX F

METHANOL CONCENTRATION PROFILES IN VAPOR PHASE THROUGH SIBS MEMBRANES

FUNCTIONALIZED WITH METALLIC CATIONS

Table F.1 Methanol permeation in vapor phase through SIBS-Mg^{2+}.

m (g.)	dm (g)	time (s.)
12.9344	…	0
12.9270	0.0074	1800
12.9205	0.0139	3600
12.9135	0.0209	5400
12.9063	0.0281	7200
12.8986	0.0358	9000
12.8910	0.0434	10800
12.8828	0.0516	12600
12.8748	0.0596	14400
12.8666	0.0678	16200
12.8580	0.0764	18000
12.8492	0.0852	19800
12.8384	0.0960	21600
12.8307	0.1037	23400
12.8209	0.1135	25200
12.8121	0.1223	27000

Table F.2 Methanol permeation in vapor phase through SIBS-Ca^{2+}.

m (g.)	dm (g)	time (s.)
12.4228	…	0
12.4203	0.0025	1860
12.4189	0.0039	3660
12.4176	0.0052	5460
12.4166	0.0062	7260
12.4156	0.0072	9060
12.4145	0.0083	10860
12.4139	0.0089	12660
12.4129	0.0099	14460
12.4121	0.0107	16260
12.4111	0.0117	18060
12.4101	0.0127	19860
12.4087	0.0141	21660
12.4075	0.0153	23460
12.4059	0.0169	25260
12.4044	0.0184	27060

Table F.3 Methanol permeation in vapor phase through SIBS-Fe^{3+}.

m (g.)	dm (g)	time (s.)
12.6383	…	0
12.6309	0.0074	1800
12.6238	0.0145	3600
12.6168	0.0215	5400
12.6103	0.0280	7200
12.6029	0.0354	9000
12.5976	0.0407	10800
12.5907	0.0476	12600
12.5841	0.0542	14400
12.5774	0.0609	16200
12.5701	0.0682	18000
12.5621	0.0762	19800
12.5330	0.1053	21600
12.5197	0.1186	23400
12.5122	0.1261	25200
12.5035	0.1348	27000

Table F.4 Methanol permeation in vapor phase through SIBS-Al^{3+}.

m (g.)	dm (g)	time (s.)
12.7476	…	0
12.7438	0.0038	1800
12.7387	0.0089	3600
12.7333	0.0143	5400
12.7280	0.0196	7200
12.7221	0.0255	9000
12.7179	0.0297	10800
12.7127	0.0349	12600
12.7075	0.0401	14400
12.7025	0.0451	16200
12.6972	0.0504	18000
12.6916	0.0560	19800
12.6868	0.0608	21600
12.6810	0.0666	23400
12.6764	0.0712	25200
12.6709	0.0767	27000

Table F.5 Methanol permeation in vapor phase through SIBS-Zn^{2+}.

m (g.)	dm (g)	time (s.)
12.1953	…	0
12.1942	0.0011	1800
12.1905	0.0048	3600
12.1866	0.0087	5400
12.1820	0.0133	7200
12.1777	0.0176	9000
12.1730	0.0223	10800
12.1683	0.0270	12600
12.1641	0.0312	14400
12.1597	0.0356	16200
12.1547	0.0406	18000
12.1507	0.0446	19800
12.1464	0.0489	21600
12.1426	0.0527	23400
12.1372	0.0581	25200

Table F.6 Methanol permeation in vapor phase through SIBS-Ba^{2+}.

m (g.)	dm (g)	time (s.)
90.0246	…	0
90.0244	0.0002	1500
90.0242	0.0004	3000
90.0241	0.0005	4500
90.0237	0.0009	6000
90.0235	0.0011	7500
90.0234	0.0012	9000
90.0233	0.0013	10500
90.0232	0.0014	12000
90.0231	0.0015	13500
90.0230	0.0016	15000
90.0227	0.0019	16500
90.0226	0.0020	18000
90.0224	0.0022	19500
90.0222	0.0024	21000

Table F.7 Methanol permeation in vapor phase through SIBS-Cu^{2+}.

m (g.)	dm (g)	time (s.)
12.0997	…	0
12.0964	0.0033	1620
12.0917	0.0080	3120
12.0866	0.0131	4620
12.0822	0.0175	6120
12.0773	0.0224	7620
12.0724	0.0273	9120
12.0685	0.0312	10620
12.0634	0.0363	12120
12.0586	0.0411	13620
12.0531	0.0466	15120
12.0483	0.0514	16620
12.0437	0.0560	18120

Table F.8 Methanol permeation in vapor phase through SIBS-Ag^{+}.

m (g.)	dm (g)	time (s.)
12.0803	…	0
12.0730	0.0073	1620
12.0652	0.0151	3120
12.0576	0.0227	4620
12.0500	0.0303	6120
12.0424	0.0379	7620
12.0346	0.0457	9120
12.0266	0.0537	10620
12.0185	0.0618	12120
12.0115	0.0688	13620
12.0037	0.0766	15120
11.9955	0.0848	16620
11.9878	0.0925	18120
11.9746	0.1057	19620

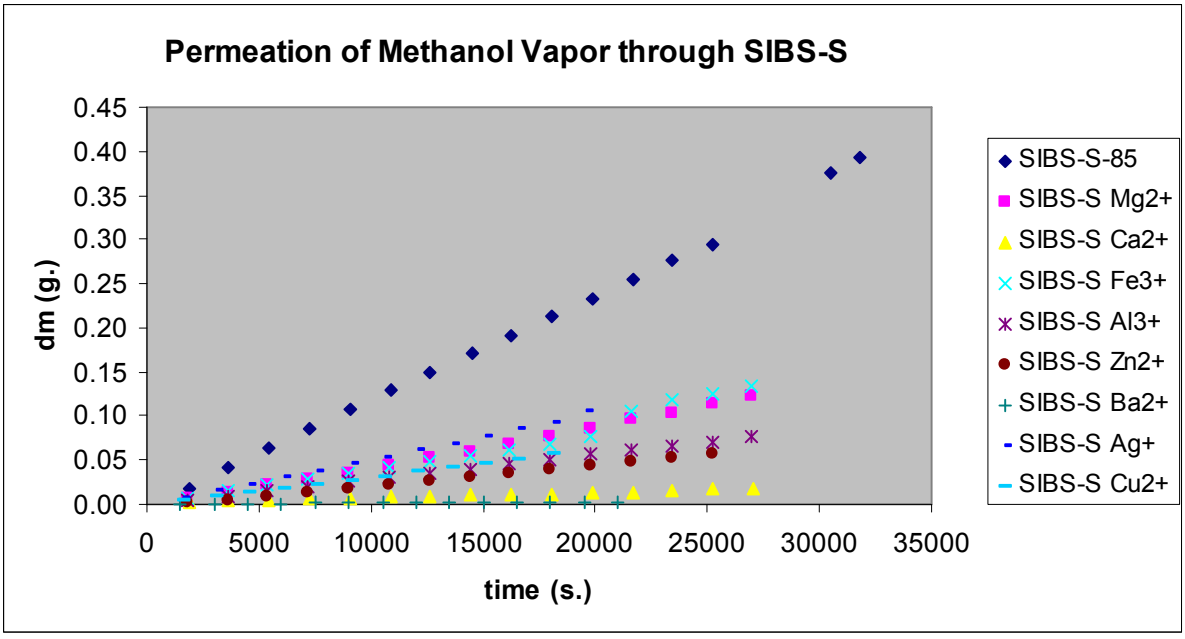

Figure F.1 Methanol permeation in vapor phase through SIBS membranes functionalized with metallic cations

APPENDIX G

THERMOGRAMS FOR SIBS MEMBRANES WITH METALLIC CATIONS

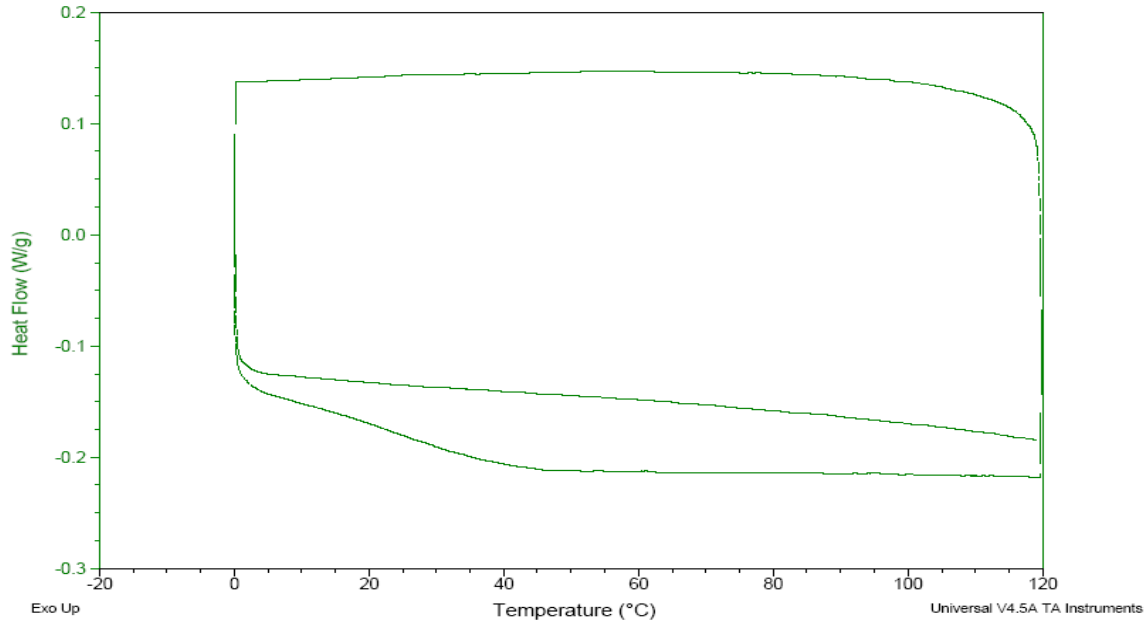

Figure G.1 Thermogram realized to SIBS-Ag^{+} membrane

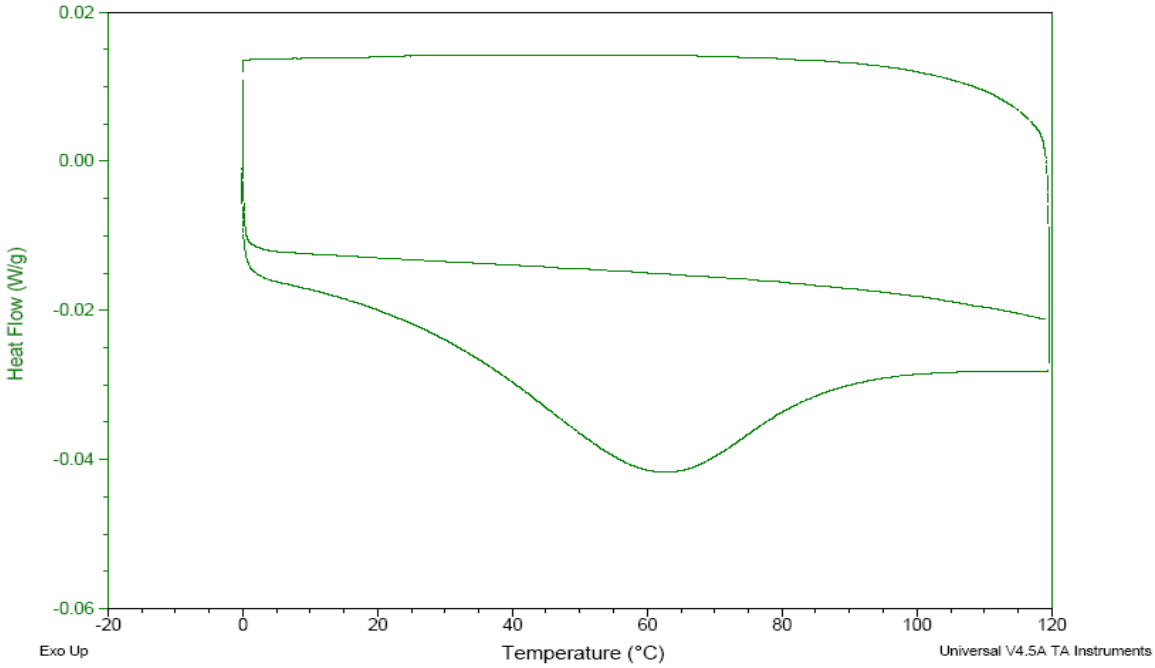

Figure G.2 Thermogram realized to SIBS-Al^{3+} membrane

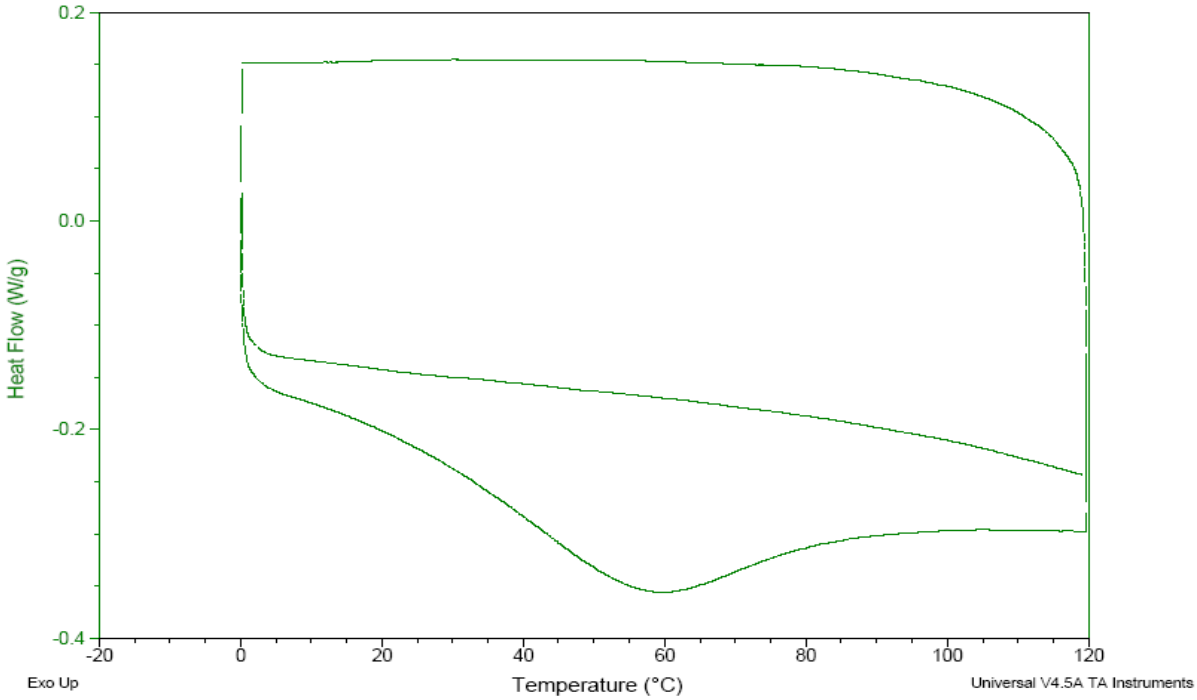

Figure G.3 Thermogram realized to SIBS-Cu^{2+} membrane

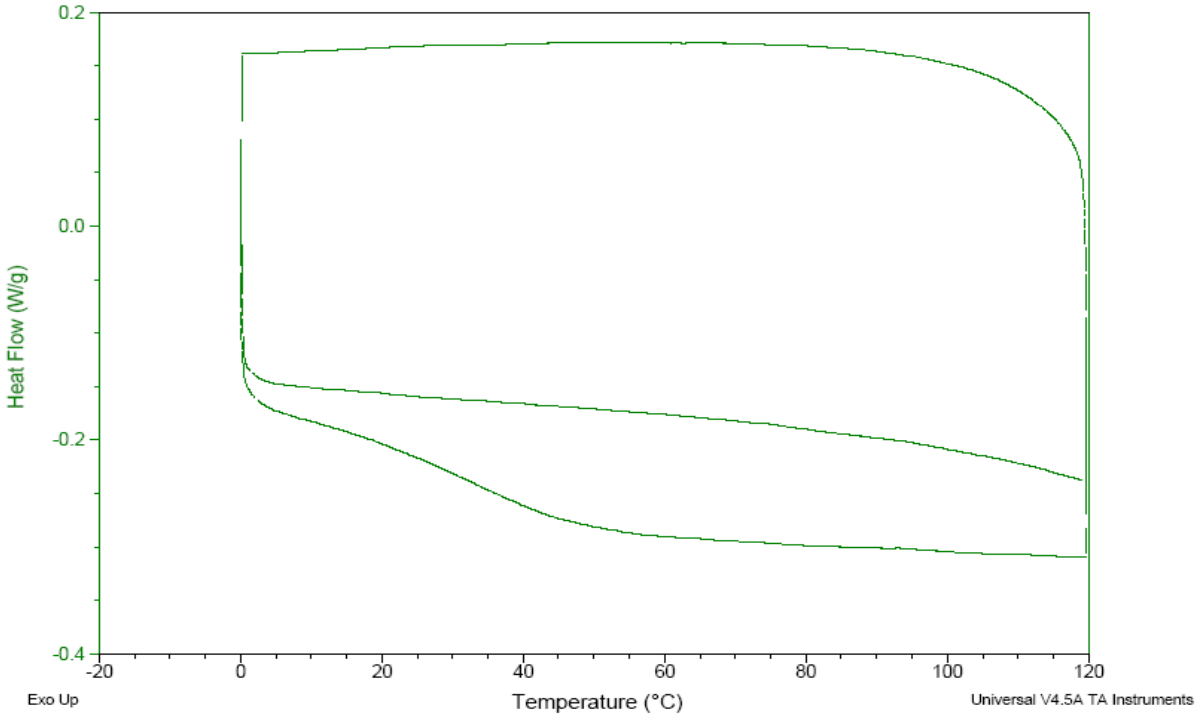

Figure G.4 Thermogram realized to SIBS-Fe^{3+} membrane

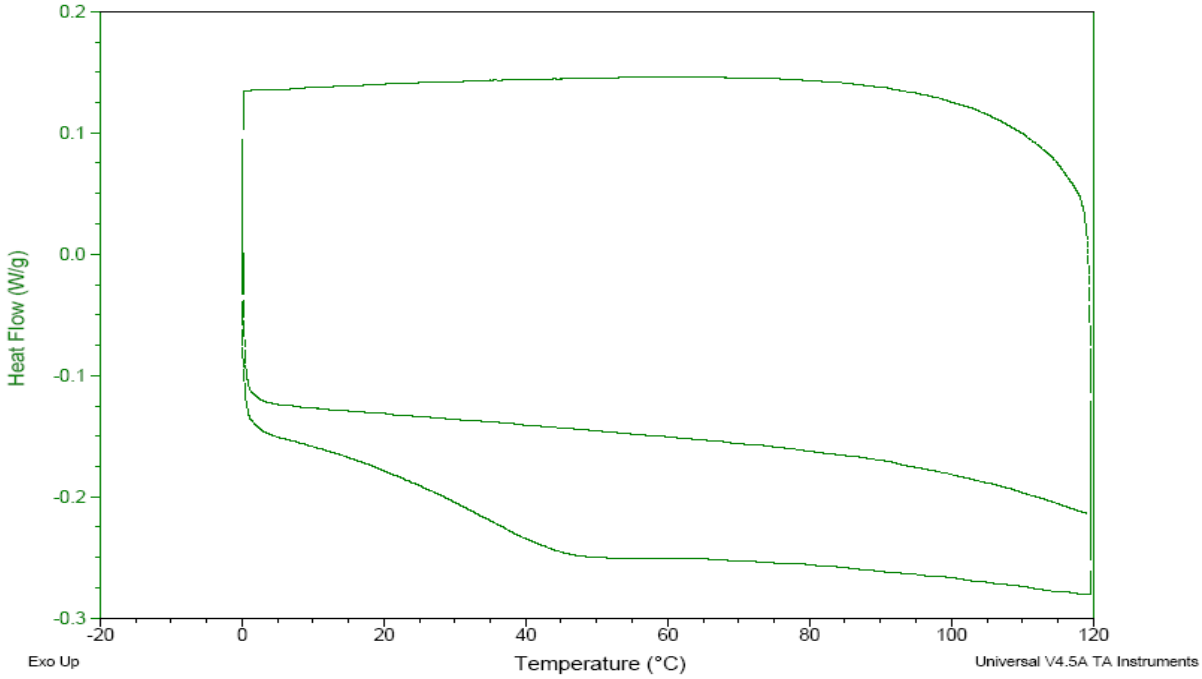

Figure G.5 Thermogram realized to SIBS-Mg^{2+} membrane

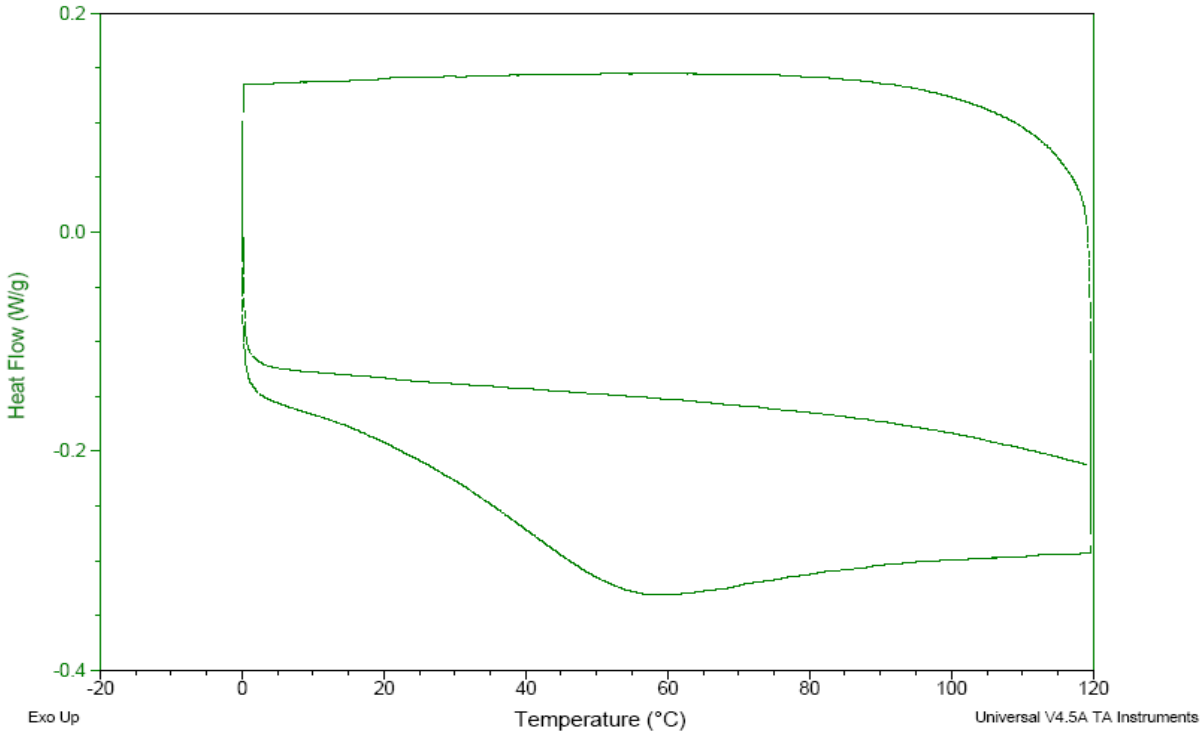

Figure G.6 Thermogram realized to SIBS-Zn^{2+} membrane

APPENDIX H

TGA SPECTRA FOR SIBS MEMBRANES WITH METALLIC CATIONS

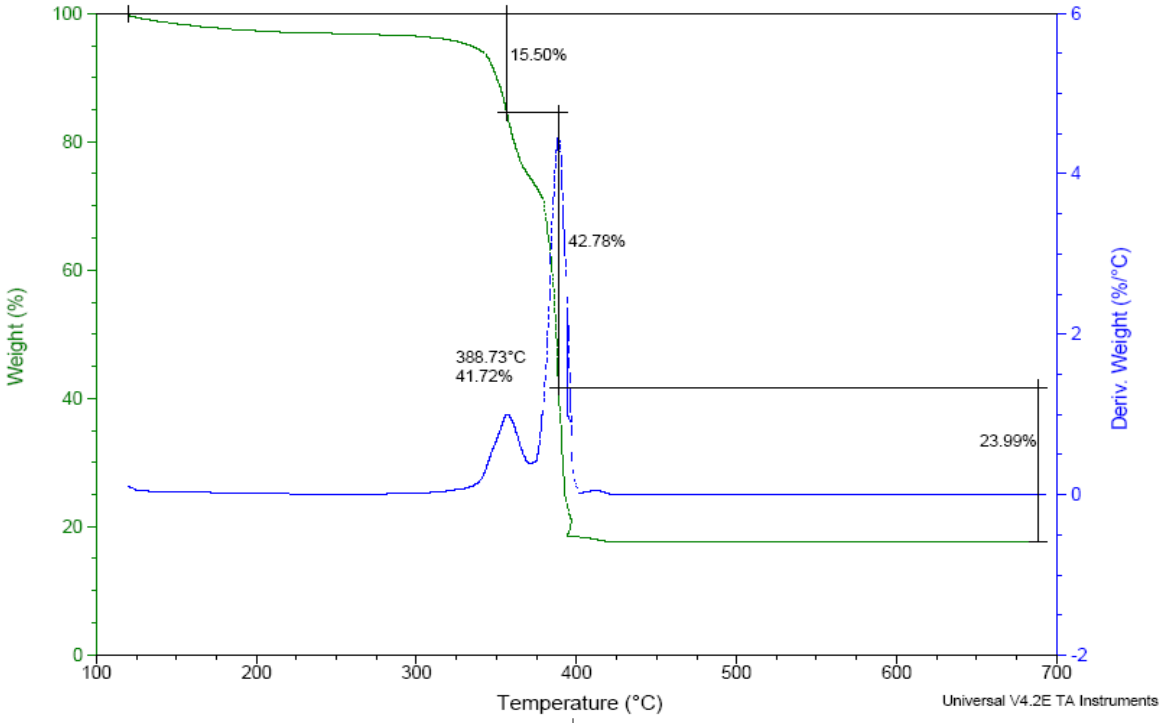

Figure H.1 TGA spectra realized to SIBS-Ag^{+} membrane

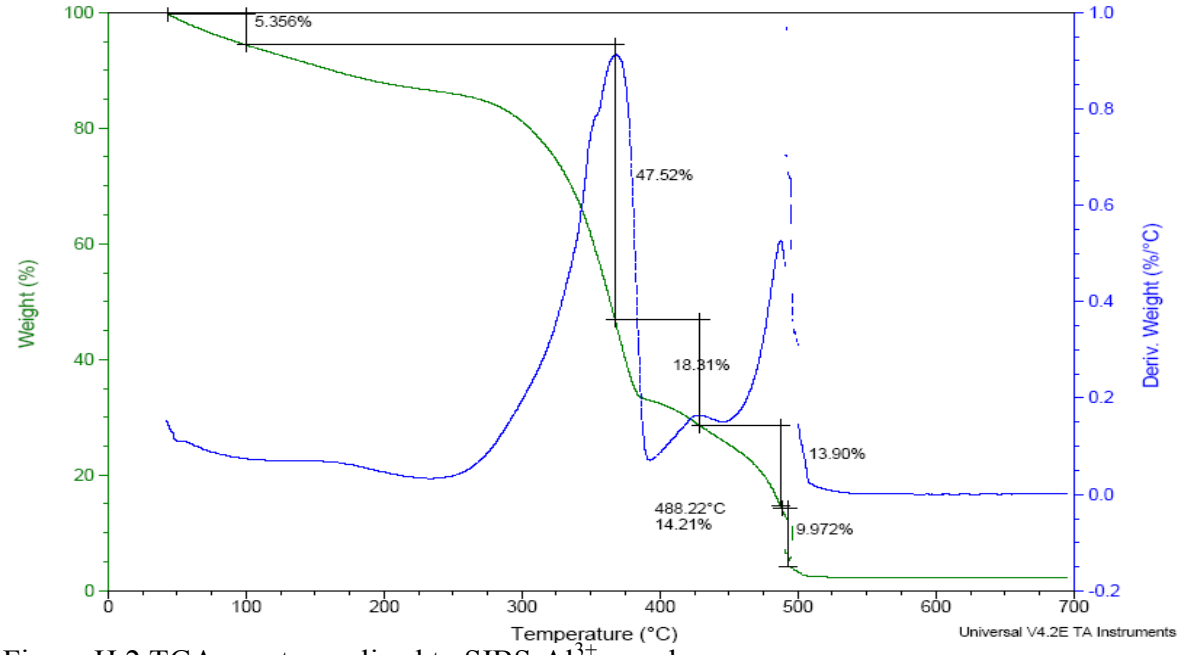

Figure H.2 TGA spectra realized to SIBS-Al^{3+} membrane

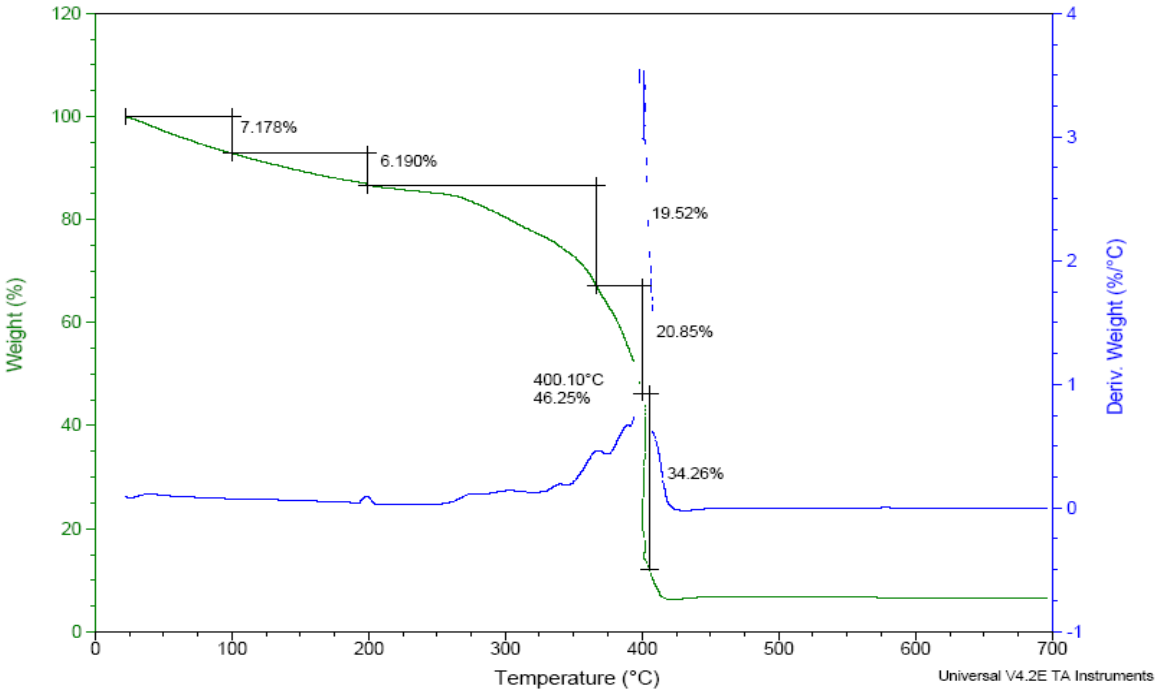

Figure H.3 TGA spectra realized to SIBS-Cu^{2+} membrane

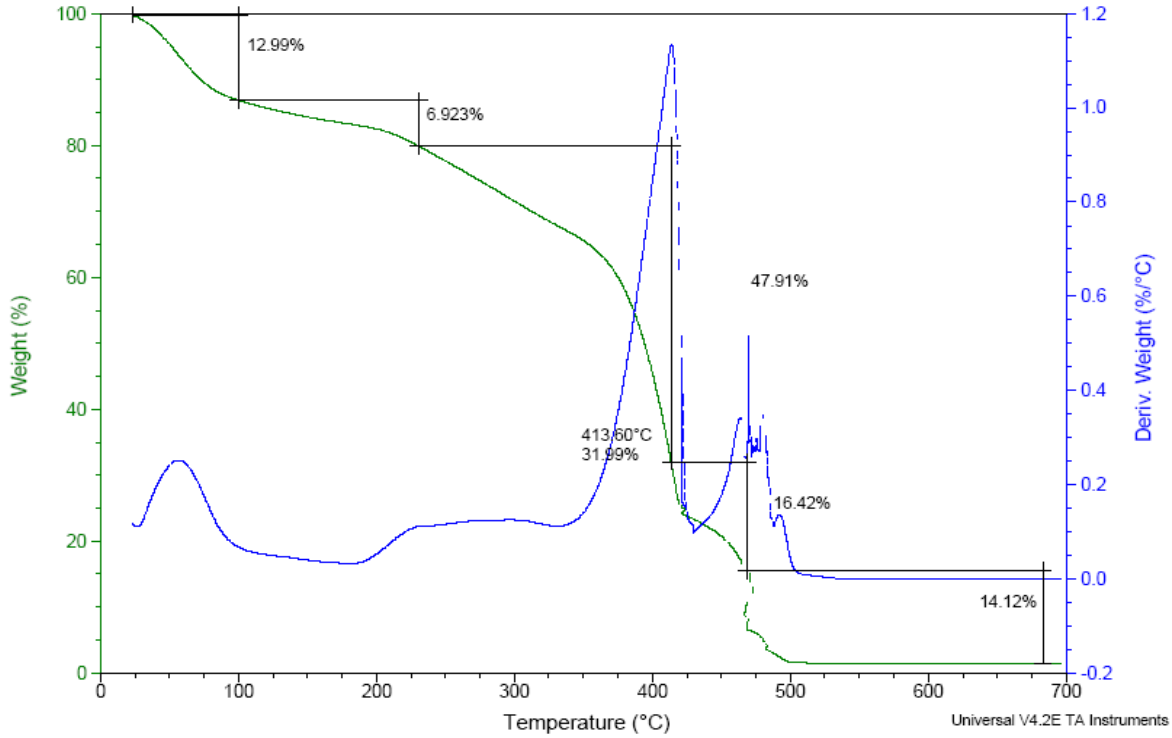

Figure H.4 TGA spectra realized to SIBS-H^{+} membrane (acid form)

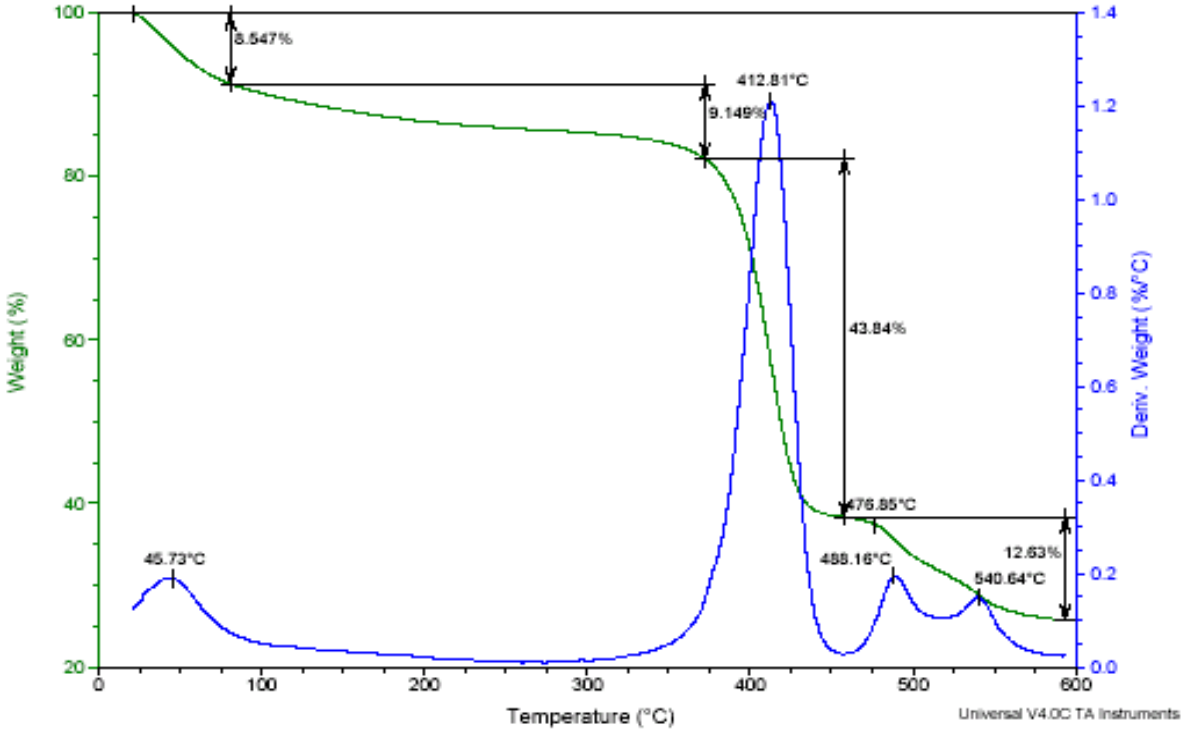

Figure H.5 TGA spectra realized to SIBS-Ca^{2+} membrane

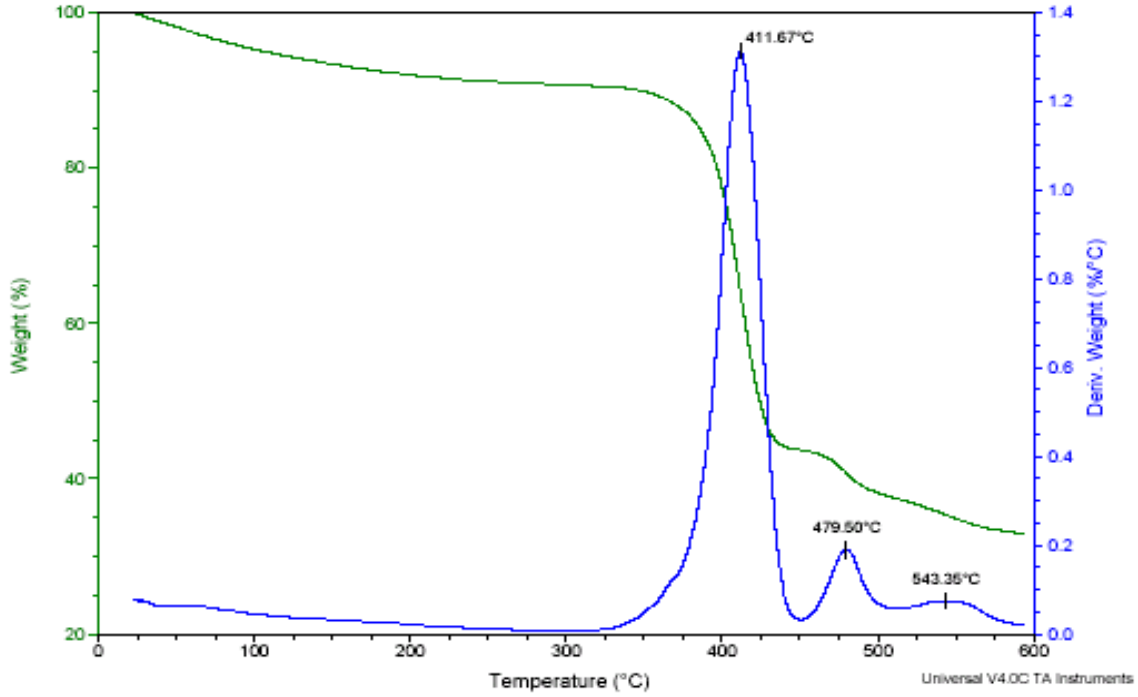

Figure H.6 TGA spectra realized to SIBS-Ba^{2+} membrane

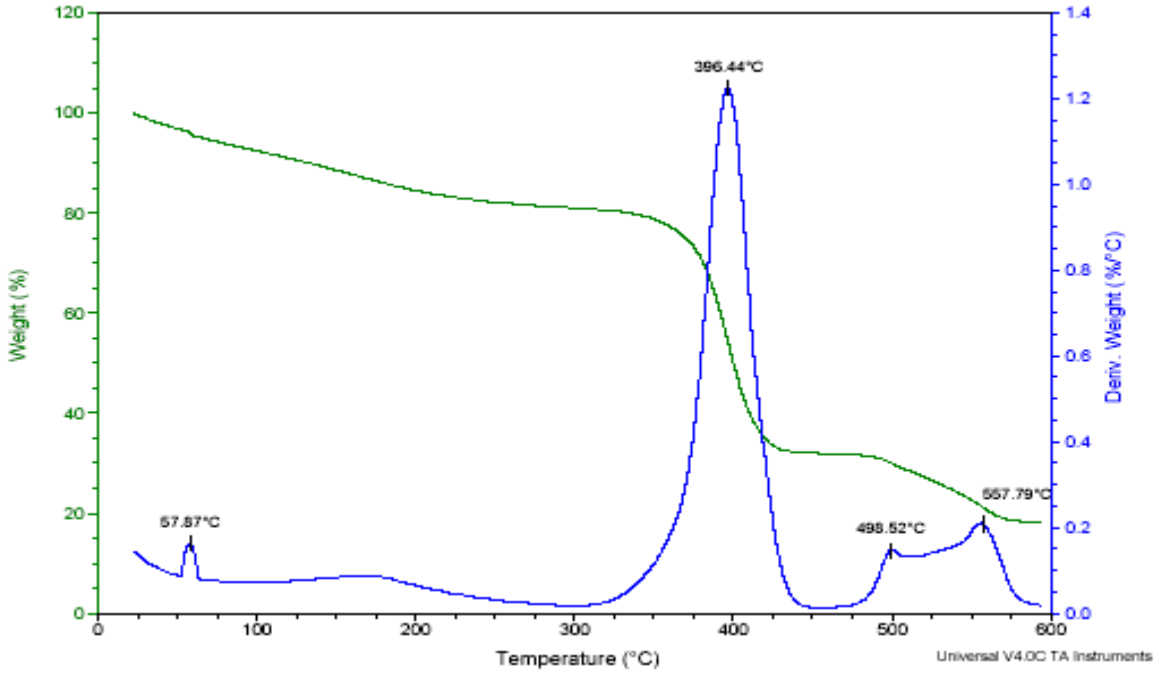

Figure H.7 TGA spectra realized to SIBS-Mg^{2+} membrane

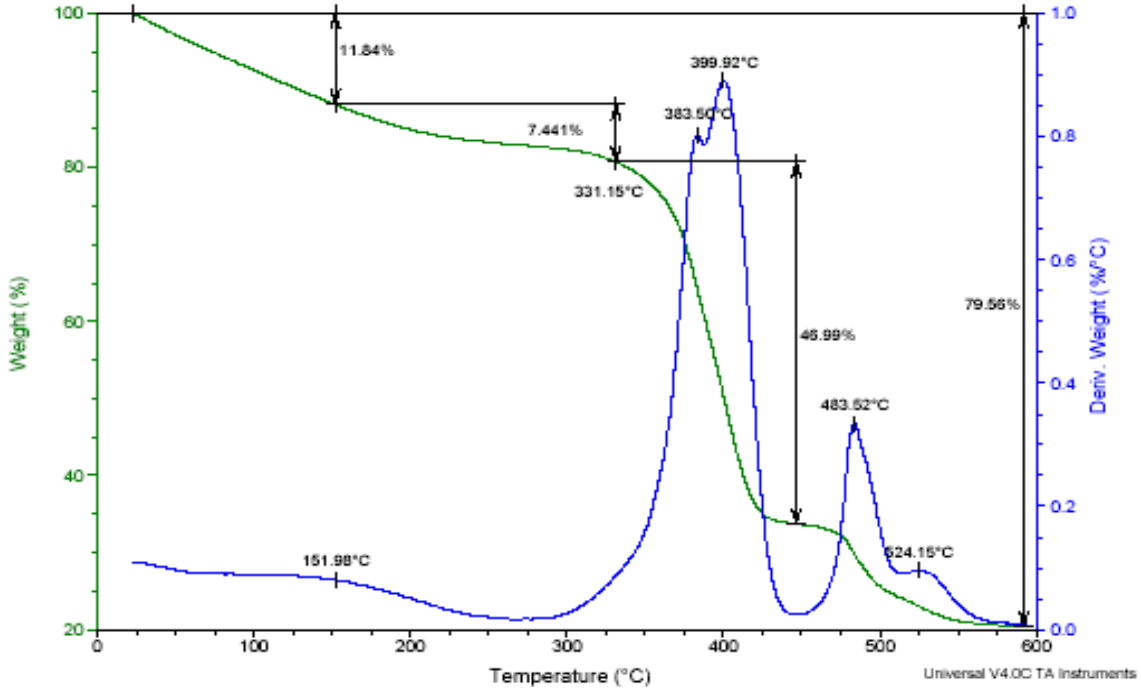

Figure H.8 TGA spectra realized to SIBS-Zn^{2+} membrane